



CONSTRUCTION  
WITH HOLLOW STEEL  
SECTIONS

3

# DESIGN GUIDE

## FOR RECTANGULAR HOLLOW SECTION (RHS) JOINTS UNDER PREDOMINANTLY STATIC LOADING

J.A. Packer, J. Wardenier, X.-L. Zhao, G.J. van der Vegte and  
Y. Kurobane

*Second Edition*



LSS Verlag



CONSTRUCTION  
WITH HOLLOW STEEL  
SECTIONS

3

# DESIGN GUIDE

## FOR RECTANGULAR HOLLOW SECTION (RHS) JOINTS UNDER PREDOMINANTLY STATIC LOADING

J.A. Packer, J. Wardenier, X.-L. Zhao, G.J. van der Vegte and  
Y. Kurobane

*Second Edition*





DESIGN GUIDE  
FOR RECTANGULAR HOLLOW SECTION (RHS) JOINTS UNDER  
PREDOMINANTLY STATIC LOADING



# CONSTRUCTION WITH HOLLOW STEEL SECTIONS

Edited by: Comité International pour le Développement et l'Étude  
de la Construction Tubulaire

Authors: Jeffrey A. Packer, University of Toronto, Canada  
Jaap Wardenier, Delft University of Technology, The  
Netherlands and National University of Singapore, Singapore  
Xiao-Ling Zhao, Monash University, Australia  
Addie van der Vegte, Delft University of Technology, The  
Netherlands  
Yoshiaki Kurobane, Kumamoto University, Japan

# DESIGN GUIDE

## **FOR RECTANGULAR HOLLOW SECTION (RHS) JOINTS UNDER PREDOMINANTLY STATIC LOADING**

Jeffrey A. Packer, Jaap Wardenier, Xiao-Ling Zhao, Addie van der Vegte  
and Yoshiaki Kurobane

**Design guide for rectangular hollow section (RHS) joints under predominantly static loading /**

[ed. by: Comité International pour le Développement et l'Étude de la Construction Tubulaire]  
Jeffrey A. Packer, 2009

(Construction with hollow steel sections)

ISBN 978-3-938817-04-9

NE: Packer, Jeffrey A.; Comité International pour le Développement et l'Étude de la Construction Tubulaire;

Design guide for rectangular hollow section (RHS) joints under predominantly static loading

ISBN 978-3-938817-04-9

© by CIDECT, 2009

## Preface

The objective of this 2<sup>nd</sup> edition of the Design Guide No. 3 for rectangular hollow section (RHS) joints under predominantly static loading is to present the most up-to-date information to designers, teachers and researchers.

Since the first publication of this Design Guide in 1992 additional research results became available and, based on these and additional analyses, the design strength formulae in the recommendations of the International Institute of Welding (IIW) have recently been modified. These recommendations are the basis for the new ISO standard in this field and also for this Design Guide.

However, these new IIW recommendations (2009) have not yet been implemented in the various national and international codes, which are still based on the previous 1989 edition of the IIW rules. Therefore, the recommendations in the previous version of (this Design Guide and) the IIW 1989 rules, which are moreover incorporated in Eurocode 3, are also given. Further, the new IIW formulae and the previous IIW (1989) recommended formulae are compared with each other.

Under the general series heading “Construction with Hollow Steel Sections”, CIDECT has published the following nine Design Guides, all of which are available in English, French, German and Spanish:

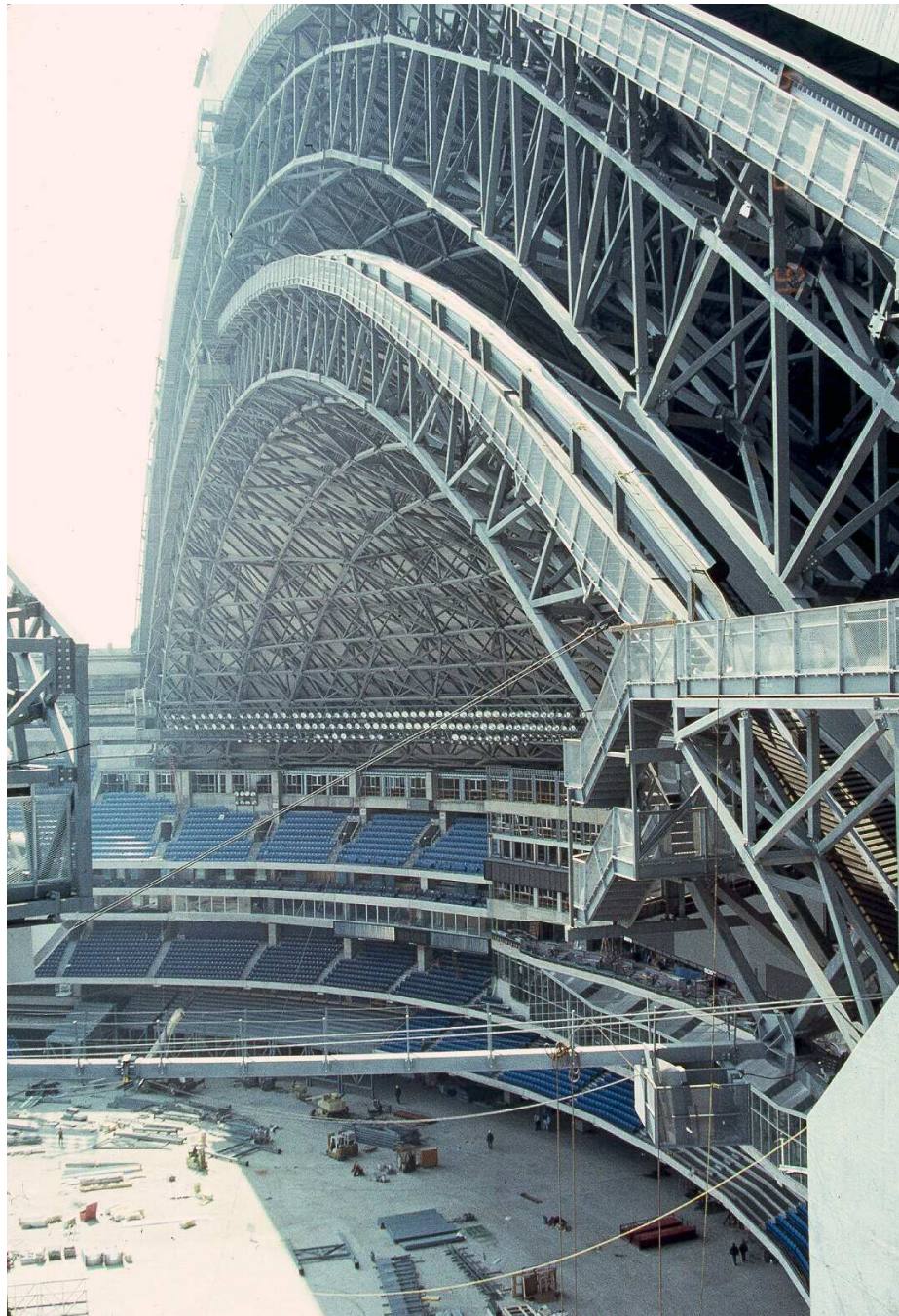
1. Design guide for circular hollow section (CHS) joints under predominantly static loading (1<sup>st</sup> edition 1991, 2<sup>nd</sup> edition 2008)
2. Structural stability of hollow sections (1992, reprinted 1996)
3. Design guide for rectangular hollow section (RHS) joints under predominantly static loading (1<sup>st</sup> edition 1992, 2<sup>nd</sup> edition 2009)
4. Design guide for structural hollow section columns exposed to fire (1995, reprinted 1996)
5. Design guide for concrete filled hollow section columns under static and seismic loading (1995)
6. Design guide for structural hollow sections in mechanical applications (1995)
7. Design guide for fabrication, assembly and erection of hollow section structures (1998)
8. Design guide for circular and rectangular hollow section welded joints under fatigue loading (2000)
9. Design guide for structural hollow section column connections (2004)

Further, the following books have been published:

“Tubular Structures in Architecture” by Prof. Mick Eekhout (1996) and “Hollow Sections in Structural Applications” by Prof. Jaap Wardenier (2002).

CIDECT wishes to express its sincere thanks to the internationally well-known authors of this Design Guide, Prof. Jeffrey Packer of University of Toronto, Canada, Prof. Jaap Wardenier of Delft University of Technology, The Netherlands and National University of Singapore, Singapore, Prof. Xiao-Ling Zhao of Monash University, Australia, Dr. Addie van der Vegte of Delft University of Technology, The Netherlands and the late Prof. Yoshiaki Kurobane of Kumamoto University, Japan for their willingness to write the 2<sup>nd</sup> edition of this Design Guide.

CIDECT, 2009



Rogers Centre (formerly SkyDome) under construction, Toronto, Canada

# CONTENTS

<b>1</b>	<b>Introduction</b> .....	9
1.1	Design philosophy and limit states .....	9
1.2	Scope and range of applicability .....	10
1.2.1	Limitations on materials .....	10
1.2.2	Limitations on geometric parameters .....	12
1.2.3	Section class limitations .....	13
1.3	Terminology and notation .....	13
1.4	Effect of geometric and mechanical tolerances on joint design strength .....	14
1.4.1	Determination of the design strength .....	14
1.4.2	Delivery standards .....	14
<b>2</b>	<b>Advantages and applications of rectangular hollow sections, and RHS relative to CHS</b> .....	16
<b>3</b>	<b>Design of tubular trusses</b> .....	21
3.1	Truss configurations .....	21
3.2	Truss analysis .....	21
3.3	Effective lengths for compression members .....	23
3.3.1	Simplified rules .....	23
3.3.2	Long, laterally unsupported compression chords .....	23
3.4	Truss deflections .....	24
3.5	General joint considerations .....	24
3.6	Truss design procedure .....	25
3.7	Arched trusses .....	26
3.8	Guidelines for earthquake design .....	26
3.9	Design of welds .....	26
<b>4</b>	<b>Welded uniplanar truss joints between RHS chords and RHS or CHS brace (web) members</b> .....	29
4.1	Joint classification .....	29
4.2	Failure modes .....	31
4.3	Joint resistance equations for T, Y, X and K gap joints .....	33
4.3.1	K and N gap joints .....	35
4.3.2	T, Y and X joints .....	35
4.4	K and N overlap joints .....	41
4.5	Special types of joints.....	46
4.6	Graphical design charts with examples.....	47
<b>5</b>	<b>Welded RHS-to-RHS joints under moment loading</b> .....	59
5.1	Vierendeel trusses and joints .....	59
5.1.1	Introduction to Vierendeel trusses .....	59
5.1.2	Joint behaviour and strength .....	60
5.2	T and X joints with brace(s) subjected to in-plane bending moment .....	61
5.3	T and X joints with brace(s) subjected to out-of-plane bending moment .....	65
5.4	T and X joints with brace(s) subjected to combinations of axial load, in-plane bending and out-of-plane bending moment .....	67
5.5	Joint flexibility .....	67
5.6	Knee joints .....	67
<b>6</b>	<b>Multiplanar welded joints</b> .....	70
6.1	KK joints .....	70
6.2	TT and XX joints .....	72

<b>7</b>	<b>Welded plate-to-RHS joints</b> .....	74
7.1	Longitudinal plate joints under axial loading .....	74
7.2	Stiffened longitudinal plate joints under axial loading .....	74
7.3	Longitudinal plate joints under shear loading .....	75
7.4	Transverse plate joints under axial loading .....	75
7.4.1	Failure mechanisms .....	75
7.4.2	Design of welds .....	76
7.5	Gusset plate-to-slotted RHS joints .....	79
7.6	Tee joints to the ends of RHS members .....	81
<b>8</b>	<b>Bolted joints</b> .....	83
8.1	Flange-plate joints .....	84
8.1.1	Bolted on two sides of the RHS – tension loading .....	84
8.1.2	Bolted on four sides of the RHS – tension loading .....	87
8.1.3	Flange-plate joints under axial load and moment loading .....	88
8.2	Gusset plate-to-RHS joints .....	89
8.2.1	Design considerations .....	89
8.2.2	Net area and effective net area .....	89
8.3	Hidden bolted joints .....	92
<b>9</b>	<b>Other uniplanar welded joints</b> .....	94
9.1	Reinforced joints .....	94
9.1.1	With stiffening plates .....	94
9.1.1.1	T, Y and X joints .....	94
9.1.1.2	K and N joints .....	95
9.1.2	With concrete filling .....	97
9.1.2.1	X joints with braces in compression .....	98
9.1.2.2	T and Y joints with brace in compression .....	98
9.1.2.3	T, Y and X joints with brace(s) in tension .....	99
9.1.2.4	Gap K joints .....	99
9.2	Cranked-chord joints .....	99
9.3	Trusses with RHS brace (web) members framing into the corners of the RHS chord (bird-beak joints) .....	100
9.4	Trusses with flattened and cropped-end CHS brace members to RHS chords .....	102
9.5	Double chord trusses .....	103
<b>10</b>	<b>Design examples</b> .....	106
10.1	Uniplanar truss .....	106
10.2	Vierendeel truss .....	114
10.3	Reinforced joints .....	117
10.3.1	Reinforcement by side plates .....	118
10.3.2	Reinforcement by concrete filling of the chord .....	119
10.4	Cranked chord joint (and overlapped joint) .....	119
10.5	Bolted flange-plate joint .....	120
<b>11</b>	<b>List of symbols and abbreviations</b> .....	123
11.1	Abbreviations of organisations .....	123
11.2	Other abbreviations .....	123
11.3	General symbols .....	123
11.4	Subscripts .....	125
11.5	Superscripts .....	126
<b>12</b>	<b>References</b> .....	127
<b>Appendix A</b>	Comparison between the new IIW (2009) design equations and the previous recommendations of IIW (1989) and/or CIDECT Design Guide No. 3 (1992) .....	136
<b>CIDECT</b>	.....	147

# 1 Introduction

Over the last forty years CIDECT has initiated many research programmes in the field of tubular structures: e.g. in the fields of stability, fire protection, wind loading, composite construction, and the static and fatigue behaviour of joints. The results of these investigations are available in extensive reports and have been incorporated into many national and international design recommendations with background information in CIDECT Monographs. Initially, many of these research programmes were a combination of experimental and analytical research. Nowadays, many problems can be solved in a numerical way and the use of the computer opens up new possibilities for developing the understanding of structural behaviour. It is important that the designer understands this behaviour and is aware of the influence of various parameters on structural performance.

This practical Design Guide shows how rectangular hollow section structures under predominantly static loading should be designed, in an optimum manner, taking account of the various influencing factors. This Design Guide concentrates on the ultimate limit states design of lattice girders or trusses. Joint resistance formulae are given and also presented in a graphical format, to give the designer a quick insight during conceptual design. The graphical format also allows a quick check of computer calculations afterwards. The design rules for the uniplanar joints satisfy the safety procedures used in the European Community, North America, Australia, Japan and China.

This Design Guide is a 2<sup>nd</sup> edition and supercedes the 1<sup>st</sup> edition, with the same title, published by CIDECT in 1992 (Packer et al., 1992). Where there is overlap in scope, the design recommendations presented herein are in accord with the most recent procedures recommended by the International Institute of Welding (IIW) Sub-commission XV-E (IIW, 2009), which are now a draft international standard for the International Organization for Standardization. Several background papers and an overall summary publication by Zhao et al. (2008) serve as a Commentary to these IIW (2009) recommendations.

Since the first publication of this Design Guide in 1992 (Packer et al., 1992), additional research results became available and, based on these and additional analyses, the design strength formulae in the IIW recommendations (2009) have been modified. These modifications have not yet been included in the various national and international codes (e.g. Eurocode 3 (CEN, 2005b); AISC, 2005) or guides (e.g. Packer and Henderson, 1997; Wardenier, 2002; Packer et al., 2009). The design strength formulae in these national and international codes/guides are still based on the previous edition of the IIW rules (IIW, 1989).

The differences with the previous formulae as used in the 1<sup>st</sup> edition of this Design Guide and adopted in Eurocode 3, are described in Appendix A.

## 1.1 Design philosophy and limit states

In designing tubular structures, it is important that the designer considers the joint behaviour right from the beginning. Designing members, e.g. of a girder, based on member loads only may result in undesirable stiffening of joints afterwards. This does not imply that the joints have to be designed in detail at the conceptual design phase. It only means that chord and brace members have to be chosen in such a way that the main governing joint parameters provide an adequate joint strength and an economical fabrication.

Since the design is always a compromise between various requirements, such as static strength, stability, economy in material use, fabrication and maintenance, which are sometimes in conflict with each other, the designer should be aware of the implications of a particular choice.

In common lattice structures (e.g. trusses), about 50% of the material weight is used for the chords in compression, roughly 30% for the chord in tension and about 20% for the web members or braces. This means that with respect to material weight, the chords in compression should likely be

optimised to result in thin-walled sections. However, for corrosion protection (painting), the outer surface area should be minimized. Furthermore, joint strength increases with decreasing chord width-to-thickness ratio  $b_0/t_0$  and increasing chord thickness to brace thickness ratio  $t_0/t_i$ . As a result, the final width-to-thickness ratio  $b_0/t_0$  for the chord in compression will be a compromise between joint strength and buckling strength of the member and relatively stocky sections will usually be chosen.

For the chord in tension, the width-to-thickness ratio  $b_0/t_0$  should be chosen to be as small as possible. In designing tubular structures, the designer should keep in mind that the costs of the structure are significantly influenced by the fabrication costs. This means that cutting, end preparation and welding costs should be minimized.

This Design Guide is written in a limit states design format (also known as LRFD or Load and Resistance Factor Design in the USA). This means that the effect of the factored loads (the specified or unfactored loads multiplied by the appropriate load factors) should not exceed the factored resistance of the joint, which is termed  $N$  or  $M$  in this Design Guide. The joint factored resistance expressions, in general, already include appropriate material and joint partial safety factors ( $\gamma_M$ ) or joint resistance (or capacity) factors ( $\phi$ ). This has been done to avoid interpretation errors, since some international structural steelwork specifications use  $\gamma_M$  values  $\geq 1.0$  as dividers (e.g. Eurocode 3 (CEN, 2005a, 2005b)), whereas others use  $\phi$  values  $\leq 1.0$  as multipliers (e.g. in North America, Australasia and Southern Africa). In general, the value of  $1/\gamma_M$  is nearly equal to  $\phi$ .

Some connection elements which arise in this Design Guide, which are not specific to hollow sections, such as plate material, bolts and welds, need to be designed in accordance with local or regional structural steel specifications. Thus, *additional safety or resistance factors should only be used where indicated*.

If allowable stress design (ASD) or working stress design is used, the joint factored resistance expressions provided herein should, in addition, be divided by an appropriate load factor. A value of 1.5 is recommended by the American Institute of Steel Construction (AISC, 2005).

Joint design in this Design Guide is based on the ultimate limit state (or states), corresponding to the "maximum load carrying capacity". The latter is defined by criteria adopted by the IIV Sub-commission XV-E, namely the lower of:

- (a) the ultimate strength of the joint, and
- (b) the load corresponding to an ultimate deformation limit.

An out-of-plane deformation of the connecting RHS face, equal to 3% of the RHS connecting face width ( $0.03b_0$ ), is generally used as the ultimate deformation limit (Lu et al., 1994) in (b) above. This serves to control joint deformations at both the factored and service load levels, which is often necessary because of the high flexibility of some RHS joints. In general, this ultimate deformation limit also restricts joint service load deformations to  $\leq 0.01b_0$ . Some design provisions for RHS joints in this Design Guide are based on experiments undertaken in the 1970s, prior to the introduction of this deformation limit and where ultimate deformations may have exceeded  $0.03b_0$ . However, such design formulae have proved to be satisfactory in practice.

## **1.2 Scope and range of applicability**

### **1.2.1 Limitations on materials**

This Design Guide is applicable to both hot-finished and cold-formed steel hollow sections, as well as cold-formed stress-relieved hollow sections. Many provisions in this Design Guide are also valid for fabricated box sections. For application of the design procedures in this Design Guide, manufactured hollow sections should comply with the applicable national (or regional) manufacturing specification for structural hollow sections. The nominal specified yield strength of

hollow sections should not exceed 460 N/mm<sup>2</sup> (MPa). This nominal yield strength refers to the finished tube product and should not be taken larger than 0.8f<sub>u</sub>.

The joint resistances given in this Design Guide are for hollow sections with a nominal yield strength of up to 355 N/mm<sup>2</sup> (MPa). For nominal yield strengths greater than this value, the joint resistances given in this Design Guide should be multiplied by 0.9. This provision considers the relatively larger deformations that take place in joints with nominal yield strengths of approximately 450 to 460 N/mm<sup>2</sup> (MPa), when plastification of the connecting RHS face occurs. (Hence, if other failure modes govern, it may be conservative). Furthermore, for any formula, the “design yield stress” used for computations should not be taken higher than 0.8 of the nominal ultimate tensile strength. This provision allows for ample connection ductility in cases where punching shear failure or failure due to local yielding of the brace govern, since strength formulae for these failure modes are based on the yield stress. For S460 steel hollow sections in Europe, the reduction factor of 0.9, combined with the limitation on f<sub>y</sub> to 0.8f<sub>u</sub>, results in a total reduction in joint resistance of about 15%, relative to just directly using a yield stress of 460 N/mm<sup>2</sup> (MPa) (Liu and Wardenier, 2004).

Some codes, e.g. Eurocode 3 (CEN, 2005b) give additional rules for the use of steel S690. These rules prescribe an elastic global analysis for structures with partial-strength joints. Further, a reduction factor of 0.8 to the joint capacity equations has to be used instead of the 0.9 factor which is used for S460.

The differences in notch toughness, for RHS manufactured internationally, can be extreme (Kosteski et al., 2005) but this property should not be of significance for statically loaded structures (which is the scope of this Design Guide). However, applications in arctic conditions or other applications under extreme conditions may be subject to special toughness requirements (Björk et al., 2003). In general, the selection of steel quality must take into account weldability, restraint, thickness, environmental conditions, rate of loading, extent of cold-forming and the consequences of failure (IIW, 2009).

Hot-dip galvanising of tubes or welded parts of tubular structures provides partial but sudden stress relief of the member or fabricated part. Besides potentially causing deformation of the element, which must be considered and compensated for before galvanising, cracking in the corners of RHS members is possible if the hollow section has very high residual strains due to cold-forming and especially if the steel is Si-killed. Such corner cracking is averted by manufacturers by avoiding tight corner radii (low radius-to-thickness values) and ensuring that the steel is fully Al-killed. Caution should be exercised when welding in the corner regions of RHS *if* there are tight corner radii or the steel is not fully Al-killed. Where cold-formed RHS corner conditions are deemed to be a potential problem for galvanising or welding, significant prior heat-treatment is recommended. Table 1.1 gives recommended minimum outside radii for *cold-formed* RHS corners which produce ideal conditions for welding or hot-dip galvanizing.

Table 1.1 – Recommended minimum outside corner radii for cold-formed RHS (from IIW (2009), which in turn is compiled from CEN (2005b, 2006b))

RHS thickness (mm)	Outside corner radius r <sub>o</sub> for fully Al-killed steel (Al ≥ 0.02%)	Outside corner radius r <sub>o</sub> for fully Al-killed steel <i>and</i> C ≤ 0.18%, P ≤ 0.020% and S ≤ 0.012%
2.5 ≤ t ≤ 6	≥ 2.0t	≥ 1.6t
6 < t ≤ 10	≥ 2.5t	≥ 2.0t
10 < t ≤ 12	≥ 3.0t	≥ 2.4t (up to t = 12.5)
12 < t ≤ 24	≥ 4.0t	N/A

## 1.2.2 Limitations on geometric parameters

Most of the joint resistance formulae in this Design Guide are subject to a particular “range of validity”. Often this represents the range of the parameters or variables over which the formulae have been validated, by either experimental or numerical research. In some cases it represents the bounds within which a particular failure mode will control, thereby making the design process simpler. These restricted ranges are given for each joint type where appropriate in this Design Guide, and several geometric constraints are discussed further in this section. Joints with parameters outside these specified ranges of validity are allowed, but they may result in lower joint efficiencies and generally require considerable engineering judgement and verification.

Also added to IIW (2009) is the minimum nominal wall thickness of hollow sections of 2.5 mm. Designers should be aware that some tube manufacturing specifications allow such a liberal tolerance on wall thickness (e.g. ASTM A500 (ASTM, 2007b) and ASTM A53 (ASTM, 2007a)) that a special “design thickness” is advocated for use in structural design calculations. The RHS nominal wall thickness for a chord member should not be greater than 25 mm, unless special measures have been taken to ensure that the through-thickness properties of the material are adequate.

Where CHS or RHS brace (web) members are welded to a RHS chord member, the included angle between a brace and chord ( $\theta$ ) should be  $\geq 30^\circ$ . This is to ensure that proper welds can be made. In some circumstances this requirement can be waived (for example at the heel of CHS braces), but only in consultation with the fabricator and the design resistance should not be taken larger than that for  $30^\circ$ . In gapped K joints, to ensure that there is adequate clearance to form satisfactory welds, the gap between adjacent brace members should be at least equal to the sum of the brace member thicknesses (i.e.  $g \geq t_1 + t_2$ ).

In overlapped K joints, the in-plane overlap should be large enough to ensure that the interconnection of the brace members is sufficient for adequate shear transfer from one brace to the other. This can be achieved by ensuring that the overlap, which is defined in figure 1.1, is at least 25%. Where overlapping brace members are of different widths, the narrower member should overlap the wider one. Where overlapping brace members, which have the same width, have different thicknesses and/or different strength grades, the member with the lowest  $t_i f_{yi}$  value should overlap the other member.

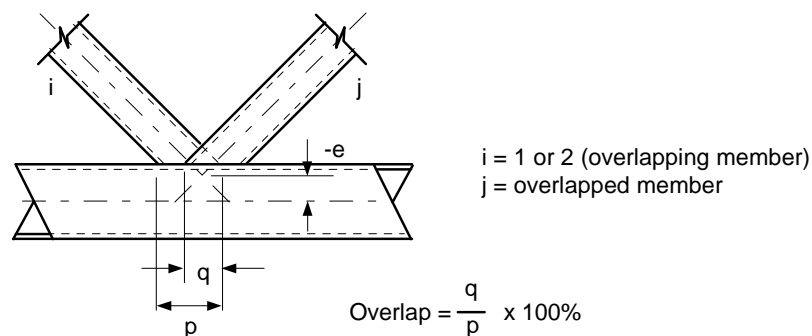


Figure 1.1 – Definition of overlap

In gapped and overlapped K joints, restrictions are placed on the noding eccentricity  $e$ , which is shown in figures 1.1 and 1.2, with a positive value of  $e$  representing an offset from the chord centerline towards the outside of the truss (away from the braces). This noding eccentricity restriction in the new IIW (2009) recommendations is  $e \leq 0.25h_0$ . The effect of the eccentricity on joint capacity is taken into account in the chord stress function  $Q_f$ . If the eccentricity exceeds  $0.25h_0$  the effect of bending moments on the joint capacity should also be considered for the brace

members. The bending moment produced by *any* nodding eccentricity  $e$ , should always be considered in member design by designing the chords as beam-columns.

With reference to figure 1.2, the gap  $g$  or overlap  $q$ , as well as the eccentricity  $e$ , may be calculated by equations 1.1 and 1.2 (Packer et al., 1992; Packer and Henderson, 1997):

$$g = \left( e + \frac{h_0}{2} \right) \frac{\sin(\theta_1 + \theta_2)}{\sin\theta_1 \sin\theta_2} - \frac{h_1}{2 \sin\theta_1} - \frac{h_2}{2 \sin\theta_2} \quad 1.1$$

Note that a negative value of gap  $g$  in equation 1.1 corresponds to an overlap  $q$ .

$$e = \left( \frac{h_1}{2 \sin\theta_1} + \frac{h_2}{2 \sin\theta_2} + g \right) \frac{\sin\theta_1 \sin\theta_2}{\sin(\theta_1 + \theta_2)} - \frac{h_0}{2} \quad 1.2$$

Note that  $g$  above will be negative for an overlap.

These equations also apply to joints which have a stiffening plate on the chord surface. Then,  $\frac{h_0}{2}$  is replaced by  $\left( \frac{h_0}{2} + t_p \right)$ , where  $t_p$  is the stiffening plate thickness.

### 1.2.3 Section class limitations

The section class gives the extent to which the resistance and rotation capacity of a cross section are limited by its local buckling resistance. For example, four classes are given in Eurocode 3 (CEN, 2005a) together with three limits on the diameter-to-thickness ratio for CHS or width-to-thickness ratio for RHS. For structures of hollow sections or combinations of hollow sections and open sections, the design rules for the joints are restricted to class 1 and 2 sections, therefore only these limits (according to Eurocode 3) are given in table 1.2. In other standards, slightly different values are used.

Table 1.2 – Section class limitations according to Eurocode 3 (CEN, 2005a)

$\epsilon = \sqrt{235/f_y}$ and $f_y$ in N/mm <sup>2</sup> (MPa)					
Limits	CHS in compression: $d/t_i$	RHS in compression (hot-finished and cold-formed): $(b_i - 2r_o)/t_i$ (*)	I sections in compression		
			Flange: $(b_i - t_w - 2r)/t_i$	Web: $(h_i - 2t_i - 2r)/t_w$	
Class 1	$50\epsilon^2$	$33\epsilon$	$18\epsilon$	$33\epsilon$	
Class 2	$70\epsilon^2$	$38\epsilon$	$20\epsilon$	$38\epsilon$	
Reduction factor $\epsilon$ for various steel grades					
$f_y$ (N/mm <sup>2</sup> )	235	275	355	420	460
$\epsilon$	1.00	0.92	0.81	0.75	0.71

(\*) For all hot-finished and cold-formed RHS, it is conservative to assume  $(b_i - 2r_o)/t_i = (b_i/t_i) - 3$  (as done by AISC (2005) and Sedlacek et al. (2006)).

### 1.3 Terminology and notation

This Design Guide uses terminology adopted by CIDECT and IIW to define joint parameters, wherever possible. The term “joint” is used to represent the zone where two or more *members* are interconnected, whereas “connection” is used to represent the location at which two or more

*elements* meet. The “through member” of a joint is termed the “chord” and attached members are termed braces (although the latter are also often termed bracings, branch members or web members). Such terminology for joints, connections and braces follows Eurocode 3 (CEN, 2005b).

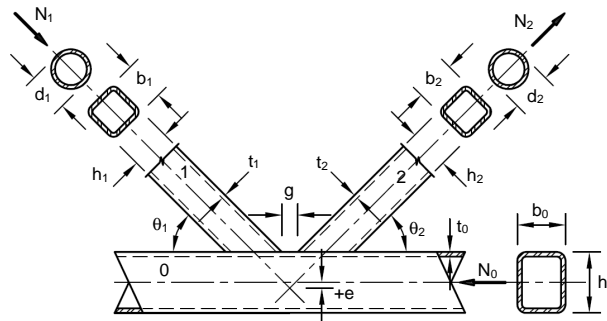


Figure 1.2 – Common notation for hollow structural section joints

Figure 1.2 shows some of the common joint notation for gapped and overlapped uniplanar K joints. Definitions of all symbols and abbreviations are given in chapter 11.

The numerical subscripts ( $i = 0, 1, 2$ ) to symbols shown in figure 1.2 are used to denote the member of a hollow section joint. The subscript  $i = 0$  designates the chord (or “through member”);  $i = 1$  refers in general to the brace for T, Y and X joints, or it refers to the compression brace member for K and N joints;  $i = 2$  refers to the tension brace member for K and N joints. For K and N overlap joints, the subscript  $i$  is used to denote the overlapping brace member and  $j$  is used to denote the overlapped brace member (see figure 1.1).

## 1.4 Effect of geometric and mechanical tolerances on joint design strength

### 1.4.1 Determination of the design strength

In the analyses for the determination of the design strengths, the mean values and coefficients of variation as shown in table 1.3 have been assumed for the dimensional, geometric and mechanical properties (IIW, 2009).

Table 1.3 – Effect of geometric and mechanical tolerances on joint design strength

Parameter	Mean value	CoV	Effect
CHS or RHS thickness $t_i$	1.0	0.05	Important
CHS diameter $d_i$ or RHS width $b_i$ or depth $h_i$	1.0	0.005	Negligible
Angle $\theta_i$	1.0	1°	Negligible
Relative chord stress parameter $n$	1.0	0.05	Important
Yield stress $f_y$	1.18	0.075	Important

In cases where hollow sections are used with mean values or tolerances significantly different from these values, it is important to note that the resulting design value may be affected.

### 1.4.2 Delivery standards

The delivery standards in various countries deviate considerably with respect to the thickness and mass tolerances (Packer, 2007). In most countries besides the thickness tolerance, a mass tolerance is given, which limits extreme deviations. However, in some production standards the thickness tolerance is not compensated by a mass tolerance – see ASTM A500 (ASTM, 2007b).

This has resulted in associated design specifications which account for this by designating a “design wall thickness” of 0.93 times the nominal thickness  $t$  (AISC, 2005) and in Canada even a design wall thickness of 0.90 $t$  is used for ASTM A500 hollow sections. However, the ASTM A501 (ASTM, 2007c) for hot-formed hollow sections has tightened its mass tolerance up to -3.5% with no thickness tolerance, resulting in small minus deviations from the nominal thickness.

The Canadian cold-formed product standard, CAN/CSA G40.20/G40.21 (CSA, 2004) has a -5% thickness tolerance throughout the thickness range and a -3.5% mass tolerance.

In Australia, the AS 1163 (Standards Australia, 1991) gives a thickness tolerance of +/- 10% and a lower mass tolerance of -4%.

In Europe, where nominal thicknesses are used in design, see EN 1993-1-1 (CEN, 2005a), the thickness tolerances are (partly) compensated by the mass tolerance. For example, table 1.4 shows the tolerances for hot-finished hollow sections according to EN 10210 (CEN, 2006a) and for cold-formed hollow sections according to EN 10219 (CEN, 2006b).

Table 1.4 – EN tolerances for hot-finished and cold-formed hollow sections

Thickness (mm)	Thickness tolerance Cold-formed (EN 10219)	Thickness tolerance Hot-finished (EN 10210)	Mass tolerance EN 10210 EN 10219	Governing (minimum) (assuming constant thickness)	
				EN 10219	EN 10210
$t \leq 5$	+/- 10%	-10%	+/- 6%	-6%	-6%
$5 < t \leq 8.33$	+/- 0.5 mm			-0.5 mm	
$8.33 < t$					

These thickness tolerances have an effect not only on the capacity of the sections but also on the joint capacity. Considering that the joint capacity criteria are a function of  $t^\alpha$  with  $1 \leq \alpha \leq 2$ , a large tolerance (as for example according to ASTM A500) can have a considerable effect on the joint capacity. Thus, in these cases a lower design thickness or an additional  $\gamma_M$  factor may have to be taken into account, for example as used in the USA.

In cases where the thickness tolerance is limited by a mass tolerance, the actual limits determine whether the nominal thickness can be used as the design thickness. Furthermore, if these tolerances are similar or smaller than those for other comparable steel sections, the same procedure can be used.

In Australia and Canada (for CSA) the tolerances on thickness and mass are such that the nominal thickness can be assumed as the design thickness. The same applies to hot-formed hollow sections according to ASTM A501.

The tolerances in Europe could, especially for the lower thicknesses, result in an effect on the joint capacity. On the other hand, joints with a smaller thickness generally have a larger mean value for the yield strength and relatively larger welds, resulting in larger capacities for small size specimens, which (partly) compensates for the effect of the minus thickness tolerance (see figure 1.4 of CIDECT Design Guide No. 1 (Wardenier et al., 2008)).

## **2 Advantages and applications of rectangular hollow sections, and RHS relative to CHS**

The structural advantages of hollow sections have become apparent to most designers, particularly for structural members loaded in compression or torsion. Circular hollow sections (CHS) have a particularly pleasing shape and offer a very efficient distribution of steel about the centroidal axes, as well as the minimum possible resistance to fluid, but specialized profiling is needed when joining circular shapes together. As a consequence, rectangular hollow sections (RHS) have evolved as a practical alternative, allowing easy connections to the flat face, and they are very popular for columns and trusses.

Fabrication costs of all structural steelwork are primarily a function of the labour hours required to produce the structural components. These need not be more with hollow section design (RHS or CHS) than with open sections, and can even be less depending on joint configurations. In this regard it is essential that the designer realizes that the selection of hollow structural section truss components, for example, determines the complexity of the joints at the panel points. It is not to be expected that members selected for minimum mass can be joined for minimum labour time. That will seldom be the case because the efficiency of hollow section joints is a subtle function of a number of parameters which are defined by relative dimensions of the connecting members.

Handling and erecting costs can be less for hollow section trusses than for alternative trusses. Their greater stiffness and lateral strength mean they are easier to pick up and more stable to erect. Furthermore, trusses comprised of hollow sections are likely to be lighter than their counterparts fabricated from non-tubular sections, as truss members are primarily axially loaded and hollow structural sections represent the most efficient use of a steel cross section in compression.

Protection costs are appreciably lower for hollow section trusses than for other trusses. A square hollow section has about  $2/3$  the surface area of the same size I section shape, and hollow section trusses may have smaller members as a result of their higher structural efficiency. The absence of re-entrant corners makes the application of paint or fire protection easier and the durability is longer. Rectangular (which includes square) hollow sections, if closed at the ends, also have only four surfaces to be painted, whereas an I section has eight flat surfaces for painting. These combined features result in less material and less labour for hollow section structures.

Regardless of the type of shape used to design a truss, it is generally false economy to attempt to minimize mass by selecting a multitude of sizes for brace members. The increased cost to source and to separately handle the various shapes more than offsets the apparent savings in materials. It is therefore better to use the same section size for a group of brace members. CHS joints are more expensive to fabricate than RHS joints. Joints of CHS require that the tube ends be profile cut when the tubes are to be fitted directly together, unless the braces are much smaller than the chords. More than that, the bevel of the end cut must generally be varied for welding access as one progresses around the tube. If automated equipment for this purpose is not available, semi automatic or manual profile cutting has to be used, which is much more expensive than straight bevel cuts on RHS.

In structures where deck or panelling is laid directly on the top chord of trusses, RHS offer superior surfaces to CHS for attaching and supporting the deck. Other aspects to consider when choosing between circular and rectangular hollow sections are the relative ease of fitting weld backing bars to RHS, and of handling and stacking RHS. The latter is important because material handling is said to be the highest cost in the shop.

Similar to CHS, the RHS combines excellent structural properties with an architecturally attractive shape. This has resulted in many applications in buildings, halls, bridges, towers, and special applications, such as sign gantries, parapets, cranes, jibs, sculptures, etc. (Eekhout, 1996; Wardenier, 2002). For indication, some examples are given in figures 2.1 to 2.7.



Figure 2.1 – Rectangular hollow sections used for the columns and trusses of a building



Figure 2.2 – Rectangular hollow sections used in the roof and for the columns of a petrol station



Figure 2.3 – Rectangular hollow sections used in a truss of a footbridge



Figure 2.4 – Rectangular hollow sections used in a crane



Figure 2.5 – Rectangular hollow sections used in sound barriers



Figure 2.6 – Rectangular hollow section columns and trusses used in a glass house

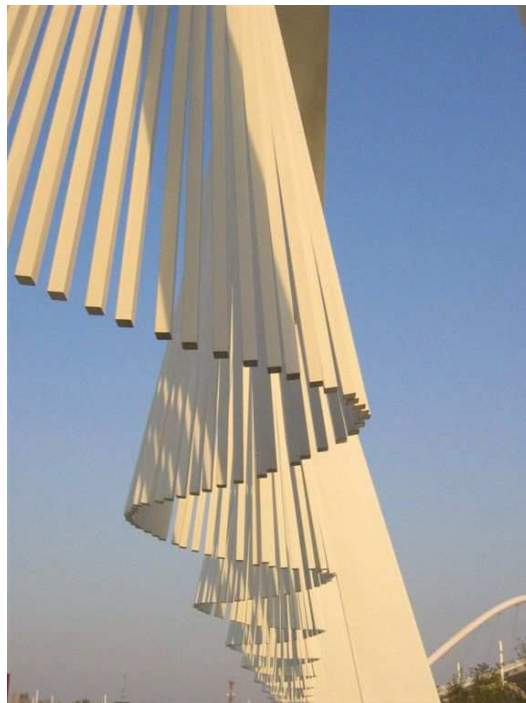


Figure 2.7 – Rectangular hollow sections used in art

## 3 Design of tubular trusses

### 3.1 Truss configurations

Some of the common truss types are shown in figure 3.1. Warren trusses will generally provide the most economical solution since their long compression brace members can take advantage of the fact that RHS are very efficient in compression. They have about half the number of brace members and half the number of joints compared to Pratt trusses, resulting in considerable labour and cost savings. The panel points of a Warren truss can be located at the load application points on the chord, if necessary with an irregular truss geometry, or even away from the panel points (thereby loading the chord in bending). If support is required at all load points to a chord (for example, to reduce the unbraced length), a modified Warren truss could be used rather than a Pratt truss by adding vertical members as shown in figure 3.1(a).

Warren trusses provide greater opportunities to use gap joints, the preferred arrangement at panel points. Also, when possible, a regular Warren truss achieves a more “open” truss suitable for practical placement of mechanical, electrical and other services. Truss depth is determined in relation to the span, loads, maximum deflection, etc., with increased truss depth reducing the loads in the chord members and increasing the lengths of the brace members. The ideal span to depth ratio is usually found to be between 10 and 15. If the total costs of the building are considered, a ratio nearer 15 will represent optimum value.

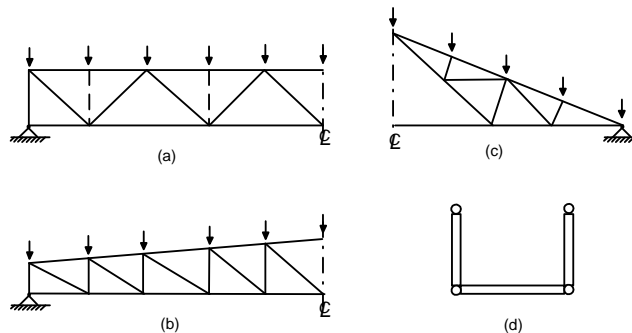


Figure 3.1 – Common RHS uniplanar trusses

- (a) Warren trusses (modified Warren with verticals)
- (b) Pratt truss (shown with a sloped roof, but may have parallel chords)
- (c) Fink truss
- (d) U-framed truss

### 3.2 Truss analysis

Elastic analysis of RHS trusses is frequently performed by assuming that all members are pin-connected. Nodal eccentricities between the centre lines of intersecting members at panel points should preferably be kept to  $e \leq 0.25h_0$ . These eccentricities produce primary bending moments which, for a pinned joint analysis, need to be taken into account in chord member design; e.g. by treating it as a beam-column. This is done by distributing the panel point moment (sum of the horizontal components of the brace member forces multiplied by the nodal eccentricity) to the chord on the basis of relative chord stiffness on either side of the joint (i.e. in proportion to the values of moment of inertia divided by chord length to the next panel point, on either side of the joint).

*Note: In the joint capacity formulae of the 1<sup>st</sup> edition of this Design Guide (Packer et al., 1992) – see Appendix A –, the eccentricity moments could be ignored for the design of the joints provided that the eccentricities were within the limits  $-0.55h_0 \leq e \leq 0.25h_0$ .*

If these eccentricity limits are violated, the eccentricity moment may have a detrimental effect on joint strength and the eccentricity moment must be distributed between the members of a joint. If moments are distributed to the brace members, the joint capacity must then be checked for the interaction between axial load and bending moment, for each brace member.

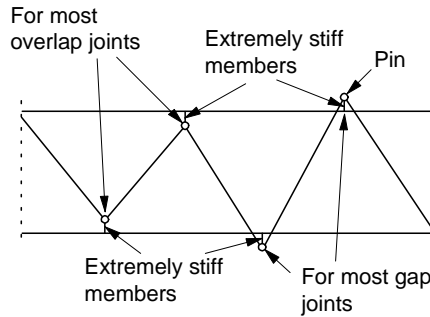


Figure 3.2 – Plane frame joint modelling assumptions to obtain realistic forces for member design

A rigid joint frame analysis is not recommended for most planar, triangulated, single-chord, directly-welded trusses, as it generally tends to exaggerate brace member moments, and the axial force distribution will still be similar to that for a pin-jointed analysis.

Transverse loads applied to either chord away from the panel points produce primary moments which must always be taken into account when designing the chords.

Computer plane frame programs are regularly used for truss analysis. In this case, the truss can be modelled by considering a continuous chord with brace members pin-connected to it at distances of +e or -e from it (e being the distance from the chord centreline to the intersection of the brace member centrelines). The links to the pins are treated as being extremely stiff as indicated in figure 3.2. The advantage of this model is that a sensible distribution of bending moments is automatically generated throughout the truss, for cases in which bending moments need to be taken into account in the design of the chords.

Secondary moments, resulting from end fixity of the brace members to a flexible chord wall, can generally be ignored for both members and joints, provided that there is deformation and rotation capacity adequate to redistribute stresses after some local yielding at the connections. This is the case when the prescribed geometric limits of validity for design formulae, given in chapter 4, are followed. Welds in particular need to have potential for adequate stress redistribution without premature failure, and this will be achieved with the recommendations given in section 3.9. Table 3.1 summarizes when moments need to be considered for designing an RHS truss.

Table 3.1 – Moments to be considered for RHS truss design

Type of moment	Primary	Primary	Secondary
Moments due to	Nodal eccentricity ( $e \leq 0.25h_0$ )	Transverse member loading	Secondary effects such as local deformations
Chord design	Yes	Yes	No
Design of other members	No	Yes	No
Design of joints	Yes, for $Q_f$ only	Yes, influences $Q_f$	No, provided parametric limits of validity are met

Plastic design could be used to proportion the chords of a truss by considering them as continuous beams with pin supports from the brace members. In such a design, the plastically designed members must be plastic design sections and the welds must be sized to develop the capacity of the connected brace members.

### 3.3 Effective lengths for compression members

To determine the effective length  $KL$  for a compression member in a truss, the effective length factor  $K$  can always be conservatively taken as 1.0. However, considerable end restraint is generally present for compression members in an RHS truss, and it has been shown that  $K$  is generally appreciably less than 1.0 (Mouty, 1981; Rondal et al., 1996). This restraint offered by members framing into a joint could disappear, or be greatly reduced, if all members were designed optimally for minimum mass, thereby achieving ultimate capacity simultaneously under static loading (Galambos, 1998). In practice, design for optimal or minimum mass will rarely coincide with minimum cost; the brace members are usually standardized to a few selected dimensions (perhaps even two) to minimize the number of section sizes for the truss. In the unlikely situation that all compression brace members are proportioned on the basis of a single load combination, and all reach their compressive resistances at approximately the same truss loading, an effective length factor of 1.0 is recommended. CIDECT has sponsored and coordinated extensive research work to specifically address the determination of effective lengths in hollow section trusses, resulting in reports from CIDECT Programmes 3E-3G and Monograph No. 4 (Mouty, 1981). A re-evaluation of all test results has been undertaken to produce recommendations for Eurocode 3. This has resulted in the following effective length recommendations.

#### 3.3.1 Simplified rules

For RHS chord members:

In the plane of the truss:

$$KL = 0.9 L \text{ where } L \text{ is the distance between chord panel points} \quad 3.1$$

In the plane perpendicular to the truss:

$$KL = 0.9 L \text{ where } L \text{ is the distance between points of lateral support for the chord} \quad 3.2$$

For RHS or CHS brace members:

In either plane:

$$KL = 0.75 L \text{ where } L \text{ is the panel point to panel point length of the member} \quad 3.3$$

These values of  $K$  are only valid for hollow section members which are connected around the full perimeter of the member, without cropping or flattening of the members. Compliance with the joint design requirements of chapter 4 will likely place even more restrictive control on the member dimensions. More detailed recommendations, resulting in lower  $K$  values are given in CIDECT Design Guide No. 2 (Rondal et al., 1996).

#### 3.3.2 Long, laterally unsupported compression chords

Long, laterally unsupported compression chords can exist in pedestrian bridges such as U-framed trusses and in roof trusses subjected to large wind uplift. The effective length of such laterally unsupported truss chords can be considerably less than the unsupported length. For example, the actual effective length of a bottom chord, loaded in compression by uplift, depends on the loading in the chord, the stiffness of the brace members, the torsional rigidity of the chords, the purlin to truss

joints and the bending stiffness of the purlins. The brace members act as local elastic supports at each panel point. When the stiffness of these elastic supports is known, the effective length of the compression chord can be calculated. A detailed method for effective length factor calculation has been given by CIDECT Monograph No. 4 (Mouty, 1981).

### 3.4 Truss deflections

For the purpose of checking the serviceability condition of overall truss deflection under specified (unfactored) loads, an analysis with all members being pin-jointed will provide a conservative (over)estimate of truss deflections when all the joints are overlapped (Coutie et al., 1987; Philiastides, 1988). A better assumption for overlap conditions is to assume continuous chord members and pin-jointed brace members. However, for gap-connected trusses, a pin-jointed analysis still generally underestimates overall truss deflections, because of the flexibility of the joints. At the service load level, gap-connected RHS truss deflections may be underestimated by up to 12-15% (Czechowski et al., 1984; Coutie et al., 1987; Philiastides, 1988; Frater, 1991). Thus, a conservative approach for gap-connected RHS trusses is to estimate the maximum truss deflection by 1.15 times that calculated from a pin-jointed analysis.

### 3.5 General joint considerations

It is essential that the designer has an appreciation of factors which make it possible for RHS members to be connected together at truss panel points without extensive (and expensive) reinforcement. Apparent economies from minimum-mass member selection will quickly vanish at the joints if a designer does not have knowledge of the critical considerations which influence joint efficiency.

1. Chords should generally have thick walls rather than thin walls. The stiffer walls resist loads from the brace members more effectively, and the joint resistance thereby increases as the width-to-thickness ratio decreases. For the compression chord, however, a large thin section is more efficient in providing buckling resistance, so for this member the final RHS wall slenderness will be a compromise between joint strength and buckling strength, and relatively stocky sections will usually be chosen.
2. Brace members should have thin walls rather than thick walls (except for the overlapped brace in overlap joints), as joint efficiency increases as the ratio of chord wall thickness to brace wall thickness increases. In addition, thin brace member walls will require smaller fillet welds for a pre-qualified connection (weld volume is proportional to  $t^2$ ).
3. Ideally, RHS brace members should have a smaller width than RHS chord members, as it is easier to weld to the flat surface of the chord section.
4. Gap joints (K and N) are preferred to overlap joints because the members are easier to prepare, fit and to weld. In good designs, a minimum gap  $g \geq t_1 + t_2$  should be provided such that the welds do not overlap each other.
5. When overlap joints are used, at least a quarter of the width (in the plane of the truss) of the overlapping member needs to be engaged in the overlap; i.e.  $q \geq 0.25p$  in figure 1.1. However,  $q \geq 0.5p$  is preferable.
6. An angle of less than  $30^\circ$  between a brace member and a chord creates serious welding difficulties at the heel location on the connecting face and is not covered by the scope of these recommendations (see section 3.9). However, angles less than  $30^\circ$  may be possible if the design is based on an angle of  $30^\circ$  and it is shown by the fabricator that a satisfactory weld can be made.

### 3.6 Truss design procedure

In summary, the design of an RHS truss should be approached in the following way to obtain an efficient and economical structure.

I. Determine the truss layout, span, depth, panel lengths, truss and lateral bracing by the usual methods, but keep the number of joints to a minimum.

II. Determine loads at joints and on members; simplify these to equivalent loads at the panel points if performing manual analysis.

III. Determine axial forces in all members by assuming that joints are either: (a) pinned and that all member centre lines are nodding, or (b) that the chord is continuous with pin-connected braces.

IV. Determine chord member sizes by considering axial loading, corrosion protection and RHS wall slenderness. (Usual width-to-thickness ratios  $b_0/t_0$  are 15 to 25.) An effective length factor of  $K = 0.9$  can be used for the design of the compression chord. Taking account of the standard mill lengths in design may reduce the end-to-end joints within chords. For large projects, it may be agreed that special lengths are delivered. Since the joint strength depends on the yield stress of the chord, the use of higher strength steel for chords (when available and practical) may offer economical possibilities. The delivery time of the required sections has to be checked.

V. Determine brace member sizes based on axial loading, preferably with thicknesses smaller than the chord thickness. The effective length factor for the compression brace members can initially be assumed to be 0.75 (see section 3.3.1).

VI. Standardize the brace members to a few selected dimensions (perhaps even two), to minimize the number of section sizes for the structure. Consider availability of all sections when making member selections. For aesthetic reasons, a constant outside member width may be preferred for all brace members, with wall thicknesses varying; but this will require special quality control procedures in the fabrication shop.

VII. Layout the joints; from a fabrication point of view, try gap joints first. Check that the joint geometry and member dimensions satisfy the validity ranges for the dimensional parameters given in chapter 4, with particular attention to the eccentricity limit. Consider the fabrication procedure when deciding on a joint layout.

VIII. If the joint resistances (efficiencies) are not adequate, modify the joint layout (for example, overlap rather than gap) or modify the brace or chord members as appropriate, and recheck the joint capacities. Generally, only a few joints will need checking.

IX. Check the effect of primary moments on the design of the chords. For example, use the proper load positions (rather than equivalent panel point loading that may have been assumed if performing manual analysis); determine the bending moments in the chords by assuming either: (a) pinned joints everywhere or (b) continuous chords with pin-ended brace members. For the compression chord, also determine the bending moments produced by any nodding eccentricities, by using either of the above analysis assumptions. Then check that the factored resistance of all chord members is still adequate, under the influence of both axial loads and total primary bending moments.

X. Check truss deflections (see section 3.4) at the specified (unfactored) load level, using the proper load positions.

XI. Design welds.

### 3.7 Arched trusses

The joints of arched trusses can be designed in a similar way to those of straight chord trusses. If the arched chords are made by bending at the joint location only, as shown in figure 3.3(a), the chord members can also be treated in a similar way to those of straight chord trusses provided that the bending radius remains within the limits to avoid distortion of the cross section (Dutta et al., 1998; Dutta, 2002). If the arched chords are made by continuous bending, the chord members have a curved shape between the joint locations, as shown in figure 3.3(b). In this case, the curvature should be taken into account in the member design by treating the chord as a beam-column. (Moment = axial force x eccentricity.)

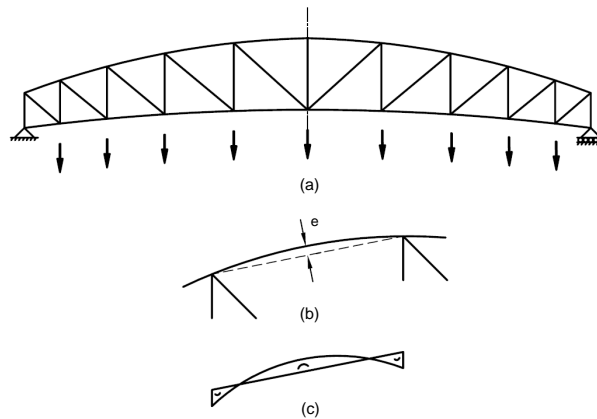


Figure 3.3 – Arched truss

### 3.8 Guidelines for earthquake design

In seismic design, the joints should meet additional requirements with regard to overstrength, resulting in the members being critical. For sufficient rotation capacity, energy-dissipating members should meet at least the class 1 requirements of table 1.1. For detailed information, reference is given to CIDECT Design Guide No. 9 (Kurobane et al., 2004).

### 3.9 Design of welds

Except for certain K and N joints with partially overlapped brace members (as noted below), a welded connection should be established around the entire perimeter of a brace member by means of a butt weld, a fillet weld, or a combination of the two. Fillet welds which are automatically prequalified for any brace member loads should be designed to give a resistance that is not less than the brace member capacity. According to Eurocode 3 (CEN, 2005b), this results in the following minimum throat thickness “a” for fillet welds around brace members, assuming matched electrodes and ISO steel grades (IIW, 2009):

- $a \geq 0.92 t$ , for S235 ( $f_{yi} = 235 \text{ N/mm}^2$ )
- $a \geq 0.96 t$ , for S275 ( $f_{yi} = 275 \text{ N/mm}^2$ )
- $a \geq 1.10 t$ , for S355 ( $f_{yi} = 355 \text{ N/mm}^2$ )
- $a \geq 1.42 t$ , for S420 ( $f_{yi} = 420 \text{ N/mm}^2$ )
- $a \geq 1.48 t$ , for S460 ( $f_{yi} = 460 \text{ N/mm}^2$ )

With overlapped K and N joints, welding of the toe of the overlapped member to the chord is particularly important for 100% overlap situations. For partial overlaps, the toe of the overlapped member need not be welded, providing the components, normal to the chord, of the brace member

forces do not differ by more than about 20%. The larger width brace member should be the “through member”. If both braces have the same width then the thicker brace should be the overlapped (through) brace and pass uninterrupted through to the chord. If both braces are of the same size (outside dimension and thickness), then the more heavily loaded brace member should be the “through member”. When the brace member force components normal to the chord member differ by more than 20%, the full circumference of the through brace should be welded to the chord.

Generally, the weaker member (defined by wall thickness times yield strength) should be attached to the stronger member, regardless of the load type, and smaller members sit on larger members.

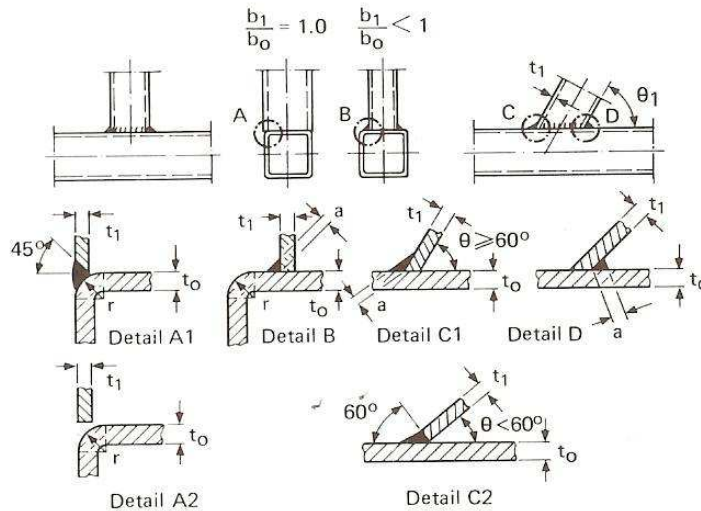


Figure 3.4 – Weld details

It is more economical to use fillet welds than butt (groove) welds. However, the upper limit on throat or leg size for fillet welds will depend on the fabricator. Most welding specifications only allow fillet welding at the toe of a brace member if  $\theta_i \geq 60^\circ$ . Because of the difficulty of welding at the heel of a brace member at low  $\theta$  values, a lower limit for the applicability of the joint design rules given herein has been set at  $\theta_i = 30^\circ$ . Some recommended weld details (IIW, 2009) are illustrated in figure 3.4.

If welds are proportioned on the basis of particular brace member loads, the designer must recognize that the entire length of the weld may not be effective, and the model for the weld resistance must be justified in terms of strength and deformation capacity. An effective length of RHS brace member welds in planar, gap K and N joints subjected to predominantly static axial load, is given by Frater and Packer (1990):

$$\text{Effective length} = \frac{2h_i}{\sin \theta_i} + b_i \quad \text{for } \theta_i \geq 60^\circ \quad 3.4$$

$$\text{Effective length} = \frac{2h_i}{\sin \theta_i} + 2b_i \quad \text{for } \theta_i \leq 50^\circ \quad 3.5$$

For  $50^\circ < \theta_i < 60^\circ$ , a linear interpolation has been suggested (AWS, 2008).

For overlapped K and N joints, limited experimental research on joints with 50% overlap has shown that the entire overlapping brace member contact perimeter can be considered as effective (Frater and Packer, 1990).

These recommendations for effective weld lengths in RHS K and N joints satisfy the required safety levels for use in conjunction with both European and North American steelwork specifications (Frater and Packer, 1990). However it is recommended that the strength enhancement for transversely loaded fillet welds – allowed by some steel codes/specifications – not be used,

because the fillet weld is loaded by a force not in the plane of the weld group (AISC, 2005; Packer et al., 2009).

Based on the weld effective lengths for K and N joints, extrapolation has been postulated for RHS T, Y and X joints under predominantly static load (Packer and Wardenier, 1992):

$$\text{Effective length} = \frac{2h_i}{\sin \theta_i} \quad \text{for } \theta_i \geq 60^\circ \quad 3.6$$

$$\text{Effective length} = \frac{2h_i}{\sin \theta_i} + b_i \quad \text{for } \theta_i \leq 50^\circ \quad 3.7$$

For  $50^\circ < \theta_i < 60^\circ$ , a linear interpolation is recommended.



Pavilion at Expo 92, Seville, Spain

## 4 Welded uniplanar truss joints between RHS chords and RHS or CHS brace (web) members

### 4.1 Joint classification

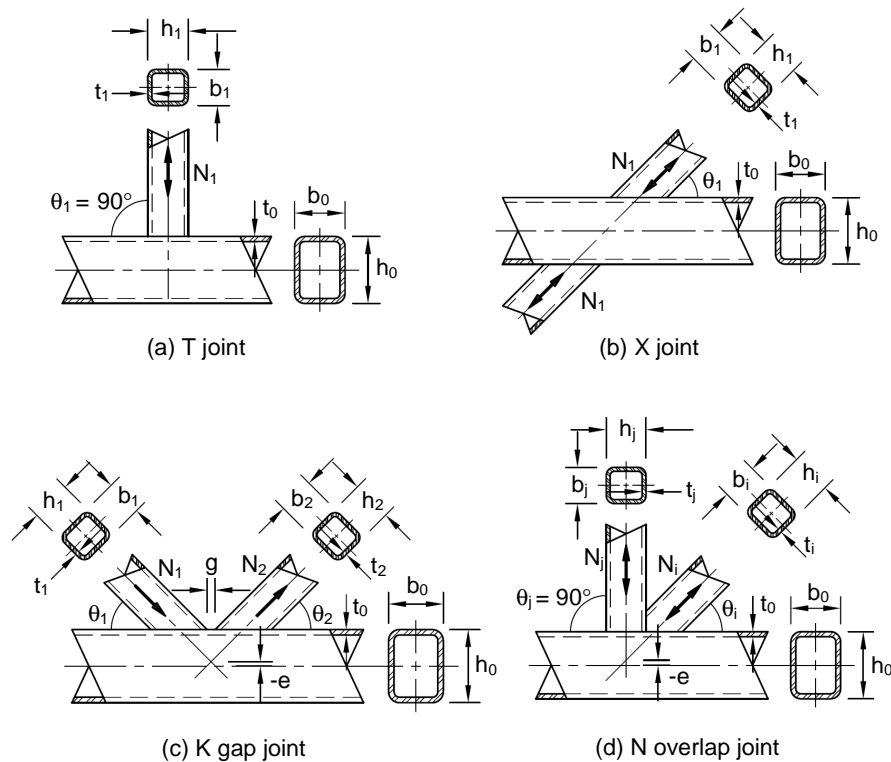


Figure 4.1 – Basic joint configurations i.e. T, X and K joints

Figure 4.1 shows the basic types of joint configurations; i.e. T, X and K or N joints. The classification of hollow section truss-type joints as K (which includes N), Y (which includes T) or X joints is based on the method of force transfer in the joint, not on the physical appearance of the joint. Examples of such classification are shown in figure 4.2, and definitions follow.

(a) When the normal component of a brace member force is equilibrated by beam shear (and bending) in the chord member, the joint is classified as a T joint when the brace is perpendicular to the chord, and a Y joint otherwise.

(b) When the normal component of a brace member force is essentially equilibrated (within 20%) by the normal force component of another brace member (or members), on the same side of the joint, the joint is classified as a K joint. The relevant gap is between the primary brace members whose loads equilibrate. An N joint can be considered as a special type of K joint.

(c) When the normal force component is transmitted through the chord member and is equilibrated by a brace member (or members) on the opposite side, the joint is classified as an X joint.

(d) When a joint has brace members in more than one plane, the joint is classified as a multiplanar joint (see chapter 6).

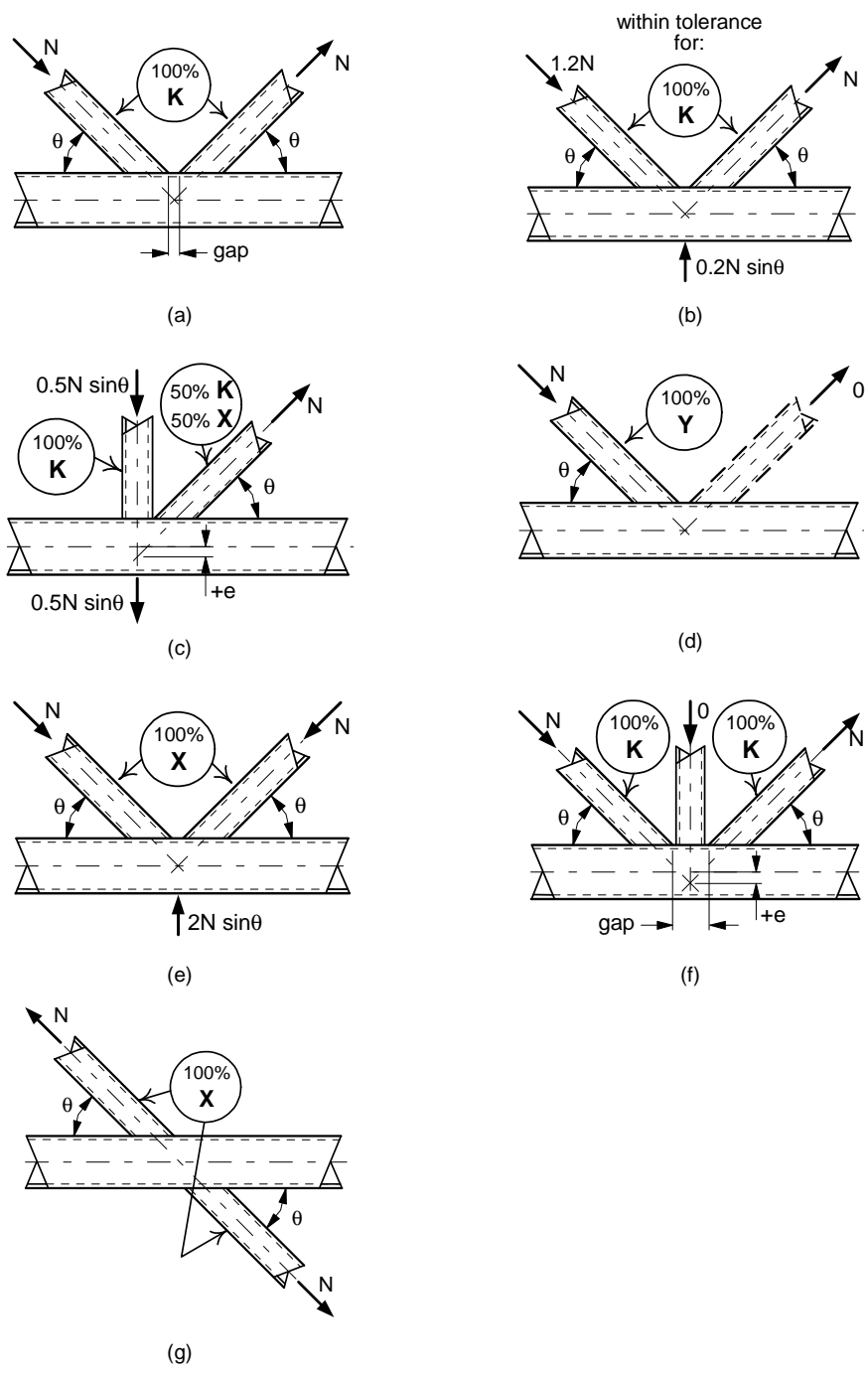


Figure 4.2 – Examples of hollow section joint classification

When brace members transmit part of their load as K joints and part of their load as T, Y, or X joints, the adequacy of each brace needs to be determined by linear interaction of the proportion of the brace load involved in each type of load transfer.

One K joint, in figure 4.2(b), illustrates that the brace force components normal to the chord member may differ by as much as 20% and still be deemed to exhibit K joint behaviour. This is to accommodate slight variations in brace member forces along a typical truss, caused by a series of panel point loads.

The N joint in figure 4.2(c), however, has a ratio of brace force components normal to the chord member of 2:1. In this case, that particular joint needs to be analysed as both a “pure” K joint (with balanced brace forces) and an X joint (because the remainder of the diagonal brace load is being transferred through the joint), as shown in figure 4.3. For the diagonal tension brace in that particular joint, one would need to check that:

$$\frac{0.5N}{\text{K joint resistance}} + \frac{0.5N}{\text{X joint resistance}} \leq 1.0$$

The three diagrams in figure 4.3 are each in equilibrium. If an additional chord “preload” force was applied to figure 4.3(a), on the left hand side of the joint, which would cause an equal and opposite additional chord force on the right hand side of the joint, then this “preload” would need to be added to either figure 4.3(b) or (c). It is recommended that this preload effect be added to the diagram which results in the more punitive outcome.

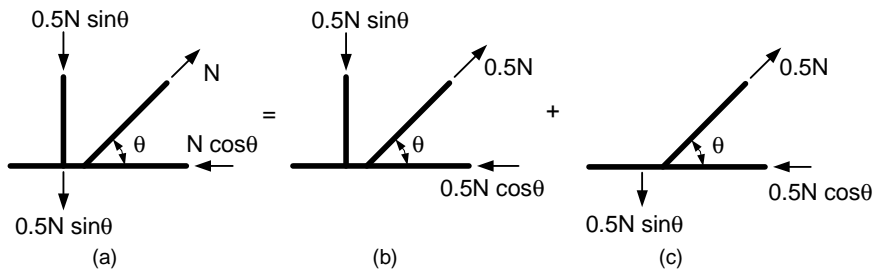


Figure 4.3 – Checking of a K joint with imbalanced brace loads

If the gap size in a gapped K (or N) joint (e.g. figure 4.2(a)) becomes large and exceeds the value permitted by the gap/eccentricity limit, then the “K joint” should also be checked as two independent Y joints.

In X joints such as figure 4.2(e), where the braces are close together or overlapping, the combined “footprint” of the two braces can be taken as the loaded area on the chord member.

In K joints such as figure 4.2(d), where a brace has very little or no loading, the joint can be treated as a Y joint, as shown.

Some special uniplanar joints with braces on both sides of the chord where the brace forces act in various ways, are dealt with in table 4.4.

## 4.2 Failure modes

The strength of RHS joints can, depending on the type of joint, geometric parameters and loading, be governed by various criteria.

The majority of RHS truss joints have one compression brace member and one tension brace member welded to the chord as shown in figure 1.2. Experimental research on RHS welded truss

joints (for example Wardenier and Stark, 1978) has shown that different failure modes exist depending on the type of joint, loading conditions, and various geometric parameters. Failure modes for RHS joints have been described by Wardenier (1982) as illustrated in figure 4.4, and the design of welded RHS joints is thus based on these potential limit states. These failure modes are:

- Mode (a): Plastic failure of the chord face (one brace member pushes the face in, and the other pulls it out)
- Mode (b): Punching shear failure of the chord face around a brace member (either compression or tension)
- Mode (c): Rupture of the tension brace or its weld, due to an uneven load distribution (also termed "local yielding of the brace")
- Mode (d): Local buckling of the compression brace, due to an uneven load distribution (also termed "local yielding of the brace")
- Mode (e): Shear failure of the chord member in the gap region (for a gapped K joint)
- Mode (f): Chord side wall bearing or local buckling failure, under the compression brace
- Mode (g): Local buckling of the connecting chord face behind the heel of the tension brace.

In addition to these failure modes, section 4.4 gives a detailed description of the typical failure modes found for K and N overlap joints.

Failure in test specimens has also been observed to be a combination of more than one failure mode.

It should be noted here that modes (c) and (d) are generally combined together under the term "local yielding of the brace" failures and are treated identically since the joint resistance in both cases is determined by the effective cross section of the critical brace member, with some brace member walls possibly being only partially effective.

Plastic failure of the chord face (mode (a)) is the most common failure mode for gap joints with small to medium ratios of the brace member widths to the chord width  $\beta$ . For medium width ratios ( $\beta = 0.6$  to  $0.8$ ), this mode generally occurs in combination with tearing in the chord (mode (b)) or the tension brace member (mode (c)) although the latter is only observed in joints with relatively thin-walled brace members.

Mode (d), involving local buckling of the compression brace member, is the most common failure mode for overlap joints.

Shear failure of the entire chord section (mode (e)) is observed in gap joints where the width (or diameter) of brace members is close to that of the chord ( $\beta \approx 1.0$ ), or where  $h_0 < b_0$ .

Local buckling failure (modes (f) and (g)) occurs occasionally in RHS joints with high chord width (or depth) to thickness ratios ( $b_0/t_0$  or  $h_0/t_0$ ). Mode (g) is taken into account by considering the total normal stress in the chord connecting face, via the term  $n$  in the function  $Q_f$  (see table 4.1).

Wardenier (1982) concluded that in selected cases, just one or two governing modes can be used to predict joint resistance.

Similar observations as above can be made for T, Y and X joints. Various formulae exist for joint failure modes analogous to those described above. Some have been derived theoretically, while others are primarily empirical. The general criterion for design is ultimate resistance, but the recommendations presented herein, and their limits of validity, have been set such that a limit state for deformation is not exceeded at specified (service) loads.

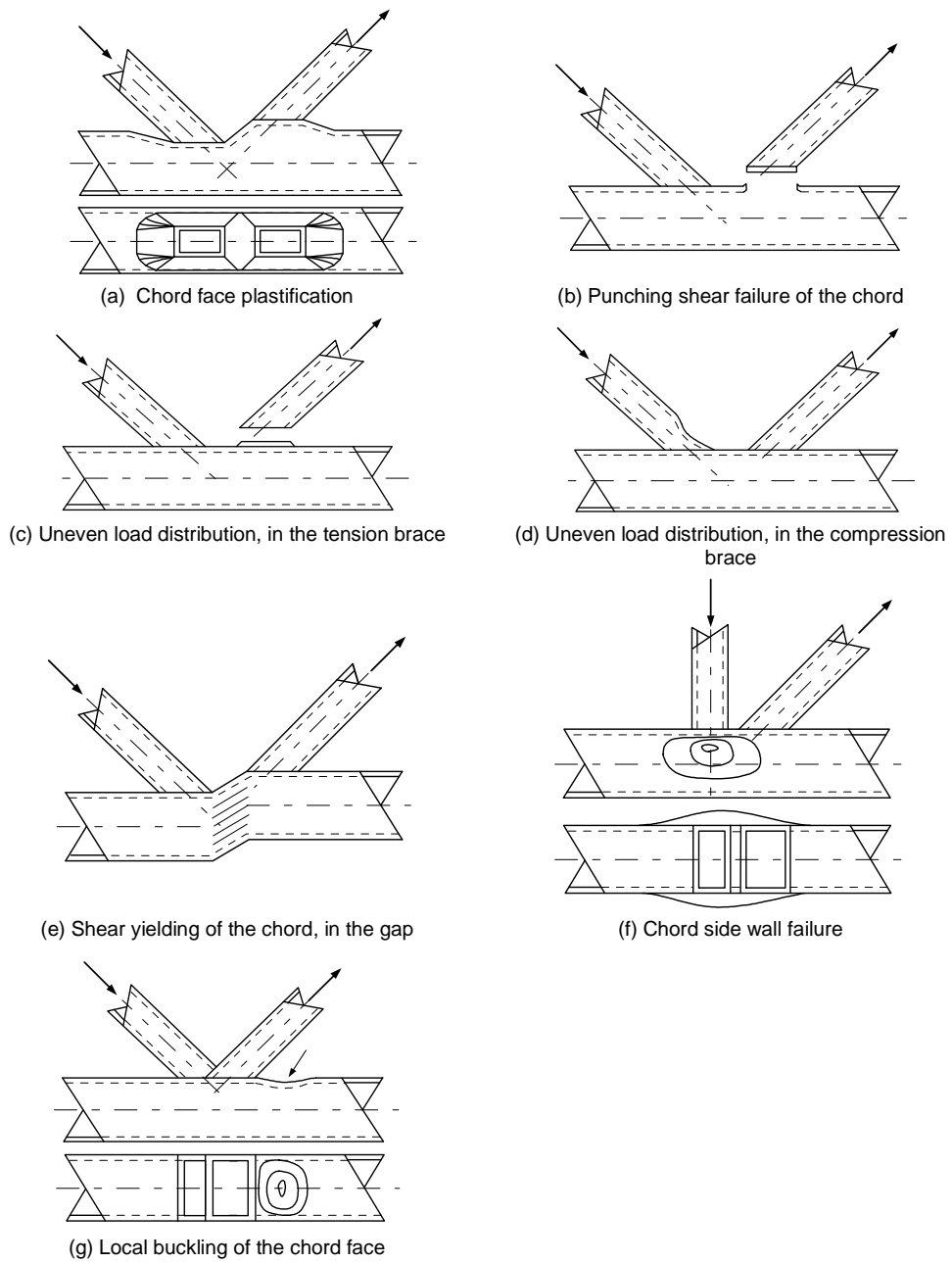


Figure 4.4 – Failure modes for K and N type RHS truss joints

### 4.3 Joint resistance equations for T, Y, X and K gap joints

Recently, Sub-commission XV-E of the International Institute of Welding has reanalysed all joint resistance formulae. Based on rigorous examinations in combination with additional finite element (FE) studies, new design resistance functions have been established (IIW, 2009; Zhao et al., 2008).

For RHS joints, the additional analyses mainly concern the modification of the chord stress functions. The reanalyses also showed that for large tensile chord loads, a reduction of the joint resistance has to be taken into account (Wardenier et al., 2007a, 2007b).

Further, as mentioned in section 1.1, the design equations for RHS K gap joints in the 1<sup>st</sup> edition of this Design Guide (Packer et al., 1992) are based on experiments undertaken in the 1970s (see e.g. Wardenier, 1982), prior to the introduction of a deformation limit of  $0.03b_0$ , and ultimate deformations may have exceeded this limit. Although these design formulae have proved to be satisfactory in practice, a modification is made to limit deformations and to extend the validity range. The new equation for K gap joints gives, compared to the previous equation, a modification in the  $\gamma$  effect and is a reasonable compromise between covering the  $N_{1(3\%)}$  data, extension of the validity range and backup by previous analyses (Packer and Haleem, 1981; Wardenier, 1982).

The new limit states design recommendations for RHS T, Y, X and K gap joints are given in tables 4.1 and 4.2. For distinction from the formulae in the previous edition, which are incorporated in many national and international codes, a slightly different presentation is used. For example, for chord (face) plastification, the general resistance equation is presented as follows:

$$N_i^* = Q_u Q_f \frac{f_{y0} t_0^2}{\sin \theta_i} \quad 4.1$$

The parameter  $Q_u$  gives the influence function for the parameters  $\beta$  and  $\gamma$ , while the parameter  $Q_f$  accounts for the influence of the chord stress on the joint capacity.

In table 4.1 the total (normal) stress ratio,  $n$ , in the chord connecting face, due to axial load plus bending moment, is computed and its effect on joint resistance determined. It should be noted that the most punitive stress effect,  $Q_f$ , in the chord on either side of the joint is to be used.

The  $Q_f$  functions are graphically presented in figures 4.5 to 4.7 for the individual effects of chord axial loading on T, Y, and X joints, chord moment loading on T, Y, and X joints, and chord axial loading on K gap joints. As shown in figures 4.5 and 4.6, the chord bending compression stress effect for T, Y and X joints is the same as that for chord axial compression loading.

The range of validity of the formulae, given in table 4.1, is about the same as in the previous edition of this Design Guide, recorded in table A1a of Appendix A. However, as indicated in section 1.2.1, the validity range has been extended to steels with yield stresses up to  $f_y = 460 \text{ N/mm}^2$  (Liu and Wardenier, 2004). For yield stresses  $f_y > 355 \text{ N/mm}^2$ , the joint resistance should be multiplied by a reduction factor of 0.9.

Fleischer and Puthli (2008) investigated the potential expansion of the validity ranges for the K joint gap size and the chord cross section slenderness, and the potential consequences this might have.

For the other criteria, the formulae are similar to those in the previous edition, although the presentation is slightly different.

The effects of the differences on the joint resistance formulae given in the previous edition of this Design Guide, are presented in Appendix A.

Table 4.2, restricted to square RHS or CHS braces and square RHS chords, is derived from the more general table 4.1 and uses more confined geometric parameters. As a result, T, Y, X and gap K and N joints with square RHS need only be examined for chord face failure, whereas those with rectangular RHS must be considered for nearly all failure modes. This approach has allowed the creation of useful graphical design charts which are later presented for joints between square RHS.

#### 4.3.1 K and N gap joints

From examination of the general limit states design recommendations, summarized in table 4.1 and those in table 4.2 for SHS, a number of observations can be made for K and N joints:

- A common design criterion for all K and N gap joints is plastic failure of the chord face. The constants in the resistance equations are derived from extensive experimental data, and the other terms reflect ultimate strength parameters such as plastic moment capacity of the chord face per unit length  $f_{y0}t_0^2/4$ , brace to chord width ratio  $\beta$ , chord wall slenderness  $2\gamma$ , and the term  $Q_f$  which accounts for the influence of chord normal stress in the connecting face.
- Tables 4.1 and 4.2 show that the resistance of a gap K or N joint with an RHS chord is largely independent of the gap size (no gap size parameter).
- In table 4.1, the check for chord shear in the gap of K and N joints involves dividing the chord cross section into two portions. The first part is the shear area  $A_V$  comprising the side walls plus part of the top flange, shown in figure 4.8, which can carry both shear and axial loads interactively. The contribution of the top flange increases with decreasing gap. The second part involves the remaining area  $A_0-A_V$ , which is effective in carrying axial forces only.

#### 4.3.2 T, Y and X joints

In the same way as an N joint is considered to be a particular case of the general K joint, the T joint is a particular case of the Y joint. The basic difference between the two types is that in T and Y joints, the component of load perpendicular to the chord is resisted by shear and bending in the chord, whereas for K or N joints, the normal component in one brace member is balanced primarily by the same component in the other brace.

The limit states design recommendations for T, Y and X joints are summarized in table 4.1 (for rectangular chords) and table 4.2 (for square chords). Various observations can be made from the tables:

- Resistance equations in tables 4.1 and 4.2 for chord face plastification (with  $\beta \leq 0.85$ ), are based on a yield line mechanism in the RHS chord face. By limiting joint design capacity under factored loads to the joint yield load, one ensures that deformations will be acceptable at specified (service) load levels.
- For full width ( $\beta = 1.0$ ) RHS T, Y and X joints, flexibility does not govern and resistance is based on either the tension capacity or the compression instability of the chord side walls, for tension and compression brace members respectively.
- Compression loaded, full-width RHS X joints are differentiated from T or Y joints as their side walls exhibit greater deformation than T joints. Accordingly, the value of  $f_k$  in the resistance equation used for X joints is reduced by a factor  $0.8\sin\theta_1$  compared to the value adopted for T or Y situations. In both instances, for  $0.85 < \beta < 1.0$ , a linear interpolation between the resistance at  $\beta = 0.85$  (where flexure of the chord face governs) and the resistance at  $\beta = 1.0$  (where chord side wall failure governs) is recommended. Furthermore, if the angle  $\theta_1$  becomes small ( $\cos\theta_1 > h_1/h_0$ ), shear failure of the chord can occur in X joints.
- All RHS T, Y and X joints with high brace width to chord width ratios ( $\beta \geq 0.85$ ) should also be checked for local yielding of the brace and for punching shear of the chord face. For this range of width ratios, the brace member loads are largely carried by their side walls parallel to the chord while the walls transverse to the chords transfer relatively little load. The upper limit of  $\beta = 1 - 1/\gamma$  for checking punching shear is determined by the physical possibility of such a failure, when one considers that the shear has to take place between the outer limits of the brace width and the inner face of the chord wall.

Table 4.1 – Design resistance of uniplanar RHS braces or CHS braces to RHS chord joints

Limit state	Axially loaded uniplanar joints with RHS chord
<b>Chord face plastification</b> (general check for K gap joints; for T, Y and X joints, if $\beta \leq 0.85$ )	$N_i^* = Q_u Q_f \frac{f_{y0} t_0^2}{\sin \theta_i}$
<b>Local yielding of brace</b> (general check)	$N_i^* = f_{yi} t_i \ell_{b,eff.}$
<b>Chord punching shear</b> (for $b_1 \leq b_0 - 2t_0$ )	$N_i^* = \frac{0.58 f_{y0} t_0}{\sin \theta_i} \ell_{p,eff.}$
<b>Chord shear</b> (general check for K gap joints; for X joints, if $\cos \theta_1 > h_1/h_0$ )	$N_i^* = \frac{0.58 f_{y0} A_v}{\sin \theta_i}$  $N_{gap,0} = (A_0 - A_v) f_{y0} + A_v f_{y0} \sqrt{1 - \left( \frac{V_{gap,0}}{V_{pl,0}} \right)^2}$
<b>Chord side wall failure</b> (only for T, Y and X joints with $\beta = 1.0$ )	$N_i^* = \frac{f_k t_0}{\sin \theta_i} b_w Q_f$

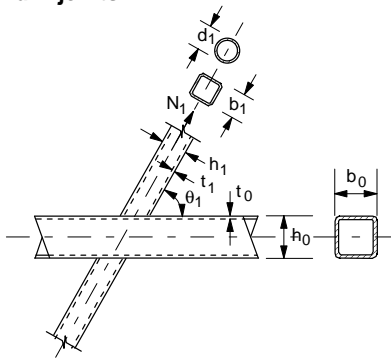
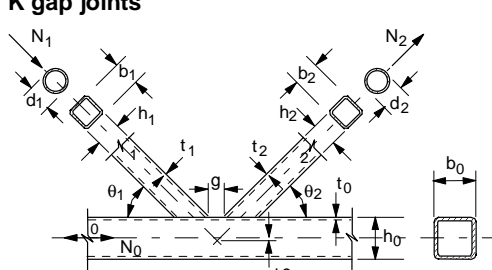
Function $Q_u$	
<p><b>T, Y and X joints</b></p> 	$Q_u = \frac{2\eta}{(1-\beta) \sin \theta_1} + \frac{4}{\sqrt{1-\beta}}$
<p><b>K gap joints</b></p> 	$Q_u = 14 \beta \gamma^{0.3}$

Table 4.1 – Design resistance of uniplanar RHS braces or CHS braces to RHS chord joints (continued)

<b>Function <math>Q_f</math></b>			
	$Q_f = (1 -  n )^{C_1}$ with $n = \frac{N_0}{N_{pl,0}} + \frac{M_0}{M_{pl,0}}$ in connecting face		
	<b>Chord compression stress (<math>n &lt; 0</math>)</b>	<b>Chord tension stress (<math>n \geq 0</math>)</b>	
<b>T, Y and X joints</b>	$C_1 = 0.6 - 0.5\beta$	$C_1 = 0.10$	
<b>K gap joints</b>	$C_1 = 0.5 - 0.5\beta$ but $\geq 0.10$		
$\ell_{b,eff.}$ and $\ell_{p,eff.}$	$\ell_{b,eff.}$	$\ell_{p,eff.}$	
<b>T, Y and X joints</b>	$\ell_{b,eff.} = (2h_1 + 2b_e - 4t_1)$	$\ell_{p,eff.} = \left( \frac{2h_1}{\sin \theta_1} + 2b_{e,p} \right)$	
<b>K gap joints</b>	$\ell_{b,eff.} = (2h_i + b_i + b_e - 4t_i)$	$\ell_{p,eff.} = \left( \frac{2h_i}{\sin \theta_1} + b_i + b_{e,p} \right)$	
	$b_e = \left( \frac{10}{b_0/t_0} \right) \left( \frac{f_{y0} t_0}{f_{yi} t_i} \right) b_i$ but $\leq b_i$	$b_{e,p} = \left( \frac{10}{b_0/t_0} \right) b_i$ but $\leq b_i$	
<b><math>A_v</math> and <math>V_{pl,0}</math></b>	$V_{pl,0} = 0.58f_{y0} A_v$		
<b>T, Y and X joints</b>	$A_v = 2h_0t_0$		
<b>K gap joints</b>	$A_v = 2h_0t_0 + \alpha b_0t_0$		
	<b>RHS braces</b>	<b>CHS braces</b>	
	$\alpha = \sqrt{\frac{1}{1 + (4g^2)/(3t_0^2)}}$	$\alpha = 0$	
<b><math>b_w</math></b>	<b><math>\beta = 1.0</math></b>	<b><math>0.85 &lt; \beta &lt; 1.0</math></b>	
<b>T, Y and X joints</b>	$b_w = \left( \frac{2h_1}{\sin \theta_1} + 10t_0 \right)$	Use linear interpolation between the resistance for chord face plastification at $\beta = 0.85$ and the resistance for chord side wall failure at $\beta = 1.0$ .	
<b>K gap joints</b>	N/A		
<b><math>f_k</math></b>	<b>Brace tension</b>	<b>Brace compression</b>	
	$f_k = f_{y0}$	<b>T and Y joints</b>	<b>X joints</b>
		$f_k = \chi f_{y0}$	$f_k = 0.8\chi f_{y0} \sin \theta_1$
		where $\chi$ = reduction factor for column buckling according to e.g. Eurocode 3 (CEN, 2005a) using the relevant buckling curve and a slenderness $\lambda = 3.46 \left( \frac{h_0}{t_0} - 2 \right) \sqrt{\frac{1}{\sin \theta_1}}$	

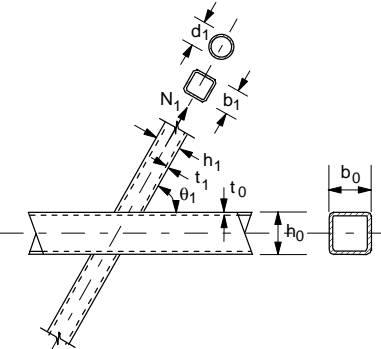
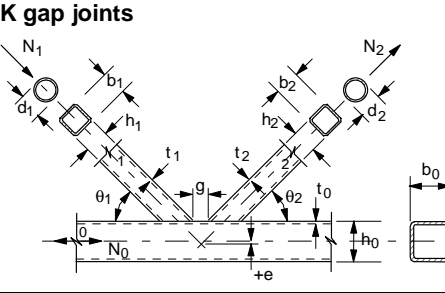
Table 4.1 – Design resistance of uniplanar RHS braces or CHS braces to RHS chord joints (continued)

<b>T, Y, X and K gap joints with CHS brace</b>		For CHS braces, multiply the above resistances by $\pi/4$ (except for chord shear criterion) and replace $b_i$ and $h_i$ by $d_i$ ( $i = 1$ or $2$ )	
<b>Range of validity</b>			
		<b>T, Y or X joints</b>	<b>K gap joints</b>
<b>Brace-to-chord ratio</b>	<b>RHS braces</b>	$b_i/b_0 \geq 0.1 + 0.01b_0/t_0$ but $\geq 0.25$	
	<b>CHS braces</b>	$d_i/b_0 \geq 0.1 + 0.01b_0/t_0$ and $0.25 \leq d_i/b_0 \leq 0.80$	
<b>RHS chord</b>	<b>Compression</b>	class 1 or 2 and $b_0/t_0 \leq 40$ and $h_0/t_0 \leq 40$	
	<b>Tension</b>	$b_0/t_0 \leq 40$ and $h_0/t_0 \leq 40$	
<b>RHS braces</b>	<b>Compression</b>	class 1 or 2 and $b_i/t_i \leq 40$ and $h_i/t_i \leq 40$	
	<b>Tension</b>	$b_i/t_i \leq 40$ and $h_i/t_i \leq 40$	
<b>CHS braces</b>	<b>Compression</b>	class 1 or 2 and $d_i/t_i \leq 50$	
	<b>Tension</b>	$d_i/t_i \leq 50$	
<b>Gap</b>		N/A	$0.5(1-\beta) \leq g/b_0 \leq 1.5(1-\beta)$ (*) and $g \geq t_1 + t_2$
<b>Eccentricity</b>		N/A	$e \leq 0.25h_0$
<b>Aspect ratio</b>		$0.5 \leq h_i/b_i \leq 2.0$	
<b>Brace angle</b>		$\theta_i \geq 30^\circ$	
<b>Yield stress</b>		$f_{yi} \leq f_{y0}$ $f_y \leq 0.8f_u$ $f_y \leq 460 \text{ N/mm}^2$ (**)	

(\*) For  $g/b_0 > 1.5(1-\beta)$ , check the joint also as two separate T or Y joints

(\*\*) For  $f_{y0} > 355 \text{ N/mm}^2$ , see section 1.2.1

Table 4.2 – Design resistance of uniplanar SHS or CHS braces to SHS chord joints

<b>Limit state</b>		<b>Axially loaded uniplanar joints with SHS chord</b>	
<b>Chord face plastification</b>		$N_i^* = Q_u Q_f \frac{f_{y0} t_0^2}{\sin \theta_i}$	
<b>Function <math>Q_u</math></b>			
<b>T, Y and X joints</b> 		$Q_u = \frac{2\eta}{(1-\beta) \sin \theta_1} + \frac{4}{\sqrt{1-\beta}}$	
<b>K gap joints</b> 		$Q_u = 14 \beta \gamma^{0.3}$	
<b>Function <math>Q_f</math></b>		Same as in table 4.1	
<b>T, Y, X and K gap joints with CHS brace</b>		For CHS braces, multiply the above resistances by $\pi/4$ and replace $b_i$ by $d_i$ ( $i = 1$ or $2$ )	
<b>Range of validity</b>			
<b>General</b>	Same as in table 4.1 with additional limits given below		
<b>SHS braces</b>	<b>T, Y and X joints</b>	$b_1/b_0 \leq 0.85$	
	<b>K gap joints</b>	$0.6 \leq (b_1 + b_2)/(2b_1) \leq 1.3$	$b_0/t_0 \geq 15$
<b>CHS braces</b>	<b>K gap joints</b>	$0.6 \leq (d_1 + d_2)/(2d_1) \leq 1.3$	$b_0/t_0 \geq 15$

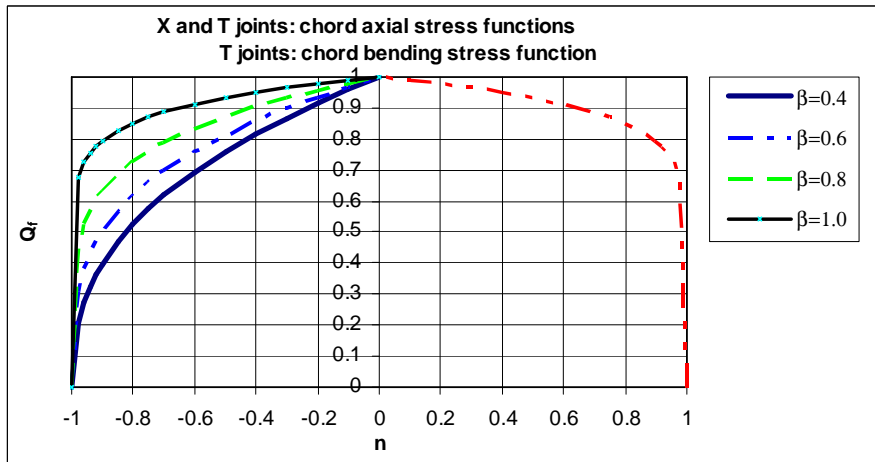


Figure 4.5 – Chord axial stress functions  $Q_r$  for T and X joints and chord bending stress function  $Q_r$  for T joints

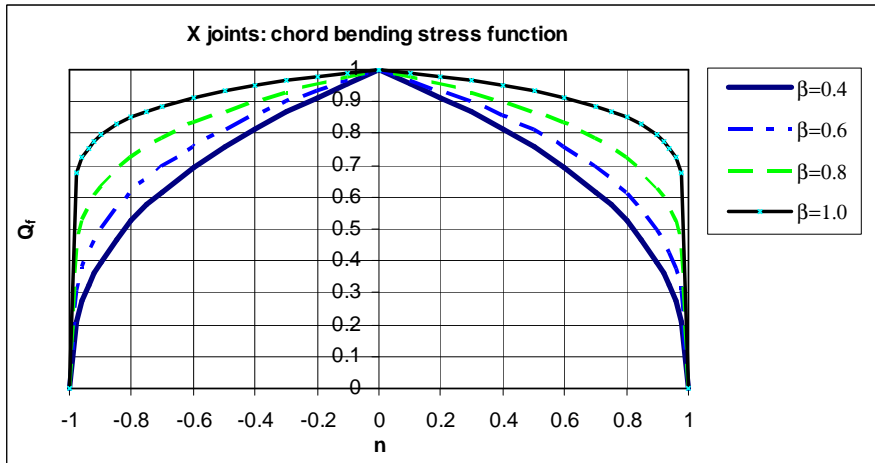


Figure 4.6 – Chord bending stress function  $Q_r$  for X joints

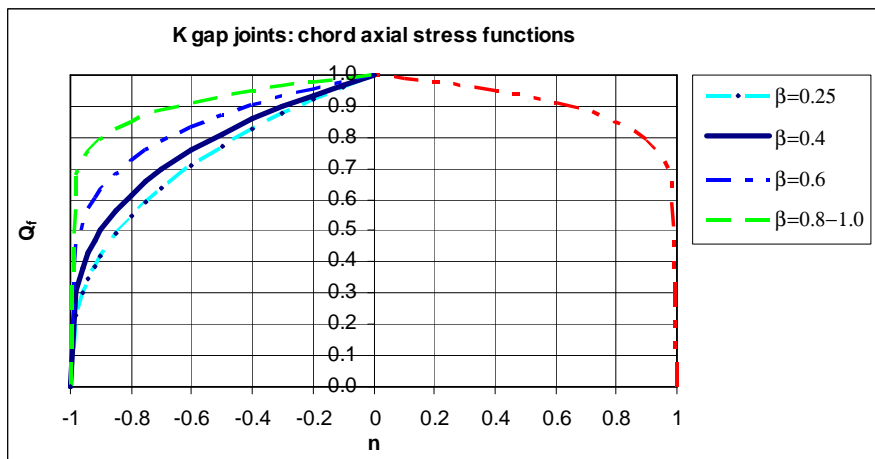


Figure 4.7 – Chord axial stress function  $Q_r$  for K gap joints

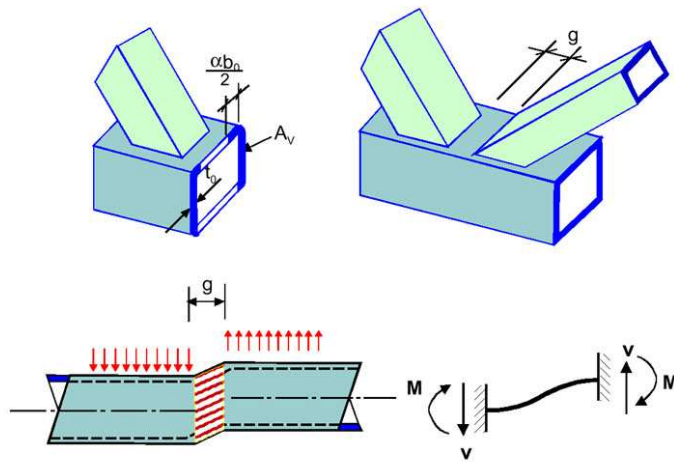


Figure 4.8 – Shear area  $A_v$  of the chord in the gap region of an RHS K or N joint

#### 4.4 K and N overlap joints

For overlap joints the same approach is adopted for all types of overlap joints, regardless of whether CHS or RHS braces are used in combination with a CHS, RHS or open section chord (Chen et al., 2005; Liu et al., 2005; Qian et al., 2007; Wardenier, 2007). Only the effective width factors depend on the type of section. The resistance of overlap joints between hollow sections with  $25\% \leq O_v \leq 100\%$  overlap is based on the following criteria:

- (1) Local yielding of the overlapping brace.
- (2) Local chord member yielding at the joint location, based on interaction between axial load and bending moment.
- (3) Shear of the connection between the brace(s) and the chord.

Figure 4.9 shows the overlap joint configuration with the cross sections to be examined for these criteria. For K and N overlap joints, the subscript  $i$  is used to denote the overlapping brace member, while the subscript  $j$  refers to the overlapped brace member.

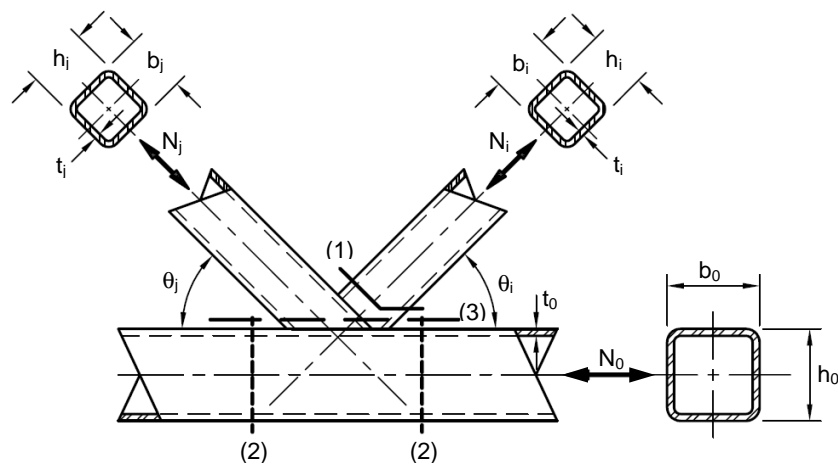


Figure 4.9 – Overlap joint configuration with cross sections to be checked

In the previous edition of this Design Guide (Packer et al., 1992), only the criterion for local yielding of the overlapping brace was given, whereas the chord member had to be checked for the combination of chord axial force and bending moment due to eccentricity. Since this last check was sometimes overlooked by the designers, it is now explicitly included in the design checks.

Furthermore, in the case of large overlaps or for  $h_i < b_i$  and/or  $h_j < b_j$ , the shear force needs to be limited in order to avoid an excessively large concentrated shear at the brace-to-chord face connection. Although no fracture has been observed in previous tests, but only shear deformation, it was found that the criterion for this failure mode can be based on the ultimate shear capacity of the effective area of the connected braces.

Table 4.3 presents the resistances for K overlap joints starting with 25% overlap, which is the minimum value to ensure overlap behaviour. The resistance increases linearly with overlap from 25% to 50%, is constant from 50% up to 100% and reaches a higher level at 100%. Figure 4.10 illustrates the physical interpretation of the expressions for the effective width given in table 4.1 for gap joints and in table 4.3 for overlap joints, whereas figure 4.11 shows this for the brace shear criterion.

Local yielding of the overlapping brace (criterion 1) should always be verified, although shear between the braces and the chord (criterion 3) may become critical for larger overlaps, i.e. larger than 60% or 80%, depending on whether or not the hidden toe location of the overlapped brace is welded to the chord. The check for local chord member yielding (criterion 2) is, in principle, a member check and may become critical for larger overlaps and/or larger  $\beta$  ratios.

For 100% overlap joints, similar criteria have to be verified. However, for such joints, shear of the overlapping brace or chord member yielding will generally be the governing criterion (Chen et al., 2005). Although an overlap can be assumed to be 100%, in general, the overlap will be slightly larger to allow proper welding of the overlapping brace to the overlapped brace.

Joints with overlaps between 0% and 25% should be avoided because for such joints, the stiffness of the connection between the overlapping brace and the overlapped brace is much larger than that of the overlapping brace to chord connection, which may lead to premature cracking and lower capacities (Wardenier, 2007).

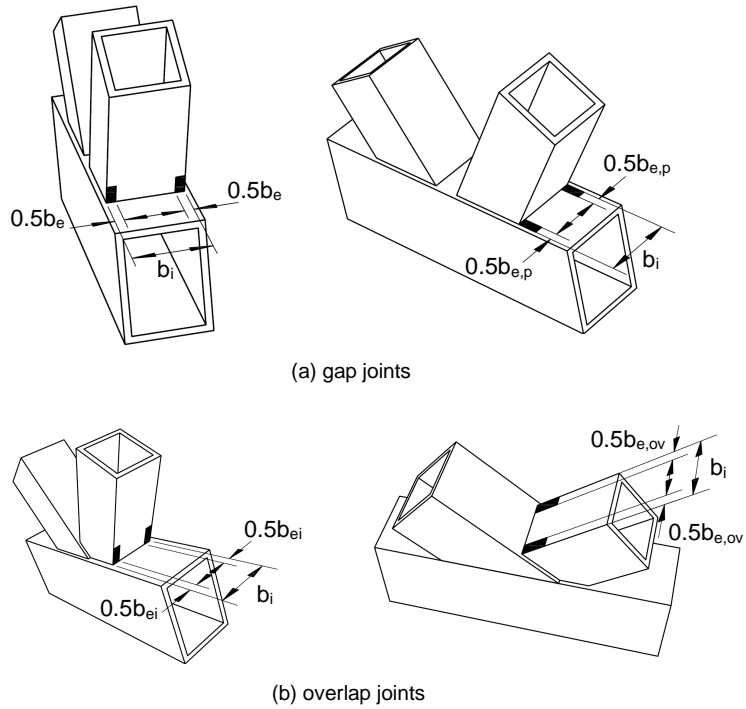


Figure 4.10 – Physical interpretation of the effective width terms for gap and overlap joints

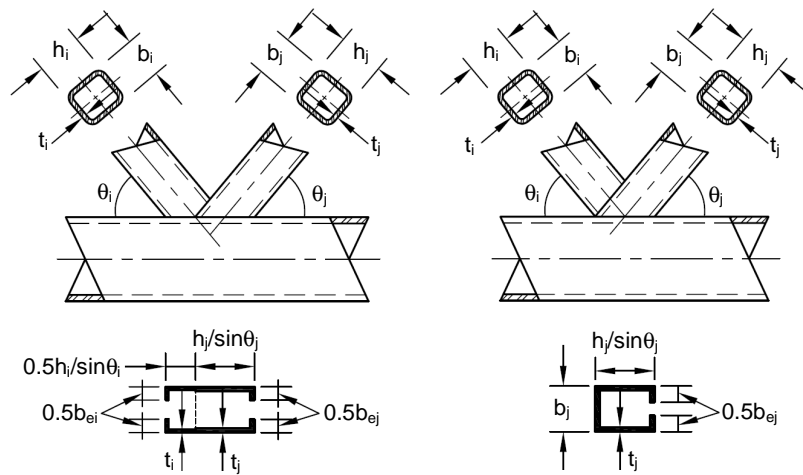


Figure 4.11 – Physical interpretation of the effective width terms for brace shear in overlap joints

Table 4.3 – Design resistance of uniplanar overlap joints with RHS braces or CHS braces to RHS chord

Limit state	Axially loaded overlap joints
Local yielding of overlapping brace	$N_i^* = f_{yi} t_i \ell_{b,eff.}$
Local chord member yielding	$\frac{N_0}{N_{pl,0}} + \frac{M_0}{M_{pl,0}} \leq 1.0$
Brace shear (*) (for $Ov_{limit} < Ov \leq 100\%$ )	$N_i \cos \theta_i + N_j \cos \theta_j \leq N_s^*$ (see table next page)

(\*)  $Ov_{limit} = 60\%$  if hidden seam of the overlapped brace is not welded  
 $Ov_{limit} = 80\%$  if hidden seam of the overlapped brace is welded

$\ell_{b,eff.}$		
	RHS braces	CHS braces
$25\% \leq Ov < 50\%$	$\ell_{b,eff.} = \left(\frac{Ov}{50}\right)2h_i + b_{ei} + b_{e,ov} - 4t_i$	$\ell_{b,eff.} = \frac{\pi}{4}(2d_i + d_{ei} + d_{e,ov} - 4t_i)$
$50\% \leq Ov < 100\%$	$\ell_{b,eff.} = 2h_i + b_{ei} + b_{e,ov} - 4t_i$	
$Ov = 100\%$	$\ell_{b,eff.} = 2h_i + b_i + b_{e,ov} - 4t_i$	$\ell_{b,eff.} = \frac{\pi}{4}(2d_i + 2d_{e,ov} - 4t_i)$

<b>General note</b>	The efficiency (i.e. design resistance divided by the yield load) of the overlapped brace j shall not exceed that of the overlapping brace i
---------------------	--

Range of validity			
<b>General</b>	$b_i/b_0$ and $b_j/b_0 \geq 0.25$	$b_i/b_j \geq 0.75$	$t_i$ and $t_j \leq t_0$
	$d_i/b_0$ and $d_j/b_0 \geq 0.25$	$d_i/d_j \geq 0.75$	$t_i \leq t_j$
	$\theta_i$ and $\theta_j \geq 30^\circ$	$Ov \geq 25\%$	$f_{yi}$ and $f_{yj} \leq f_{y0}$ $f_y \leq 0.8f_u$ $f_y \leq 460 \text{ N/mm}^2$ (**)
<b>RHS chord</b>	<b>Compression</b>	class 1 or 2 and $b_0/t_0 \leq 40$ and $h_0/t_0 \leq 40$	
	<b>Tension</b>	$b_0/t_0 \leq 40$ and $h_0/t_0 \leq 40$	
	<b>Aspect ratio</b>	$0.5 \leq h_0/b_0 \leq 2.0$	
<b>RHS braces</b>	<b>Compression</b>	class 1 or 2 and $b_1/t_1 \leq 40$ and $h_1/t_1 \leq 40$	
	<b>Tension</b>	$b_2/t_2 \leq 40$ and $h_2/t_2 \leq 40$	
	<b>Aspect ratio</b>	$0.5 \leq h_i/b_i \leq 2.0$ and $0.5 \leq h_j/b_j \leq 2.0$	
<b>CHS braces</b>	<b>Compression</b>	class 1 or 2 and $d_1/t_1 \leq 50$	
	<b>Tension</b>	$d_2/t_2 \leq 50$	

(\*\*) For  $f_{y0} > 355 \text{ N/mm}^2$ , see section 1.2.1

Table 4.3 – Design resistance of uniplanar overlap joints with RHS braces or CHS braces to RHS chord  
(continued)

<b><math>N_s^*</math> for brace shear criterion (only to be checked for <math>Ov_{limit} &lt; Ov \leq 100\%</math>) (***)</b>	
<b>RHS braces</b> $Ov_{limit} < Ov < 100\%$	$N_s^* = 0.58f_{ui} \frac{\left[ \left( \frac{100 - Ov}{100} \right) 2h_i + b_{ei} \right] t_i}{\sin \theta_i} + 0.58f_{uj} \frac{(2h_j + c_s b_{ej}) t_j}{\sin \theta_j}$
<b>RHS braces</b> $Ov = 100\%$	$N_s^* = 0.58f_{uj} \frac{(2h_j + b_j + b_{ej}) t_j}{\sin \theta_j}$
<b>CHS braces</b> $Ov_{limit} < Ov < 100\%$	$N_s^* = \frac{\pi}{4} \left[ 0.58f_{ui} \frac{\left[ \left( \frac{100 - Ov}{100} \right) 2d_i + d_{ei} \right] t_i}{\sin \theta_i} + 0.58f_{uj} \frac{(2d_j + c_s d_{ej}) t_j}{\sin \theta_j} \right]$
<b>CHS braces</b> $Ov = 100\%$	$N_s^* = 0.58f_{uj} \frac{\pi (3d_j + d_{ej}) t_j}{4 \sin \theta_j}$

(\*\*\*)  $Ov_{limit} = 60\%$  and  $c_s = 1$  if hidden seam of overlapped brace is not welded  
 $Ov_{limit} = 80\%$  and  $c_s = 2$  if hidden seam of overlapped brace is welded  
 In case of overlap joints with  $h_i < b_i$  and/or  $h_j < b_j$ , the brace shear criterion shall always be checked.

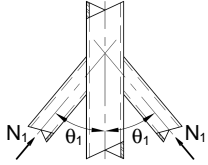
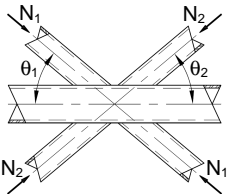
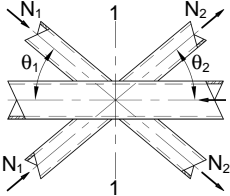
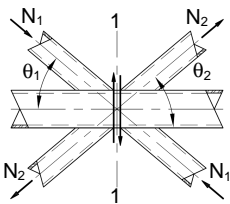
<b>Factors for RHS or CHS braces to RHS chords</b>	
<b>RHS braces</b>	<b>CHS braces</b>
<b>Overlapping RHS brace to RHS chord:</b> $b_{ei} = \left( \frac{10}{b_0/t_0} \right) \left( \frac{f_{y0} t_0}{f_{yi} t_i} \right) b_i \text{ but } \leq b_i$	<b>Overlapping CHS brace to RHS chord:</b> $d_{ei} = \left( \frac{10}{b_0/t_0} \right) \left( \frac{f_{y0} t_0}{f_{yi} t_i} \right) d_i \text{ but } \leq d_i$
<b>Overlapped RHS brace to RHS chord:</b> $b_{ej} = \left( \frac{10}{b_0/t_0} \right) \left( \frac{f_{y0} t_0}{f_{yj} t_j} \right) b_j \text{ but } \leq b_j$	<b>Overlapped CHS brace to RHS chord:</b> $d_{ej} = \left( \frac{10}{b_0/t_0} \right) \left( \frac{f_{y0} t_0}{f_{yj} t_j} \right) d_j \text{ but } \leq d_j$
<b>Overlapping RHS brace to overlapped RHS brace:</b> $b_{e,ov} = \left( \frac{10}{b_j/t_j} \right) \left( \frac{f_{yj} t_j}{f_{yi} t_i} \right) b_i \text{ but } \leq b_i$	<b>Overlapping CHS brace to overlapped CHS brace:</b> $d_{e,ov} = \left( \frac{12}{d_i/t_j} \right) \left( \frac{f_{yj} t_j}{f_{yi} t_i} \right) d_i \text{ but } \leq d_i$

#### 4.5 Special types of joints

In tubular structures, various joint configurations exist which have not been discussed in the previous chapters. However, the resistance of several types of joints can be directly related to the basic types presented in tables 4.1 and 4.2.

Table 4.4 shows some special types of RHS uniplanar joints with braces directly welded to the chord.

Table 4.4 – Special types of uniplanar joints

Type of joint	Relationship to the formulae of tables 4.1 and 4.2
	$N_1 \leq N_1^*$ <p>with <math>N_1^*</math> from X joint</p>
	$N_1 \sin \theta_1 + N_2 \sin \theta_2 \leq N_i^* \sin \theta_i$ <p>with <math>N_i^*</math> (<math>i = 1</math> or <math>2</math>) from X joint</p> <p>where <math>N_i^* \sin \theta_i</math> is the larger of <math>N_1^* \sin \theta_1</math> and <math>N_2^* \sin \theta_2</math></p>
	$N_i \leq N_i^* \quad (i = 1 \text{ or } 2)$ <p>with <math>N_i^*</math> (<math>i = 1</math> or <math>2</math>) from K joint, but with the actual chord force</p>
	$N_i \leq N_i^* \quad (i = 1 \text{ or } 2)$ <p>with <math>N_i^*</math> (<math>i = 1</math> or <math>2</math>) from K joint</p> <p>Note: Check cross section 1-1 for shear failure in the gap:</p> $V_{\text{gap},0} \leq V_{\text{pl},0} = 0.58 f_{y0} A_v$ $N_{\text{gap},0} \leq N_{\text{gap},0}^* = (A_0 - A_v) f_{y0} + A_v f_{y0} \sqrt{1 - \left( \frac{V_{\text{gap},0}}{V_{\text{pl},0}} \right)^2}$

#### 4.6 Graphical design charts with examples

The joint design strength for joints *with square hollow section members*, as given in table 4.2, may be expressed in terms of the efficiency of the connected braces; i.e. the joint design resistance for axially loaded joints  $N_i^*$  may be divided by the yield load  $A_i f_{yi}$  of the connected brace. This results in an efficiency formula of the following type:

$$\frac{N_i^*}{A_i f_{yi}} = C_e \frac{f_{y0} t_0}{f_{yi} t_i} \frac{Q_f}{\sin \theta_i} \quad 4.2$$

For each type of joint, the efficiency parameter  $C_e$  is given in the diagrams in tables 4.5 to 4.9. In general,  $C_e$  is a function of the width ratio  $\beta$  and the chord width-to-thickness ratio  $2\gamma$ .

*In the case of  $b_1 \neq b_2$  for K joints, equation 4.2 has to be multiplied by  $\frac{b_1 + b_2}{2b_i}$ , where  $b_i$  is the width of the brace considered.*

The value of the parameter  $C_e$  in equation 4.2 gives the joint efficiency for the brace of a joint with a chord stress effect  $Q_f = 1.0$ , a brace angle  $\theta_i = 90^\circ$  and the same wall thickness and design yield stress for chord and brace. Except for overlapped K joints, the efficiencies given in the charts are termed  $C_T$ ,  $C_X$ , or  $C_K$  depending on the type of joint. Hence, these latter efficiencies need to be multiplied by the following three factors (see equation 4.2) to obtain the final joint efficiency in each case:

- The first factor, correcting for differing strengths between the chord and the brace member, is  $(f_{y0} t_0)/(f_{yi} t_i)$ . In general, this term is reduced to  $t_0/t_i$ , because the same grade of steel would normally be used throughout.
- The second factor, adjusting for the angle between the brace member and the chord, is  $1/\sin \theta_i$  for square RHS T, Y, X and gap K joints. One should note that such an angle function is not considered for square RHS overlap joints because the efficiencies of these joints are based on the criterion for local yielding of the overlapping brace.
- The third factor, correcting for the influence of chord longitudinal stresses on the joint efficiency, is  $Q_f$ . For RHS,  $Q_f$  is defined in table 4.1 and plotted in figures 4.5 to 4.7. This function  $Q_f$  is not included for overlap joints because for these joints, the strength function is based on the criterion for local yielding of the overlapping brace.

Simplifying assumptions and narrower validity parameters were sometimes necessary to simplify the presentation of the charts. Still, use of the design charts for T and X joints with  $\theta_1 = 90^\circ$  and K joints in general, produces results close to the actual formulae. For Y and X joints with  $\beta \leq 0.85$ , the results obtained with the design charts can be very conservative for  $\theta_1 < 90^\circ$ . On the other hand, for Y and X joints with  $\beta > 0.85$  subjected to brace compression, the design charts may give unconservative predictions for  $\theta_1 < 90^\circ$ .

*Furthermore, it should be considered that the design charts have been based on a brace cross sectional area of  $0.96(4b_1t_1)$ . Hence, for sections with relatively large corner radii and/or stocky members, the graphs may give too optimistic results. In those cases it is recommended to reduce the calculated efficiency by about 10%.*

From the efficiency equation, it is evident that the yield stress and thickness ratio between the chord and brace is extremely important for an efficient material use of the brace. Furthermore, decreasing the angle  $\theta_i$  increases the efficiency.

The efficiency formula shows directly that the following measures are favourable for the joint efficiency:

- brace wall thickness as small as possible ( $t_i < t_0$ ), but such that the limits for local buckling are satisfied
- higher strength steel for chords than for braces ( $f_{y0} > f_{yi}$ )
- angle  $\theta_i \ll 90^\circ$ ; hence, prefer K joints to N joints

Three charts are presented for T, Y and X joints (tables 4.5 to 4.7). The first graph applies to each of the three joint types when the braces are loaded in tension; the second applies to T and Y joints when the braces are loaded in compression; the third to X joints with the braces loaded in compression.

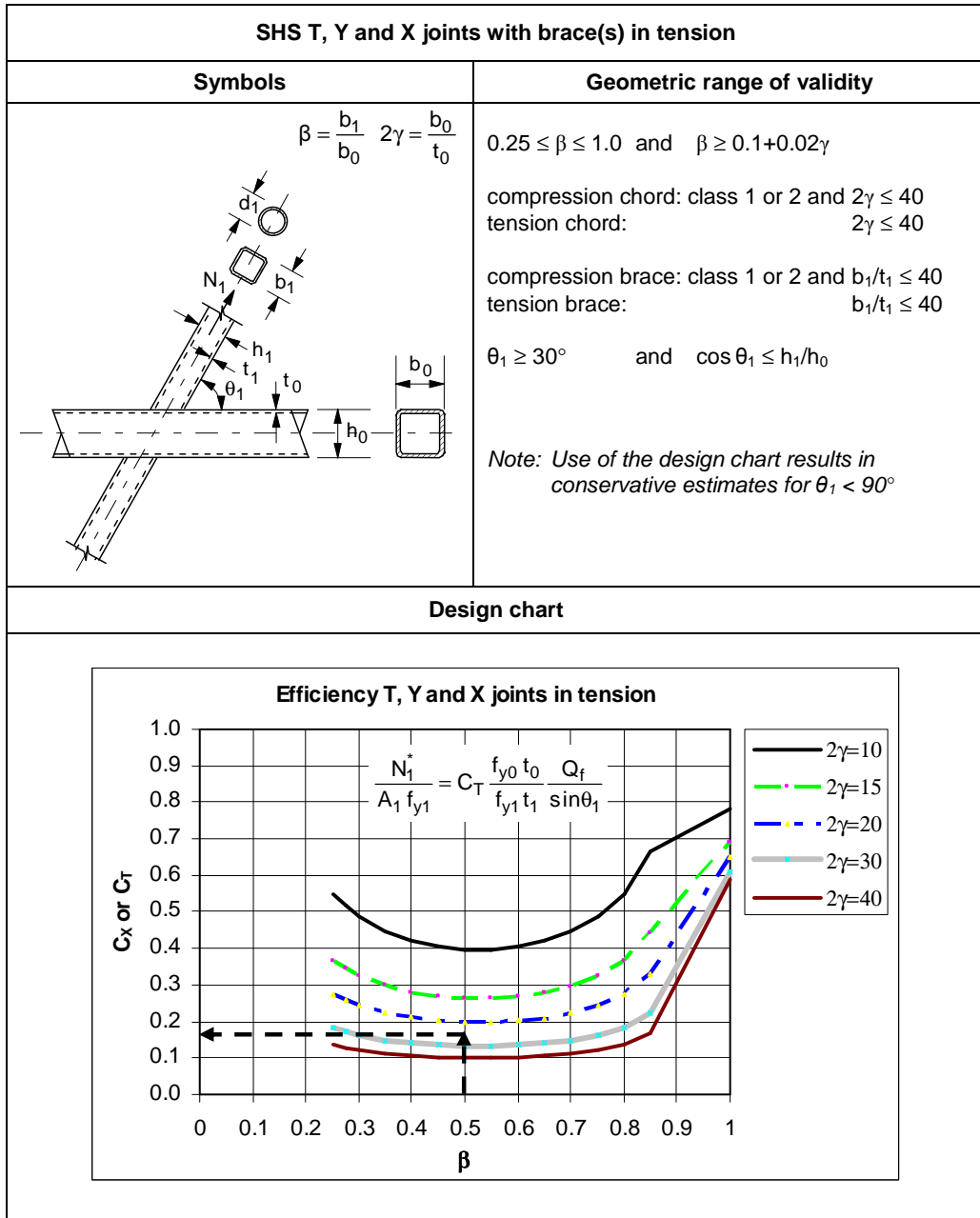
In addition to the failure mode listed in table 4.2 (chord face plastification for joints with  $\beta \leq 0.85$ ), the first three design charts also include chord side wall failure (for joints with  $\beta > 0.85$ ). The three charts are identical for  $\beta$  values up to 0.85. However, when  $\beta$  exceeds 0.85, the behaviour of the chord side walls is different for the three situations, resulting in three separate charts. The graphs further show linear interpolations between the calculated resistances at  $\beta = 0.85$  and  $\beta = 1.0$ .

For gap K and N joints, the efficiency chart is given in table 4.8, which is slightly different from the graphs used for T, Y and X joints. For gap K joints, the efficiency  $C_K$  is plotted as a function of  $2\gamma$  instead of  $\beta$ . Furthermore, for K gap joints, the correction with  $\frac{b_1 + b_2}{2b_i}$  for  $b_1 \neq b_2$  should be included, where  $b_i$  represents the width of the brace considered.

Observation of the design resistances for joints with CHS braces shows that the efficiency for these joints can be directly obtained from the design graphs for square braces by using  $d_i$  instead of  $b_i$ . The design resistance of joints with CHS braces is  $\pi/4$  times that of RHS braces, which is about the ratio between the cross sectional areas of the braces for  $d_i = b_i$  and the same  $t_i$ .

The range of overlap for SHS K and N joints, given in table 4.9, is from 50% to  $OV_{limit}$  rather than for  $OV \geq 25\%$  as presented in table 4.3. This avoids the more complex lower range where the resistance varies with the amount of overlap. However, above  $OV_{limit}$ , which is 60 or 80%, the brace shear criterion has to be checked separately.

Table 4.5 – Efficiency design chart for SHS T, Y and X joints with brace(s) in tension

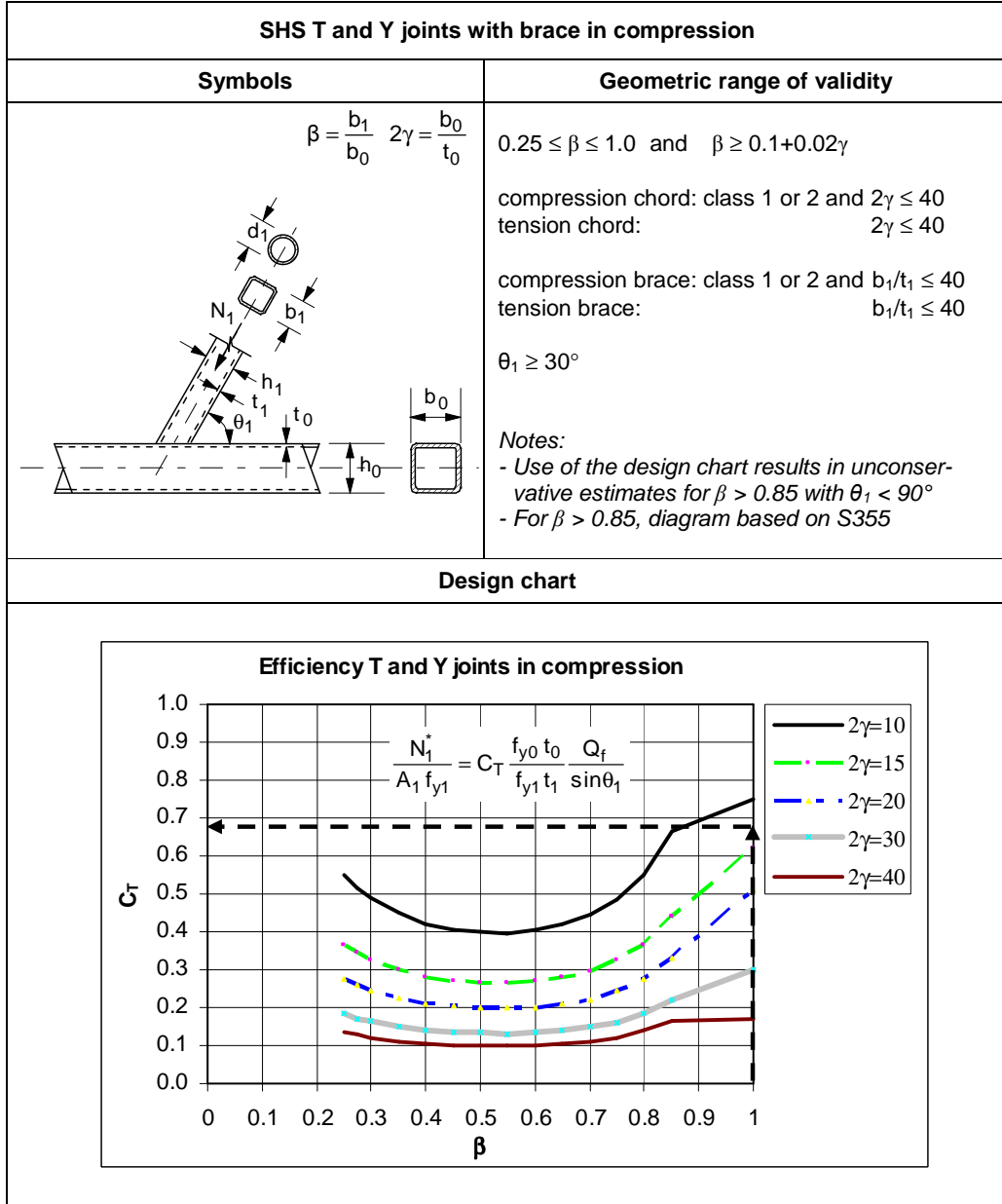


<b>Calculation example for SHS T, Y and X joints with brace(s) in tension</b> with sections according to EN 10210-2 (CEN, 2006a)				
chord: 200 x 200 x 8	$A_0 = 6080 \text{ mm}^2$	$b_0/t_0 = 25$	$\theta_1 = 45^\circ$	$\sin \theta_1 = 0.707$
brace: 100 x 100 x 5	$A_1 = 1870 \text{ mm}^2$	$b_1/t_1 = 20$		
S355	$f_{y0} = f_{y1} = 355 \text{ N/mm}^2$	$\beta = \frac{b_1}{b_0} = \frac{100}{200} = 0.5$		<b><math>C_x = 0.17</math></b>
Assume for this example $n = -0.48$ :		$Q_f = 0.80$ (see figure 4.5)		
$\frac{N_1^*}{A_1 f_{y1}} = 0.17 \times \frac{8}{5} \times \frac{0.8}{0.707} = 0.31$		or	$N_1^* = 0.31 \times 1870 \times 0.355 = 206 \text{ kN}$	



Federation Square, Melbourne, Australia

Table 4.6 – Efficiency design chart for SHS T and Y joints with brace in compression



**Calculation example for SHS T and Y joints with brace in compression**  
with sections according to EN 10210-2 (CEN, 2006a)

chord: 100 x 100 x 8	A <sub>0</sub> = 2880 mm <sup>2</sup>	b <sub>0</sub> /t <sub>0</sub> = 12.5	
brace: 100 x 100 x 5	A <sub>1</sub> = 1870 mm <sup>2</sup>	b <sub>1</sub> /t <sub>1</sub> = 20	θ <sub>1</sub> = 90°     sin θ <sub>1</sub> = 1.0

S355	f <sub>y0</sub> = f <sub>y1</sub> = 355 N/mm	β = $\frac{b_1}{b_0} = \frac{100}{100} = 1.0$	<b>C<sub>T</sub> = 0.68</b>
------	--	---	-----------------------------

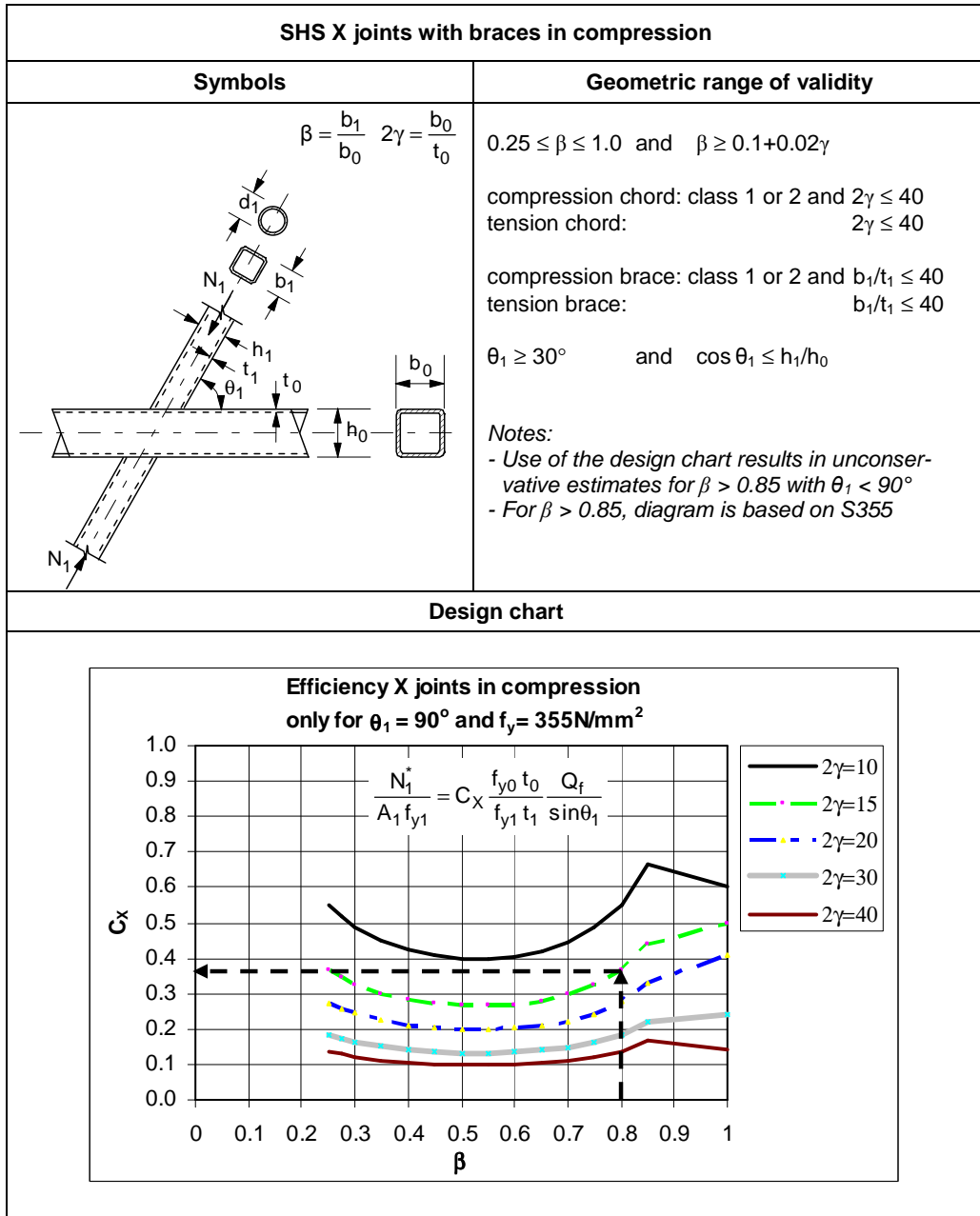
Assume for this example n = -0.60 in bending:     Q<sub>f</sub> = 0.91 (see figure 4.5)

$\frac{N_1^*}{A_1 f_{y1}} = 0.68 \times \frac{8}{5} \times 0.91 = 0.99$	or	$N_1^* = 0.99 \times 1870 \times 0.355 = 657 \text{ kN}$
---	----	--



RHS lattice girder

Table 4.7 – Efficiency design chart for SHS X joints with braces in compression



**Calculation example for SHS X joints with braces in compression**  
with sections according to EN 10210-2 (CEN, 2006a)

chord: 150 x 150 x 10     $A_0 = 5490 \text{ mm}^2$      $b_0/t_0 = 15$   
brace: 120 x 120 x 5     $A_1 = 2270 \text{ mm}^2$      $b_1/t_1 = 24$      $\theta_1 = 90^\circ$      $\sin \theta_1 = 1.0$

S355     $f_{y0} = f_{y1} = 355 \text{ N/mm}^2$      $\beta = \frac{b_1}{b_0} = \frac{120}{150} = 0.8$      **$C_x = 0.37$**

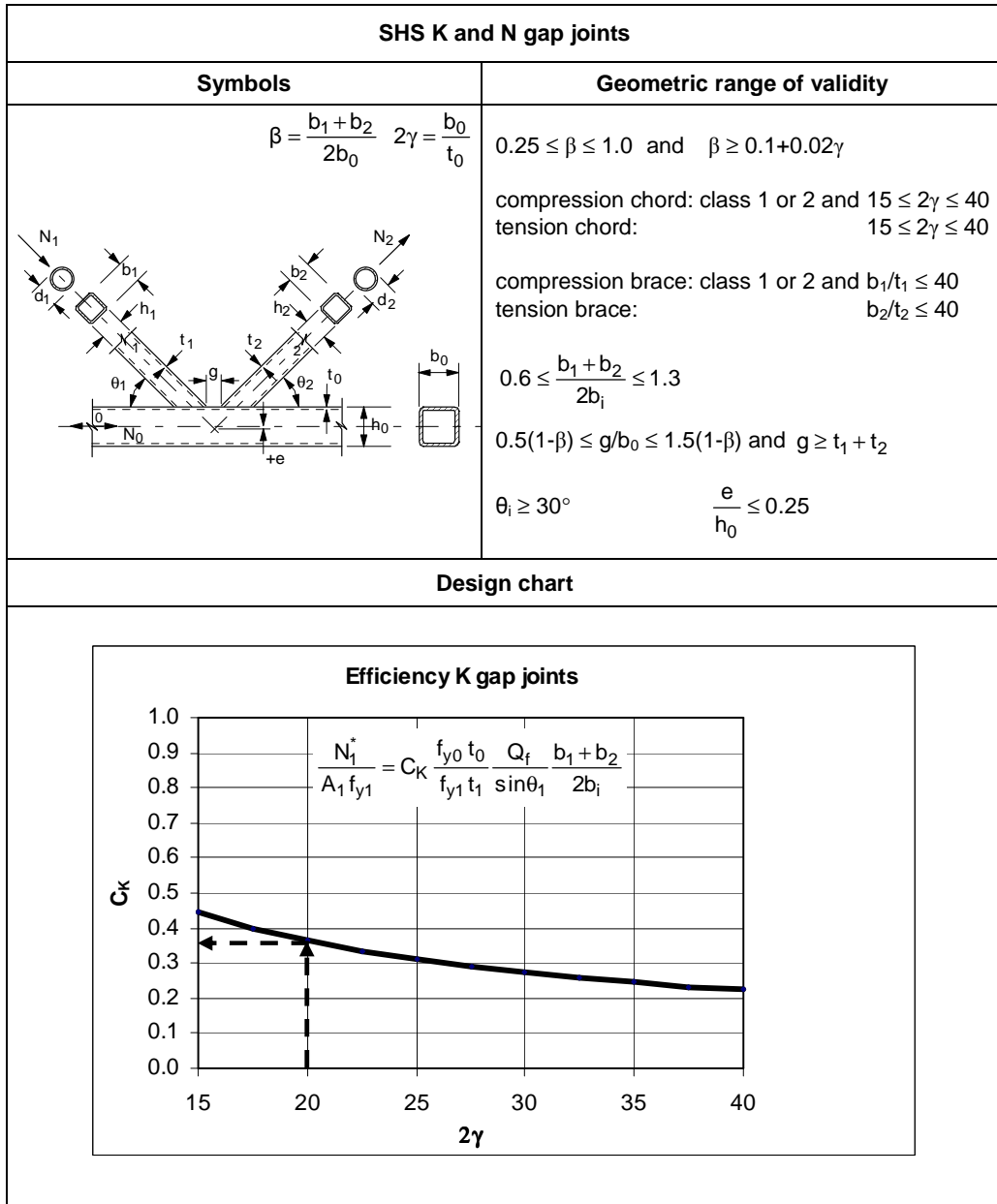
Assume for this example  $n = +0.60$  in tension:     $Q_f = 0.91$  (see figure 4.5)

$$\frac{N_1^*}{A_1 f_{y1}} = 0.37 \times \frac{10}{5} \times 0.91 = 0.67 \quad \text{or} \quad N_1^* = 0.67 \times 2270 \times 0.355 = 540 \text{ kN}$$



Pedestrian "Pony Truss" bridge

Table 4.8 – Efficiency design charts for SHS K and N gap joints



**Calculation example for SHS K and N gap joints**  
with sections according to EN 10210-2 (CEN, 2006a)

chord : 200 x 200 x 10	$A_0 = 7490 \text{ mm}^2$	$b_0/t_0 = 20$	$f_{y0} = f_{y1} = f_{y2} = 355 \text{ N/mm}^2$
brace 1: 140 x 140 x 5	$A_1 = 2670 \text{ mm}^2$	$b_1/t_1 = 28$	$e = 0 \text{ mm}$
brace 2: 120 x 120 x 5	$A_2 = 2270 \text{ mm}^2$	$b_2/t_2 = 24$	$g = 36 \text{ mm}$

$\theta_1 = \theta_2 = 40^\circ$                        $\sin \theta_1 = \sin \theta_2 = 0.643$

$$2\gamma = \frac{b_0}{t_0} = \frac{200}{10} = 20 \qquad \beta = \frac{b_1 + b_2}{2b_0} = \frac{140 + 120}{2 \times 200} = 0.65$$

Assume  $n = -0.8$ :                       $Q_f = 0.75$  (see figure 4.7)

Thus:  **$C_K = 0.36$**                       with  $\frac{b_1 + b_2}{2b_i} = 0.93$  for brace 1, and 1.08 for brace 2

$$\frac{N_1^*}{A_1 f_{y1}} = 0.36 \times \frac{10}{5} \times \frac{0.75}{0.643} \times 0.93 = 0.78 \qquad \frac{N_2^*}{A_2 f_{y2}} = 0.36 \times \frac{10}{5} \times \frac{0.75}{0.643} \times 1.08 = 0.91$$

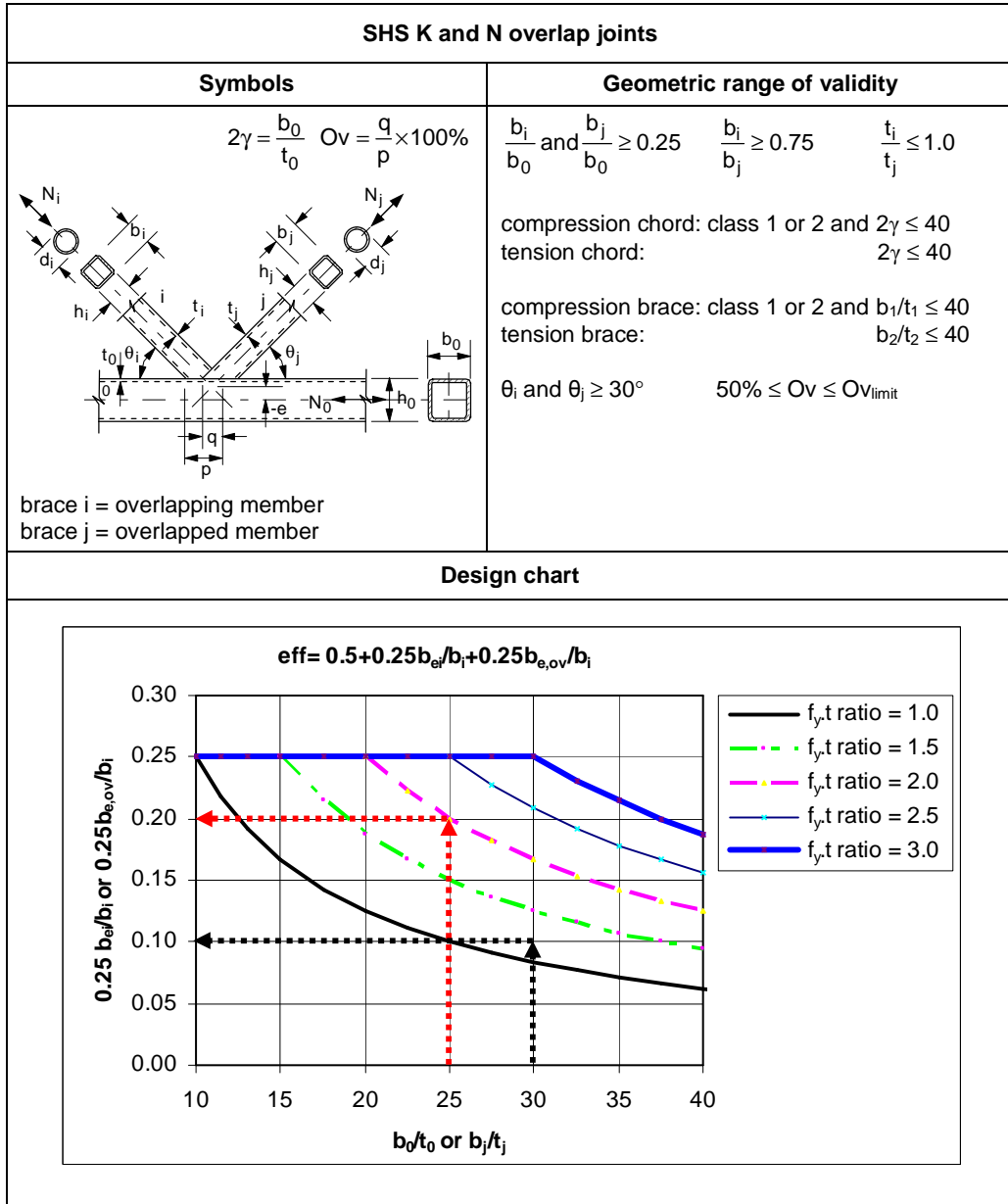
$$N_1^* = 0.78 \times 2670 \times 0.355 = 739 \text{ kN}$$

$$N_2^* = 0.91 \times 2270 \times 0.355 = 733 \text{ kN}$$



Rack structure, for automated retrieval of pallets

Table 4.9 – Efficiency design chart for SHS K and N overlap joints (for  $50\% \leq Ov \leq Ov_{limit} = 60\%$  or  $80\%$ )



**Calculation example for SHS K and N overlap joints**  
with sections according to EN 10210-2 (CEN, 2006a)

chord : 200 x 200 x 8	A <sub>0</sub> = 6080 mm <sup>2</sup>	b <sub>0</sub> /t <sub>0</sub> = 25	f <sub>y0</sub> = f <sub>yi</sub> = f <sub>yj</sub> = 355 N/mm <sup>2</sup>
brace i : 140 x 140 x 4	A <sub>i</sub> = 2130 mm <sup>2</sup>	b <sub>i</sub> /t <sub>i</sub> = 35 (tension)	Ov = 50%
brace j : 150 x 150 x 5	A <sub>j</sub> = 2870 mm <sup>2</sup>	b <sub>j</sub> /t <sub>j</sub> = 30 (compression)	

For Ov = 50%, besides member checks, only local yielding of the overlapping brace needs to be checked:

$$\frac{f_{y0} t_0}{f_{yi} t_i} = \frac{8}{4} = 2.0 \quad \text{with } b_0/t_0 = 25: \quad 0.25b_{e,i}/b_i = 0.20$$

$$\frac{f_{yj} t_j}{f_{yi} t_i} = \frac{5}{4} = 1.25 \quad \text{with } b_j/t_j = 30: \quad 0.25b_{e,ov}/b_i = 0.10$$

Hence, the brace efficiency for both braces is:

$$\text{Eff.} = 0.50 + 0.25b_{e,i}/b_i + 0.25b_{e,ov}/b_i = 0.50 + 0.20 + 0.10 = 0.80$$

$$N_i^* = 0.8 \times 2130 \times 0.355 = 605 \text{ kN}$$

$$N_j^* = 0.8 \times 2870 \times 0.355 = 815 \text{ kN}$$



Truss with 100% overlapped joint

## 5 Welded RHS-to-RHS joints under moment loading

### 5.1 Vierendeel trusses and joints

#### 5.1.1 Introduction to Vierendeel trusses

Arthur Vierendeel first proposed Vierendeel trusses in 1896. They are comprised of brace members connected to chord members usually at 90° angles (see figure 5.1).



Figure 5.1 – Application of RHS Vierendeel trusses in the foyer of a building

The typical design premise with Vierendeel trusses has been to assume full joint rigidity, but this is rarely the case with RHS to RHS Vierendeel joints. Unlike triangulated Warren or Pratt trusses, in which the joints approximately behave as a pinned joint at their ultimate limit state and cause the brace members to be loaded by predominantly axial forces, Vierendeel joints have brace members subjected to substantial bending moments as well as axial and shear forces. Until recently, most of the testing performed on Vierendeel joints has been on isolated joint specimens as shown in figure 5.2, with a lateral load applied to the vertical brace member. Thus, the joint strength and moment-rotation behaviour have been assessed mainly by researchers under moment plus shear loading.

Square and rectangular RHS single chord joints loaded by in-plane bending moments have been studied by Duff (1963), Redwood (1965), Cote et al. (1968), Mehrotra and Redwood (1970), Lazar and Fang (1971), Wardenier (1972), Mehrotra and Govil (1972), Staples and Harrison (undated), Brockenbough (1972), Korol et al. (1977), Korol and Mansour (1979), Kanatani et al. (1980), Korol et al. (1982), Korol and Mirza (1982), Mang et al. (1983), Davies and Panjeh Shahi (1984), Szlendak and Brodka (1985, 1986a, 1986b), Szlendak (1986,1991), Kanatani et al. (1986), and Yeomans and Giddings (1988).

Researchers concur that both the strength and flexural rigidity of an unstiffened joint decrease as the chord slenderness ratio  $b_0/t_0$  increases, and as the brace-to-chord width ratio  $b_1/b_0$  (or  $\beta$ ) decreases. Joints with  $\beta = 1.0$  and a low  $b_0/t_0$  value almost attain full rigidity, but all other unstiffened joints can be classed as semi-rigid. For such semi-rigid joints, figures 5.2(b) to (e) give a variety of means of stiffening which have been used to achieve full rigidity. From these alternatives, figures 5.2(c) and (d) are recommended since the resistance of figure 5.2(b) is limited by local yielding of the brace, while figure 5.2(e) is rather expensive to fabricate.

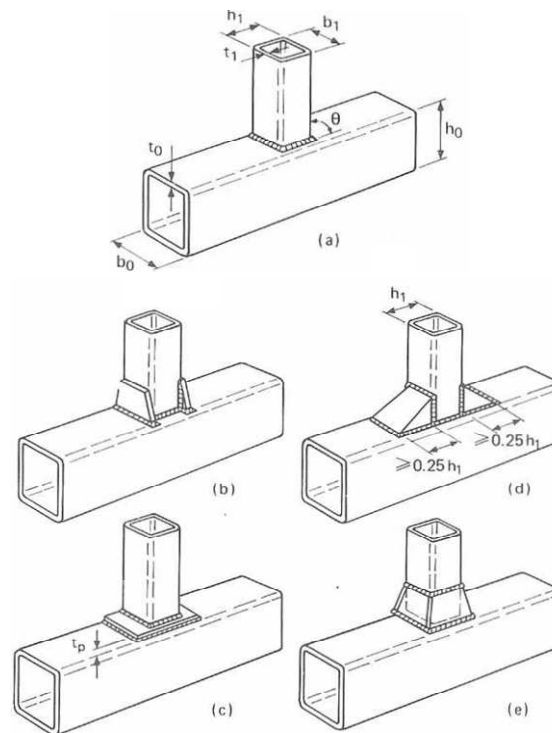


Figure 5.2 – RHS Vierendeel joint types (Korol et al., 1977)  
 (a) Unreinforced  
 (b) With brace plate stiffeners  
 (c) With chord plate stiffener  
 (d) With haunch stiffeners  
 (e) With truncated pyramid stiffeners

### 5.1.2 Joint behaviour and strength

Korol et al. (1977) developed an empirical formula for estimating the maximum joint moment, but this moment typically occurs at excessively large joint deformations. Thus, for all practical design purposes, the moment capacity of a joint can be determined in a manner similar to that used for axially loaded RHS T joints, whereby the strength is characterized by an ultimate bearing capacity or by a deformation- or rotation limit (Wardenier, 1982). This design approach is more apparent if one considers the possible failure modes for such joints, which are shown in figure 5.3.

The failure modes represented in figure 5.3 for brace in-plane bending presume that neither the welds nor the members themselves are critical (e.g. local buckling of the brace is precluded). Cracking in the chord (chord punching shear) has not been observed in any test, and chord shear failure is strictly a member failure. Hence, analytical solutions for failure modes (b) and (e) are not considered herein.

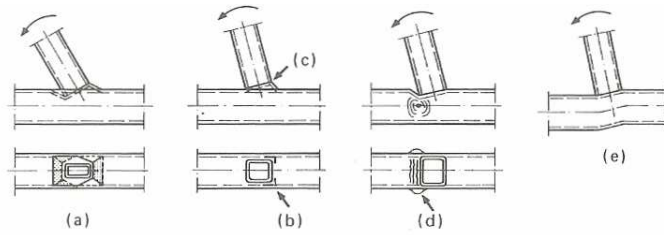


Figure 5.3 – Possible failure modes for RHS joints loaded by brace in-plane bending moment (Wardenier, 1982)

- (a) Chord face plastification
- (b) Cracking in chord (punching shear)
- (c) Cracking in brace member
- (d) Crippling of the chord side walls
- (e) Chord shear failure

## 5.2 T and X joints with brace(s) subjected to in-plane bending moment

For mode (a), the moment capacity of joints with low to moderate  $\beta$  values can be determined by the yield line mechanism illustrated in figure 5.4. Neglecting the influence of membrane effects and strain hardening, the in-plane bending moment resistance is given by:

$$M_{ip,1}^* = f_{y0} t_0^2 h_1 \left( \frac{\sin \theta_1}{2\eta} + \frac{2}{\sqrt{1-\beta}} + \frac{\eta}{(1-\beta) \sin \theta_1} \right) \frac{Q_f}{\sin \theta_1} \quad 5.1$$

with  $\eta = h_1/b_0$  and for  $\beta \leq 0.85$ .

The term  $Q_f$  (referred to as  $f(n)$  in the 1<sup>st</sup> edition of this Design Guide, see table A6 in Appendix A) is a function to allow for the reduction in joint moment resistance due to the presence of chord stresses. This function is now based on the numerical and test results of Yu (1997) and the reanalysis by Wardenier et al. (2007a). Here the same influence function is taken as for axially loaded T and X joints, see table 4.1 and figures 4.5 and 4.6.

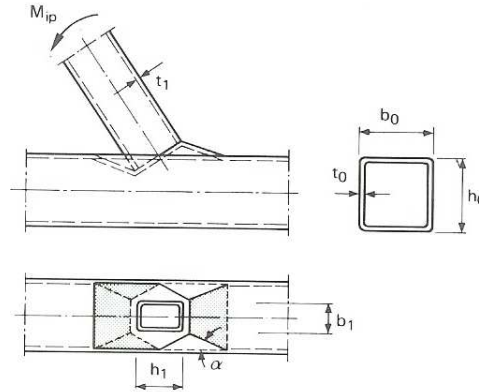


Figure 5.4 – Yield line mechanism for chord face plastification under brace in-plane bending (failure mode (a))

Nearly all Vierendeel joints have a brace to chord angle  $\theta_1 = 90^\circ$ , which simplifies equation 5.1 to:

$$M_{ip,1}^* = f_{y0} t_0^2 h_1 \left( \frac{1}{2\eta} + \frac{2}{\sqrt{1-\beta}} + \frac{\eta}{(1-\beta)} \right) Q_f \quad 5.2$$

for  $\beta \leq 0.85$ .

For mode (c), local yielding of the brace is used to relate the reduced capacity of the brace member (considered to be the same for the tension and compression flanges of the brace member) to the applied brace moment as follows (Wardenier, 1982):

$$M_{ip,1}^* = f_{y1} \left[ W_{pl,1} - \left(1 - \frac{b_e}{b_1}\right) b_1 (h_1 - t_1) t_1 \right] \quad 5.3$$

The term  $b_e$  in equation 5.3 is the effective width of the brace member flange, and is given by:

$$b_e = \left( \frac{10}{b_0/t_0} \right) \left( \frac{f_{y0} t_0}{f_{y1} t_1} \right) b_1 \text{ but } \leq b_1 \quad 5.4$$

For mode (d), a chord side wall bearing or buckling capacity can conservatively be given by equation 5.5 (Wardenier, 1982) which is illustrated in figure 5.5.

$$M_{ip,1}^* = 0.5 f_k t_0 (h_1 + 5t_0)^2 Q_f \quad 5.5$$

This moment is derived from stress blocks of twice (two walls)  $f_k t_0 (h_1/2 + 2.5t_0)$  acting as a couple at centres of  $(h_1/2 + 2.5t_0)$ . Since the compression is very localized, tests by Mang et al. (1983) and de Koning and Wardenier (1984) have shown that buckling is less critical for moment loaded T joints than for axially loaded T joints. Hence, within the parameter range of validity given, the chord yield stress  $f_{y0}$  can be used instead of the buckling stress for T joints. For X joints, this is reduced by 20% and inclusion of the buckling coefficient  $\chi$  in order to be consistent with table 4.1. For simplicity, the stress blocks are taken to be symmetrical, although a stress distribution with  $f_{y0}$  for the tension side would be more realistic.

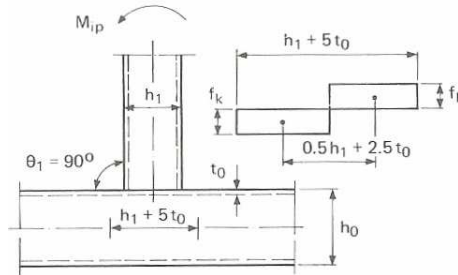


Figure 5.5 – Chord side wall bearing or buckling failure model under brace in-plane bending (failure mode (d))

Hence, for design purposes an estimate of the joint moment resistance can be obtained from the lower of the  $M_{ip,1}^*$  values obtained from equations 5.2, 5.3 and 5.5.

It can be seen that the moment resistance predicted by equation 5.2 tends towards infinity as  $\beta$  tends towards unity (similar to axially loaded joints, see table 4.1). Hence, this failure mode, which corresponds to a state of complete joint face plastification, is not critical in the high  $\beta$  range. This explains the  $\beta \leq 0.85$  limit attached to equation 5.2. For high  $\beta$  values, failure due to web crippling, expressed by equation 5.5, will likely govern. A summary of the design equations for in-plane moment loading is given in table 5.1.

Table 5.1 – Design moment resistance of uniplanar RHS braces to RHS chord joints

Limit state	T and X joints ( $\theta_1 = 90^\circ$ ) (*)	
	Brace in-plane bending	Brace out-of-plane bending (**)
<b>Chord face plastification</b> (for $\beta \leq 0.85$ )	$M_{ip,1}^* = Q_u Q_f f_{y0} t_0^2 h_1$	$M_{op,1}^* = Q_u Q_f f_{y0} t_0^2 b_1$
<b>Local yielding of brace</b> (for $0.85 < \beta \leq 1.0$ )	$M_{ip,1}^* = f_{y1} \left[ W_{pl,1} - \left(1 - \frac{b_e}{b_1}\right) b_1 (h_1 - t_1) t_1 \right]$	$M_{op,1}^* = f_{y1} [W_{pl,1} - 0.5 t_1 (b_1 - b_e)^2]$
<b>Chord side wall failure</b> (for $\beta = 1.0$ ) (***)	$M_{ip,1}^* = 0.5 f_k t_0 (h_1 + 5t_0)^2 Q_f$	$M_{op,1}^* = f_k t_0 (b_0 - t_0) (h_1 + 5t_0) Q_f$

(\*) The equations are conservative for  $\theta_1 < 90^\circ$ .

(\*\*) Chord distortion to be prevented for brace out-of-plane bending.

(\*\*\*) For  $0.85 < \beta < 1.0$ , use linear interpolation between the resistance for chord face plastification at  $\beta = 0.85$  and the resistance for chord side wall failure at  $\beta = 1.0$ .

Function $Q_u$	Brace in-plane bending	Brace out-of-plane bending
	$Q_u = \left( \frac{1}{2\eta} + \frac{2}{\sqrt{1-\beta}} + \frac{\eta}{1-\beta} \right)$	$Q_u = \left( \frac{h_1(1+\beta)}{2b_1(1-\beta)} + \sqrt{\frac{2(1+\beta)}{\beta(1-\beta)}} \right)$

Function $Q_f$	Same as in table 4.1
----------------	----------------------

$b_e$	$b_e = \left( \frac{10}{b_0/t_0} \right) \left( \frac{f_{y0} t_0}{f_{y1} t_1} \right) b_1$ but $\leq b_1$
-------	---

$f_k$	Brace in-plane bending		Brace out-of-plane bending	
	T and Y joints	X joints	T and Y joints	X joints
	$f_k = f_{y0}$	$f_k = 0.8\chi f_{y0}$	$f_k = \chi f_{y0}$	$f_k = 0.8\chi f_{y0}$
where $\chi$ = reduction factor for column buckling according to e.g. Eurocode 3 (CEN, 2005a) using the relevant buckling curve and a slenderness $\lambda = 3.46 \left( \frac{h_0}{t_0} - 2 \right)$				

Range of validity	Same as in table 4.1, but with $\theta_1 \approx 90^\circ$ (*)
-------------------	--

From the above expressions for  $M_{ip,1}^*$ , it can be observed that full width ( $\beta = 1.0$ ) unstiffened RHS Vierendeel joints are capable of developing the full moment capacity of the brace member, provided that  $b_0/t_0$  is sufficiently low. For  $h_0 = b_0 = h_1 = b_1$  and  $h_0/t_0 \leq 16$ , the chord side wall web crippling capacity is approximately given by (Wardenier, 1982):

$$M_{ip,1}^* = 12 f_{y0} t_0^2 h_1 Q_f \quad 5.6$$

Further, the plastic moment capacity of a hot-formed square RHS brace member (small corner radii) is approximately given by:

$$M_{pl,1} = 1.5 b_1^2 t_1 f_{y1} \quad 5.7$$

Hence,

$$\frac{M_{ip,1}^*}{M_{pl,1}} = \frac{8}{b_0/t_0} \frac{f_{y0} t_0}{f_{y1} t_1} Q_f \quad 5.8$$

As a result, for the same steel grades used throughout, a truss with  $\beta \approx 1.0$  and with dimensional ratios of  $b_0/t_0 \leq 16$  and  $t_0/t_1 \geq 2$  will produce a joint with a moment capacity close or approximately equal to the plastic moment capacity of the brace, provided that the chord stress ratio  $n$  is not too high. In this case, the brace member cross section is fully effective ( $b_e = b_1$  in equations 5.3 and 5.4). The above is similar to the recommendation by Korol et al. (1977) for cold-formed stress-relieved RHS that  $b_0/t_0$  be less than 16 with  $\beta = 1.0$  for full moment transfer to be assumed at the joint.

Any resistance factor ( $\phi$ ) or partial safety factor ( $\gamma_M$ ) is already included, where necessary, in the above resistance expressions of  $M_{ip,1}^*$  for their use in a limit states design format. The expressions for  $M_{ip,1}^*$  further have a limited range of validity, which corresponds to the limits of the test data against which the equations have been checked. This validity range is equal to that in table 4.1 with  $\theta_1 \approx 90^\circ$  and the compression brace member is restricted to plastic design sections.

The welds in RHS moment joints are loaded in a highly non-uniform manner and should also be capable of sustaining significant joint rotations. To enable adequate load redistribution to take place, the fillet weld sizes should be at least as large as those specified for axially loaded RHS truss joints to develop the capacity of the brace member (see section 3.9).

The previous expressions for moment capacity are based on moment loading only, whereas in Vierendeel trusses significant axial loads may also exist in the brace members. The effect of the axial load on the joint moment capacity depends on the critical failure mode, and hence, a complex set of interactions is developed. Consequently, it is conservatively proposed that a linear interaction relationship be used to reduce the in-plane moment capacity of a Vierendeel joint as follows:

$$\frac{N_1}{N_1^*} + \frac{M_{ip,1}}{M_{ip,1}^*} \leq 1.0 \quad 5.9$$

where:

$N_1$  = the applied axial load in the brace member

$N_1^*$  = the joint resistance with only axial load applied to the brace member (table 4.1)

$M_{ip,1}$  = the applied bending moment in the brace member

$M_{ip,1}^*$  = the lower of the values obtained from equations 5.2, 5.3 and 5.5

The resistance of an RHS T joint *under brace axial load* is given in table 4.1 and discussed in section 4.3.2 but is reproduced below for the most relevant case of  $\beta = 1.0$  (and  $\theta_1 = 90^\circ$ ). There



where  $Q_f$  is given by the same equation as in table 4.1. It should be noted that for this failure, all deformation takes place in the chord face and the chord will therefore not distort as a rhombus.

(b) For  $0.85 < \beta \leq 1.0$ , design would likely be governed by the more critical failure mode between reduced brace member capacity (or local yielding of the brace), and chord side wall bearing or buckling capacity (see figure 5.7).

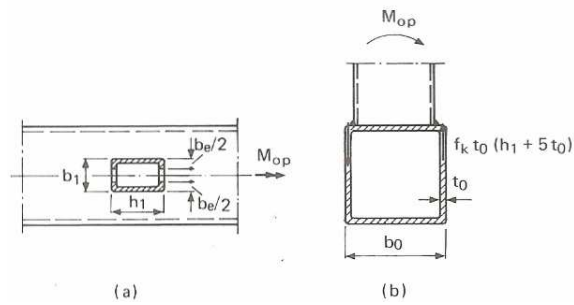


Figure 5.7 – T joint subjected to brace out-of-plane bending moment, showing the basis of design models for:  
(a) Local yielding of the brace  
(b) Chord side wall failure

For local yielding of the brace:

$$M_{op,1}^* = f_{y1} [W_{pl,1} - 0.5t_1(b_1 - b_e)^2] \quad 5.13$$

where  $W_{pl,1}$  is the plastic section modulus about the correct axis of bending, and plastic design sections should be selected for the brace member. The term  $b_e$  is defined by equation 5.4.

For chord side wall failure:

$$M_{op,1}^* = f_k t_0 (b_0 - t_0)(h_1 + 5t_0) Q_f \quad 5.14$$

For RHS T joints subjected to (brace) out-of-plane bending, the term  $f_k$  is taken equal to the buckling stress given for T joints under brace compression (see table 4.1).

The design provisions for RHS T joints subjected to out-of-plane bending moment are summarized in table 5.1.

Equations 5.13 and 5.14 are only applicable for determining the out-of-plane moment capacity if rhomboidal distortion of the chord is prevented.

One can see that the design criteria for RHS X joints subjected to equal and opposite (self-equilibrating) out-of-plane bending moments applied to the brace members, are again taken equal to those given above for T joints with one exception. The difference is that for chord side wall failure,  $f_k$  should be reduced to  $0.8\chi f_{y0}$ .

The design formulae for RHS X joints subjected to brace out-of-plane bending are also covered by table 5.1.

#### 5.4 T and X joints with brace(s) subjected to combinations of axial load, in-plane bending and out-of-plane bending moment

The interaction of (brace) axial load and in-plane bending moment on the (brace) out-of-plane bending moment capacity depends on the critical failure mode, resulting in a complex set of interactions. Consequently, it is conservatively proposed that a linear interaction relationship be used:

$$\frac{N_1}{N_1^*} + \frac{M_{ip,1}}{M_{ip,1}^*} + \frac{M_{op,1}}{M_{op,1}^*} \leq 1.0 \quad 5.15$$

#### 5.5 Joint flexibility

In the foregoing, it was shown that unstiffened RHS joints with  $\beta = 1.0$  and selected  $b_0/t_0$  and  $t_0/t_1$  values could achieve the full moment capacity of the brace member, but it should be noticed that any in-plane bending moment resistance calculated ( $M_{ip,1}^*$ ) must be reduced to take account of the influence of axial load in the brace member (see equation 5.9). Such joints, which still develop a moment resistance exceeding the moment capacity of the brace member, can be considered as fully rigid for the purpose of analysis of a Vierendeel truss. All other joints (which covers most possible joint combinations) should be considered as semi-rigid. To analyse a frame which is connected by semi-rigid joints, one needs the load-deformation characteristics of the joints being used, and these can be obtained by either reliable finite element analysis, from laboratory tests or published databases.

#### 5.6 Knee joints

Research on mitred RHS knee joints (such as illustrated in figure 5.8) has been performed by Mang et al. (1980) at the University of Karlsruhe. Their recommendations have also been included in Eurocode 3 (CEN, 2005b). They cover both stiffened and unstiffened knee joints, and are intended for use in corner joints of frames.

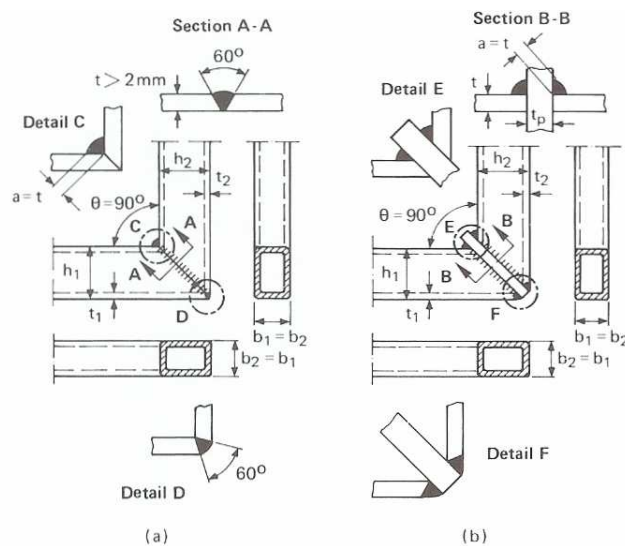


Figure 5.8 – Details of RHS knee joints  
 (a) Unstiffened  
 (b) With a transverse stiffening plate

Mang et al. (1980) recommend that these joints be designed based on the following requirements for both members:

$$\frac{N_i}{N_{pl,i}} + \frac{M_i}{M_{pl,i}} \leq \alpha \quad (\text{with } i = 1 \text{ or } 2, \text{ see figure 5.8}) \quad 5.16$$

where:

$N_{pl,i}$  = axial yield capacity of a member, either in compression or tension as applicable.

$M_{pl,i}$  = plastic moment capacity of member  $i$ .

$\alpha$  = a stress reduction factor, which can be taken as 1.0 for mitred joints with stiffening plates.

For the mitred joints without stiffening plates,  $\alpha$  is a function of the cross sectional parameters as shown in figures 5.9 and 5.10.

Based on the work of Mang et al. (1980), it is recommended that for joints without stiffening plates, the shear force  $V_i$  and the axial force  $N_i$  in the members should not exceed:

$$\frac{V_i}{V_{pl,i}} \leq 0.5 \text{ and } \frac{N_i}{N_{pl,i}} \leq 0.2 \quad 5.17$$

where:

$V_{pl,i}$  = shear yield capacity in the member under consideration.  $V_{pl,i}$  can be taken as the yield stress in pure shear ( $0.58f_{yi}$ ) multiplied by the cross sectional area of the RHS webs ( $2 h_i t_i$ ).

$N_{pl,i}$  = axial yield capacity of the member

For those structural applications where a reasonable strength, stiffness and rotational capacity are required, it is recommended that a stiffened joint with class 1 sections is used. For other structural applications, it is recommended to use unstiffened joints only if the sections satisfy at least the plastic design requirements. Karcher and Puthli (2001) recommended for CHS knee joints, that the stiffening plate thickness should satisfy  $t_p > 2t_i$  and not be taken smaller than 10 mm, which is also adopted for RHS knee joints.

The fabrication details with  $a = t_i$  shown in figure 5.8 are based on a steel grade S235. The weld size can be considered to be adequate when the throat thickness ( $a$ ) of the fillet weld is in accordance with the recommendations given in section 3.9.

If mitred knee joints are used with an obtuse angle between the RHS members (i.e.  $\theta > 90^\circ$  in figure 5.8), the same design checks can be undertaken as for right-angle joints, since obtuse angle knee joints behave more favourably than right-angle ones (CIDECT, 1984). For unstiffened knee joints with  $90^\circ < \theta < 180^\circ$ , a strength enhancement can be used by increasing the value of  $\alpha$  as follows:

$$\alpha = 1 - \left( \sqrt{2} \cos \frac{\theta}{2} \right) (1 - \alpha_{\theta=90^\circ}) \quad 5.18$$

where  $\alpha_{\theta=90^\circ}$  is the value obtained from figure 5.9 or figure 5.10.

An alternative form of joint reinforcement (other than a transverse stiffening plate) is a haunch on the inside of the knee. This haunch piece needs to be of the same width as the two main members, and can easily be provided by taking a cutting from one of the RHS sections. Provided the haunch length is sufficient to ensure that the bending moment does not exceed the section yield moment in either member, the joint resistance will be adequate and does not require checking (CIDECT, 1984).

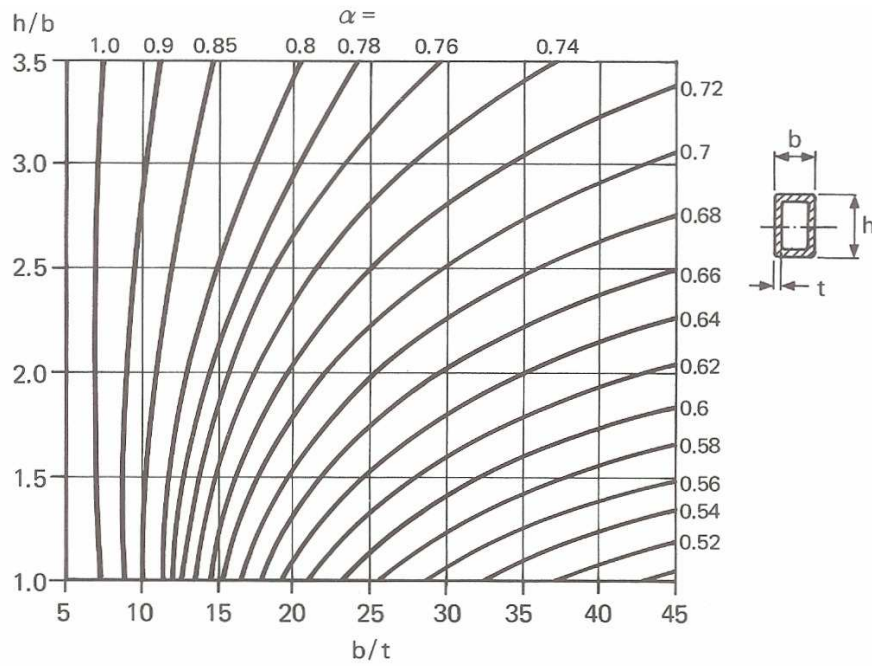


Figure 5.9 – Stress reduction factors  $\alpha$  for RHS subjected to bending about the major axis in 90° unstiffened mitred knee joints (Mang et al., 1980)

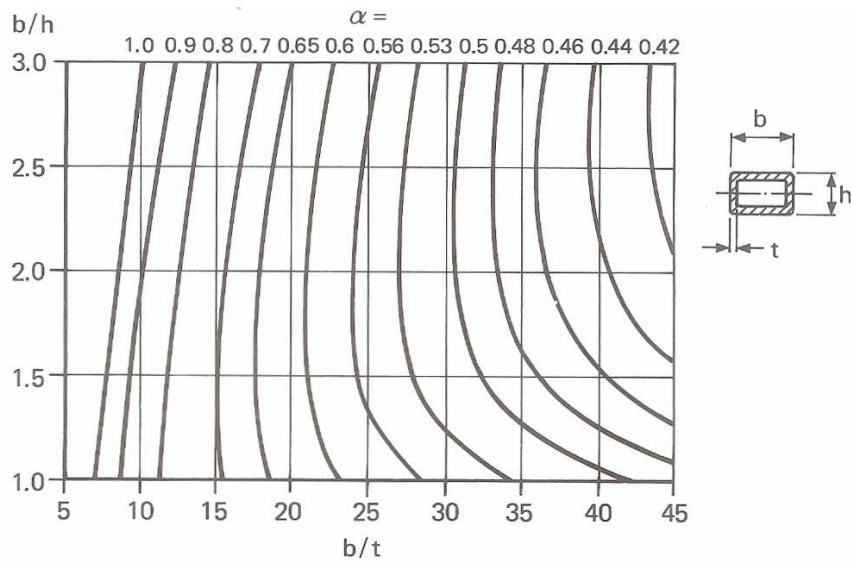


Figure 5.10 – Stress reduction factors  $\alpha$  for RHS subjected to bending about the minor axis in 90° unstiffened mitred knee joints (Mang et al., 1980)

## 6 Multiplanar welded joints

Multiplanar joints are frequently used in tubular structures such as towers, space frames, offshore structures, triangular trusses (Delta trusses), quadrangular trusses and many other applications. Triangular trusses, as illustrated in figure 6.1, have several advantages over single plane trusses, such as the increased lateral stability offered by the twin, separated, but connected compression chords. They are frequently used as exposed structures and considered equivalent in appearance, but less expensive than space frames. Furthermore, in general, purlins are not necessary with triangular trusses, as the usual practice is to space the top chords of the trusses at a distance suitable for the roof deck, and then fasten the roof deck directly to the flat surfaces of the RHS top chords.

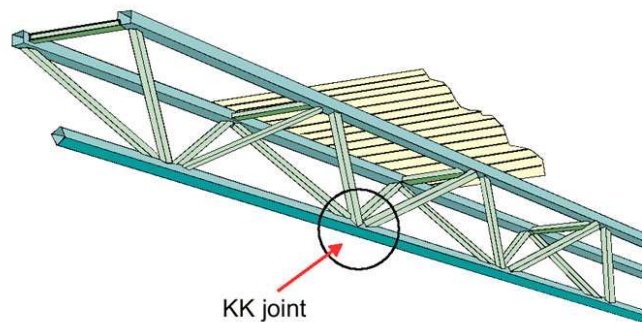


Figure 6.1 – RHS triangular truss with double compression chords

### 6.1 KK joints

Initial tests by Coutie et al. (1983) on RHS multiplanar KK joints found a small decrease compared to the strength of the in-plane K joint due to out-of-plane loaded brace members. Bauer and Redwood (1988) deduced that for KK joints to the single RHS chord of a triangular truss, as shown in figure 6.1, there was little interactive effect produced by identical loading (same sense) on an adjacent wall of the chord.

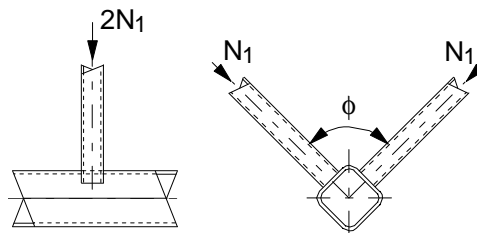


Figure 6.2 – Elevation view of a KK joint to triangular truss tension chord

As further failure modes may exist over a wider range of joint parameters than those studied by Coutie et al. (1983) and Bauer and Redwood (1988), in the 1<sup>st</sup> edition of this Design Guide (Packer et al., 1992) it was suggested to use a reduction factor of 0.9 in conjunction with the uniplanar K joint design formulae (see table A7 of Appendix A). This applied to cases where the angle between brace member planes  $\phi$  was equal to or less than  $90^\circ$  and with the brace members attached to the chord face with no eccentricity, as illustrated in figure 6.2. This was the same reduction factor as given for CHS KK joints in the 1<sup>st</sup> edition of CIDECT Design Guide No. 1 (Wardenier et al., 1991).

The recommendation for RHS KK joints in the 1<sup>st</sup> edition of this Design Guide (Packer et al., 1992) was made for  $60^\circ \leq \phi \leq 90^\circ$ . In addition, it was advised always to perform a chord shear check for gap KK joints, as shown in table A7 of Appendix A.

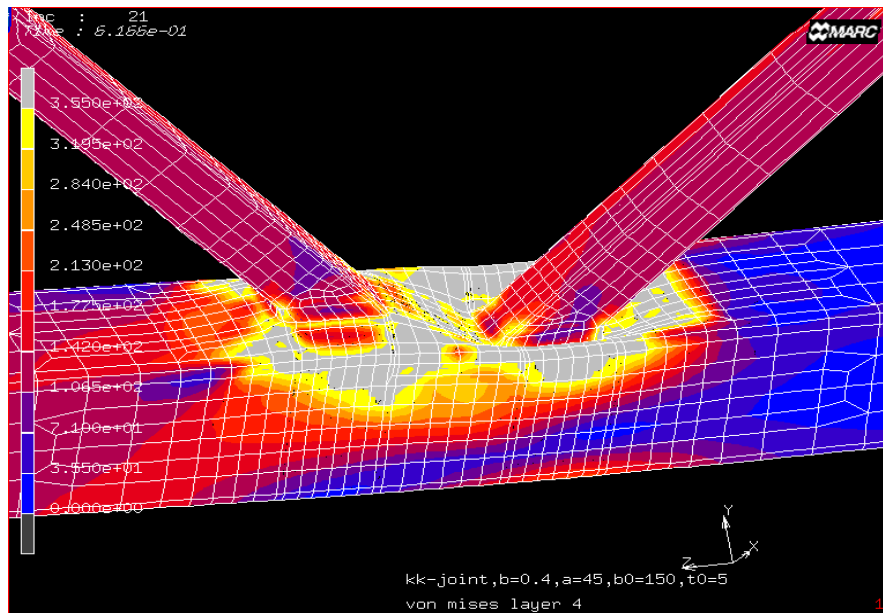
Since then, extensive analytical and numerical research has been carried out by Liu and Wardenier (2001a, 2001b, 2002, 2003). It was concluded that the differences in capacity between uniplanar K gap and multiplanar KK gap joints are caused by the different chord force. Based on this work, the following recommendations can be made, summarized in table 6.1:

*Multiplanar KK gap joints:*

- For chord face plastification (small or medium  $\beta$ ), the strength of the joint can be based on the joint resistance formulae for uniplanar joints given in tables 4.1 and 4.2, and no further multiplanar correction is necessary, provided that the actual total chord force is used for the chord stress function  $Q_f$ .
- For large  $\beta$  ratios or rectangular chord sections, the strength of a KK gap joint is governed by chord shear and chord axial force interaction, presented in table 6.1. The K gap joint (with  $\phi = 90^\circ$ ) is subjected to a shear force of  $0.5\sqrt{2} V_{\text{gap},0}$  in each plane, where  $V_{\text{gap},0}$  is the total "vertical" shear force. The shear force in each plane is resisted by the two walls of the RHS chord. The horizontal components from the two planes equilibrate.

*Multiplanar overlap KK joints:*

- For multiplanar overlap KK joints, the strength of the joint is similar to the current recommendations for uniplanar overlap joints in table 4.3. Thus, compared to the previous recommendations in the 1<sup>st</sup> edition of this Design Guide (Packer et al., 1992), a brace shear criterion and a local chord yielding criterion have been added.



Multiplanar RHS KK gap joint

## 6.2 TT and XX joints

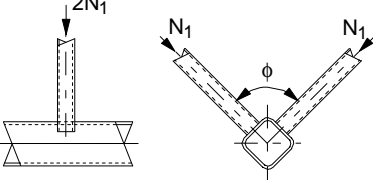
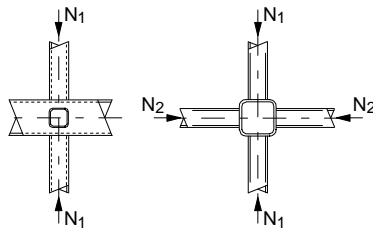
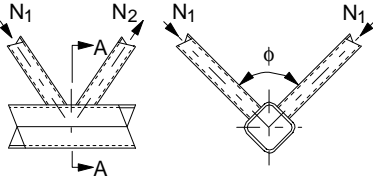
Initial, theoretical research by Davies and Morita (1991) on TT and XX joints showed that little difference exists between the design strengths of planar and multiplanar 90° TT and XX joints. Because of a lack in experimental evidence, the 1<sup>st</sup> edition of this Design Guide recommended to apply a correction factor of 0.9 to the uniplanar T and X joint resistances to account for out-of-plane loaded braces (see table A7 of Appendix A).

Extensive research by Yu (1997) on XX and TT joints revealed that the multiplanar effect is caused by geometric and loading effects. The geometric effect is a function of the width ratio  $\beta$  and the chord width-to-thickness ratio  $2\gamma$ , with  $\beta$  as the most important influence. Based on Yu's work, table 6.1 gives simplified recommendations for multiplanar TT and XX joints.



Erection of an RHS pipeline bridge

Table 6.1 – Correction factors for RHS multiplanar joints

Type of joint	Correction factor $\mu$ to uniplanar joint strength
<p><b>TT joints</b></p>  <p>Members 1 may be either in tension or compression</p>	<p><math>\mu = 1.0</math></p>
<p><b>XX joints</b></p>  <p>Members 1 and 2 can be either in compression or tension</p>	<p><math>\mu = 1 + 0.35 \frac{N_2}{N_1}</math> for <math>\beta \leq 0.85</math></p> <p>Notes:</p> <ul style="list-style-type: none"> <li>- Take account of the sign of <math>N_2</math> and <math>N_1</math>, with <math> N_1  \geq  N_2 </math></li> <li>- <math>N_2/N_1</math> is negative if the members in one plane are in tension and in the other plane in compression.</li> </ul>
<p><b>KK gap and overlap joints</b></p>  <p>Members 1: compression Members 2: tension</p>	<p><math>\mu = 1.0</math></p> <p>Note: In a gap joint, the cross section in the gap should be checked for shear failure:</p> $\left( \frac{N_{gap,0}}{N_{pl,0}} \right)^2 + \left( \frac{0.71 V_{gap,0}}{V_{pl,0}} \right)^2 \leq 1.0$ <p>where:</p> <ul style="list-style-type: none"> <li><math>N_{gap,0}</math> = axial force in gap</li> <li><math>N_{pl,0} = A_0 f_{y0}</math></li> <li><math>V_{gap,0}</math> = shear force in gap</li> <li><math>V_{pl,0} = 0.58 f_{y0} (0.5 A_0)</math> for an SHS chord</li> </ul>
<p><b>Range of validity</b></p>	<p>Same as for uniplanar joints (tables 4.1 and 4.2) <math>\phi \approx 90^\circ</math></p>

## 7 Welded plate-to-RHS joints

Branch plate joints are one of the most popular joint types due to their ease of fabrication and handling. Originally, longitudinal branch plate joints were used with I section beams or columns with the branch plate welded along the centre of the flange, so that the force introduced by the branch plate was directly transmitted to the web of the I section. This practice was carried over to hollow section construction, but then the branch plate was attached in a similar manner to the middle of the hollow section face which is very flexible and often deforms excessively, frequently exceeding the deformation limit at relatively low loads. For welded RHS joints, a serviceability deformation limit of 1% and an ultimate deformation limit of 3% of the width of the connecting chord face ( $0.03b_0$ ) have been employed, as it has been shown that this ultimate deformation limit reasonably corresponds to the yield load of these joints (Lu et al., 1994).

Besides the yield strength or deformation criteria, punching shear of the hollow section connecting face is a further critical limit state which has to be checked, among others. All pertinent limit state checks are summarized in table 7.1 and are further explained below. Generally, the presented formulae have been simplified by considering only loads perpendicular to the hollow section member and disregarding the (generally positive) effect of fillet welds. The orientation (longitudinal or transverse) and width of the branch plate has a major effect on the strength and failure mode of branch plate joints. Hence, the following discussion distinguishes between the longitudinal and transverse plate joints.

### 7.1 Longitudinal plate joints under axial loading

Due to their very low  $\beta$  ratios, longitudinal plate-to-RHS joints tend to have excessive distortion or plastification of the RHS connecting face. An analytical approach is used to predict the limit state of chord face plastification and is based on a flexural model using yield line analysis (Cao et al., 1998a, 1998b). The influence of compressive stress in the RHS chord member, either due to axial load or bending moment, has been taken into account by the term  $Q_f$ . In table 7.1 this term is the result of recent research to harmonize the chord stress effects on RHS and CHS welded joints (Wardenier et al., 2007a, 2007b). If the longitudinal plate is loaded by an axial force that is not at  $90^\circ$  to the RHS member axis, the joint resistance can be evaluated using the normal component ( $N_1 \sin \theta_1$ ).

The foregoing design recommendation has been validated by research in which the longitudinal branch plate was located along the RHS member axis. A slight variant is sometimes produced when the longitudinal branch plate is offset from the RHS centreline so that the centreline of the connected member can coincide with that of the RHS. This should cause minimal difference in behaviour of the RHS face and this detailing arrangement is also acceptable. However, as noted in the last paragraph of section 7.6, for eccentrically-connected lap splice plates *under compression loading, the effect of the eccentricity must be taken into account in the design of both connected plates*.

### 7.2 Stiffened longitudinal plate joints under axial loading

Longitudinal plate-to-RHS joints in particular are only suitable for lightly loaded branch plates, so methods of strengthening this joint type have been examined. Research on longitudinal through-plate joints (Kosteski, 2001; Kosteski and Packer, 2003b) verified the assumption that a through-plate joint has approximately double the resistance of a simple longitudinal branch plate joint, which is reflected in the design equation for this joint type in table 7.1. This is because of the plastification of two RHS walls rather than one. While the single plate joint is one of the least expensive plate-to-RHS joints, the through-plate joint is deemed to be the most expensive because of the slotting procedure (Sherman, 1996). Designers should also bear in mind that a part of the through-plate protrudes beyond the far side of the RHS (see table 7.1) and this may affect joints to that face of the RHS.

Another means of strengthening a longitudinal plate joint is to use a stiffened longitudinal plate (T stub) to RHS joint. By adding the stiffening plate at the end of the branch plate, the “footprint” of the branch becomes much enlarged (an increased  $\beta$  ratio). Provided that the stiffening plate is rigid enough, the stiffened longitudinal plate-to-RHS joint can then be regarded as a RHS-to-RHS T joint, whereby the width of the stiffening plate becomes the new width of the “branch/brace member”. Based on work by Kosteski (2001) and Kosteski and Packer (2003a) a minimum thickness was derived for the stiffening plate to ensure the required rigidity (see table 7.1).

### 7.3 Longitudinal plate joints under shear loading

This type of joint is primarily found in “simple” shear joints to hollow section columns, where the plate is typically referred to as a “shear tab” or “fin plate”. Over a wide range of joints tested by Sherman (1995, 1996) only one limit state was identified for the RHS member. This was a punching shear failure related to end rotation of the beam when a thick shear tab was connected to a relatively thin-walled RHS. A simple criterion to avoid this failure mode is to ensure that the tension resistance of the tab under axial load (per unit plate length) is less than the shear resistance of the RHS wall along two planes (per unit plate length). This is achieved if (Sherman, 1995):

$$t_p < 1.16 \frac{f_{y0}}{f_{yp}} t_0 \quad 7.1$$

This design check is valid for RHS members that do not have slender cross sections (i.e. which are not thin-walled; i.e. are not class 4 according to Eurocode 3 (CEN 2005a)). Further details regarding this design criterion, along with a design example, are provided in CIDECT Design Guide No. 9 (Kurobane et al., 2004), where a variant of the above equation is used, basing the shear resistance instead on shear ultimate stress of the RHS wall rather than shear yielding.

### 7.4 Transverse plate joints under axial loading

#### 7.4.1 Failure mechanisms

Joints with transverse plates typically have higher  $\beta$  values than comparable joints with a longitudinal branch plate. Thus, they are less flexible and can have different failure mechanisms than joints with a longitudinal plate. For branch plate-to-RHS joints with transverse plates, four basic failure mechanisms have now been identified, with each limit state having the potential to govern in the plate-to-RHS width ratio ( $\beta$ ) ranges stipulated below (see table 7.1):

- Chord face plastification (for  $0.4 \leq \beta \leq 0.85$ )
- Chord punching shear (for  $0.85 \leq \beta \leq 1-1/\gamma$ )
- Chord side wall failure (for  $\beta \approx 1.0$ )
- Local yielding of the plate (for all  $\beta$ )

Initial research on transverse branch plate joints to RHS was carried out by Wardenier et al. (1981) and Davies and Packer (1982). Davies and Packer observed a combination of flexural failure and punching shear for joints with high  $\beta$  values (but slightly less than  $1-1/\gamma$ ). Based on the work of Wardenier et al. (1981), an effective punching shear width of the branch member was introduced, which was incorporated into a standard punching shear model. A similar effective branch width was further used to calculate the local yielding strength of the branch.

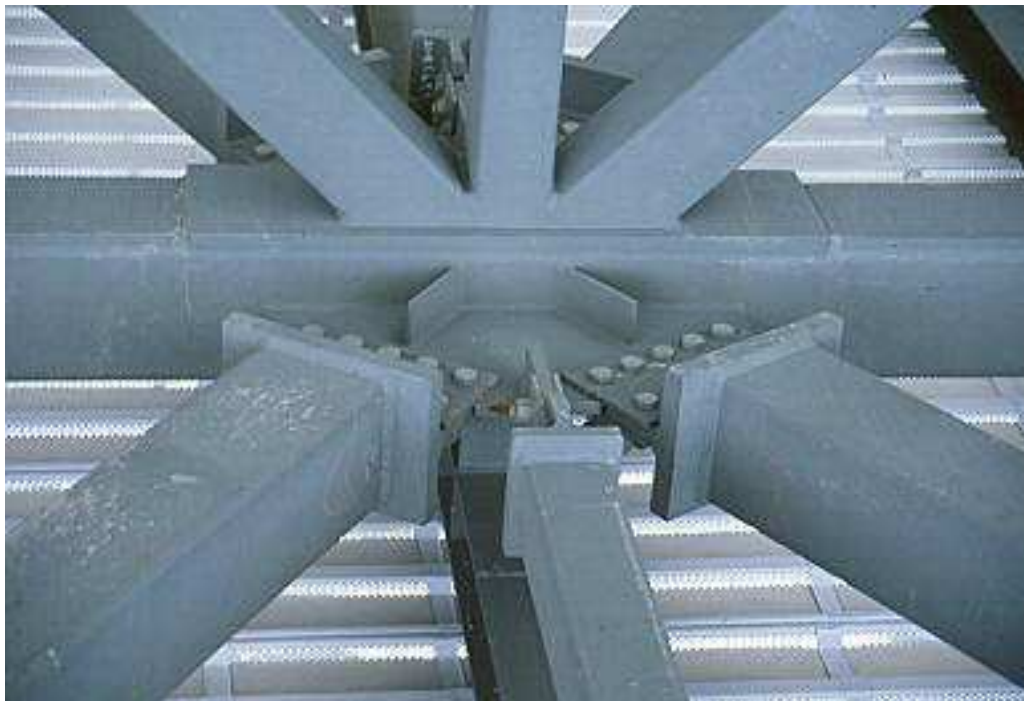
Chord face plastification was initially deemed a non-critical failure mode, for all transverse plate joints, and was hence omitted as a design check in the 1<sup>st</sup> edition of CIDECT Design Guide No. 3 (Packer et al., 1992). Plastification of the connecting chord face is well represented by the formation of a yield line mechanism. Lu (1997), however, subsequently found that the yield capacity of the connecting RHS face could be severely lowered in the presence of high normal compressive stresses in the connecting chord face. Lu hence determined an appropriate reduction factor,  $Q_f$ , and the application of this – for high RHS compression stresses – may make the chord face

plastification failure mode critical. Hence, this failure mode was introduced into CIDECT Design Guide No. 9 (Kurobane et al., 2004). The limit state expression used herein for this failure mode is a result of recent reanalyses by Wardenier et al. (2007a, 2007b).

For transverse plates in which the width of the plate is about the width of the chord or hollow section ( $\beta \approx 1.0$ ), the plate will bear directly on the RHS side walls. In this case, chord side wall failure is the pertinent failure mode for which the joint must be designed. The chord side wall failure stress is taken as the yield stress because the plate applies the compression load in a very localised manner. However, Lu (1997) has also noted that the chord side wall failure resistance can also be decreased by compressive normal stresses in the RHS if the hollow section has a high  $h_0/t_0$  value. Hence, a  $Q_f$  chord stress term has been included with this limit state expression.

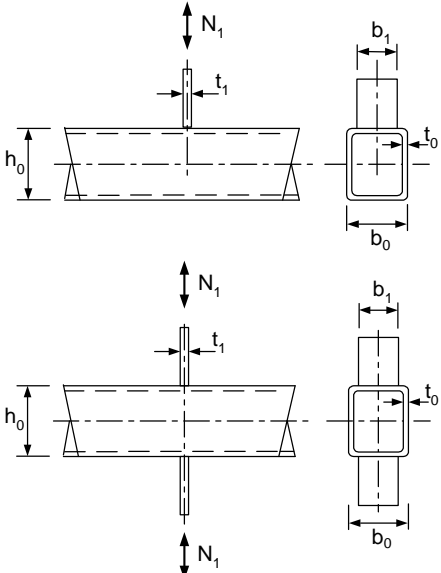
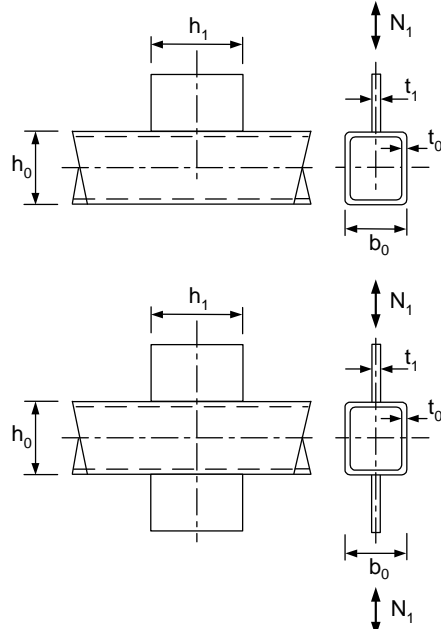
#### 7.4.2 Design of welds

The non-uniformity of load transfer along the line of weld, due to the flexibility of the RHS connecting face in a transverse plate joint, must be taken into account in proportioning such welds. This can be satisfied by limiting the total effective weld length (between the plate and RHS) to  $2b_e$ , as defined in table 7.1, where the factor 2 accounts for welds on both sides of the transverse plate. An upper limit on weld size will be given by the weld that develops the full yield strength of the connected transverse plate ( $A_f f_{y1}$ ), which then ensures that the weld is non-critical. Even if one uses just a particular length of weld as being effective, for weld design purposes, the actual weld should have the same weld size and extend over the entire plate width ( $b_1$ ).



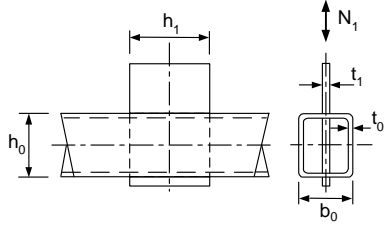
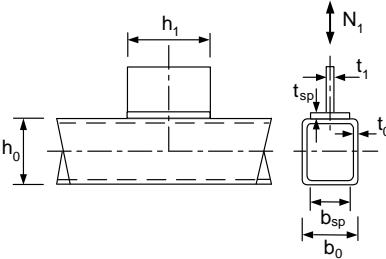
Complex joint in the Rogers Centre, Toronto, Canada

Table 7.1 – Design resistances of uniplanar branch plate-to-RHS joints

Type of joint	Design limit state
<p><b>T and X joints – transverse plate</b></p> 	<p><b>Chord face plastification</b> (for <math>0.4 \leq \beta \leq 0.85</math>)</p> $N_1^* = f_{y0} t_0^2 \left[ \frac{2 + 2.8\beta}{\sqrt{1 - 0.9\beta}} \right] Q_f$ <hr/> <p><b>Chord punching shear</b> (for <math>0.85 b_0 \leq b_1 \leq b_0 - 2t_0</math>)</p> $N_1^* = 0.58 f_{y0} t_0 (2t_1 + 2b_{e,p})$ <hr/> <p><b>Chord side wall failure</b> (for <math>\beta \approx 1.0</math>) (*)</p> $N_1^* = 2 f_{y0} t_0 (t_1 + 5t_0) Q_f$ <hr/> <p><b>Local yielding of plate</b> (for all <math>\beta</math>)</p> $N_1^* = f_{y1} t_1 b_e$
<p><b>T and X joints – longitudinal plate</b></p> 	<p><b>Chord face plastification</b></p> $N_1^* = 2 f_{y0} t_0^2 \left[ \eta + 2 \sqrt{1 - \frac{t_1}{b_0}} \right] Q_f$

(\*) For  $0.85 < \beta < 1.0$ , use linear interpolation between the resistance for chord face plastification at  $\beta = 0.85$  and the resistance for chord side wall failure at  $\beta = 1.0$ .

Table 7.1 – Design resistances of uniplanar branch plate-to-RHS joints (continued)

Type of joint	Design limit state
<p><b>T joints - longitudinal through-plate</b></p> 	<p><b>Chord face plastification</b></p> $N_1^* = 4 f_{y0} t_0^2 \left[ \eta + 2 \sqrt{1 - \frac{t_1}{b_0}} \right] Q_f$
<p><b>T stub joints - stiffened longitudinal plate</b></p> 	$t_{sp} \geq 0.5 t_0 e^{3\beta^*}$ <p>with: <math>\beta^* = \frac{b_{sp} - t_1}{b_0 - t_0}</math></p> <p>If <math>t_{sp}</math> fulfils the above requirement, the joint can be regarded as an RHS-to-RHS T joint. In the design equations for RHS-to-RHS T joints, the stiffening plate width <math>b_{sp}</math> is then used for the branch width <math>b_1</math>.</p>

Function $Q_f$		
	$Q_f = (1 -  n )^{C_1}$ with $n = \frac{N_0}{N_{pl,0}} + \frac{M_0}{M_{pl,0}}$ in connecting face	
	Chord compression stress ( $n < 0$ )	Chord tension stress ( $n \geq 0$ )
Transverse plate	$C_1 = 0.03\gamma$ but $\geq 0.10$	$C_1 = 0.10$
Longitudinal plate	$C_1 = 0.20$	

Factors		
$b_e$ and $b_{e,p}$	$b_e = \left( \frac{10}{b_0/t_0} \right) \left( \frac{f_{y0} t_0}{f_{y1} t_1} \right) b_1$ but $\leq b_1$	$b_{e,p} = \left( \frac{10}{b_0/t_0} \right) b_1$ but $\leq b_1$

Range of validity		
RHS chord	Compression	class 1 or 2 and $b_0/t_0 \leq 40$ and $h_0/t_0 \leq 40$
	Tension	$b_0/t_0 \leq 40$ and $h_0/t_0 \leq 40$
	Aspect ratio	$0.5 \leq h_0/b_0 \leq 2.0$
Transverse plate	$\beta = b_1/b_0 \geq 0.4$	
Longitudinal plate	$1 \leq \eta = h_1/b_0 \leq 4$	
Plate angle	$\theta_1 \approx 90^\circ$	
Yield stress	$f_{y1} \leq f_{y0}$ $f_y \leq 0.8f_u$ $f_y \leq 460 \text{ N/mm}^2$ (**)	

(\*\*) For  $f_{y0} > 355 \text{ N/mm}^2$ , see section 1.2.1

## 7.5 Gusset plate-to-slotted RHS joints

Single gusset plates, slotted into the ends of hollow section members and concentrically aligned with the axis of the member, as shown in figures 7.1 to 7.3, are commonly found in diagonal brace members of steel framed buildings (see figure 7.4) and also in roof brace-to-chord member joints.

Slotted RHS joints are noted by the presence (or lack) of an open slot at the end of the slotted RHS. An open slot allows for liberal construction and fabrication tolerances, if the longitudinal welds are performed on site. If the gusset plate bears against the end of the slot (common for shop fabrication) the ends of the gusset plate are typically welded with “end return welds”.

As a consequence of only part of the RHS cross section being connected, an uneven stress distribution around the RHS perimeter always occurs during load transfer at the connection. This phenomenon, known as shear lag, is illustrated in figure 7.1.

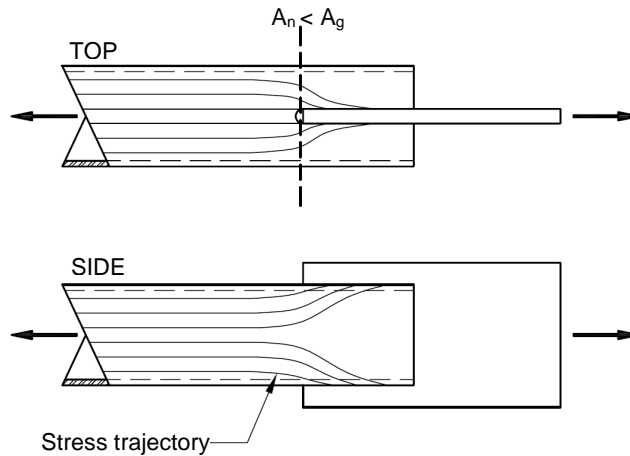


Figure 7.1 – Shear lag in gusset plate-to-slotted RHS joints

Two possible failure modes have been identified for gusset plate-to-slotted RHS joints loaded in tension: circumferential failure (CF) of the RHS (see figure 7.2) and tear out (TO) – or “block shear” – failure of the RHS (see figure 7.3). Shear lag is principally influenced by the weld length,  $L_w$ , or the “stick-in length”. For long weld lengths, shear lag effects become negligible, while for short weld lengths ( $L_w/w < 0.7$ ), tear out governs over circumferential fracture of the RHS, where the dimension  $w$  is the distance between the welds measured from plate face-to-plate face, around the perimeter of the RHS.

For both cases shown in figure 7.2, Martinez-Saucedo and Packer (2006) have shown that the RHS circumferential failure limit state design resistance *in tension* can be determined by:

$$N_t^* = 0.9A_n f_{ui} \left( 1 - \frac{1}{\left[ 1 + \left( \frac{L_w}{w} \right)^{2.4} \right]^{5.7}} \right) \quad \text{for } L_w/w \geq 0.7 \quad 7.2$$

For the RHS tear out limit state (see figure 7.3), the design resistance in tension can be determined by summing the fracture resistance of the net area in tension and the resistance of the gross area in shear (Martinez-Saucedo and Packer, 2006):

$$N_i^* = 0.9 \left( A_{nt} f_{ui} + 0.58 A_{gv} \left( \frac{f_{yi} + f_{ui}}{2} \right) \right) \quad \text{for } L_w/w < 0.7 \quad 7.3$$

Note that for the gusset plate-to-slotted RHS with longitudinal welds only, as shown in figure 7.3(a),  $A_{nt}$  is  $0 \text{ mm}^2$ .

Depending on the weld length,  $L_w$ , only one of these two limit states (failure modes) needs to be checked (unlike in many contemporary steel specifications). The 0.9 factor in these equations represents a  $1/\gamma_M = \phi$  term, determined by a reliability analysis. As indicated in figure 7.2(a) and figure 7.3(a), when there is an opening at the end of the slot, cracking starts at the end of the weld. Thus, under static loading, the cutting of the slot end does not need to be smooth, drilled or machined, and some roughness is tolerable. (Under dynamic loading conditions the slot end should be very smooth).

For these joints *in compression*, the member axial load is limited by overall buckling of the brace and hence, the member compression load is typically well below the capacity of the joint in compression.

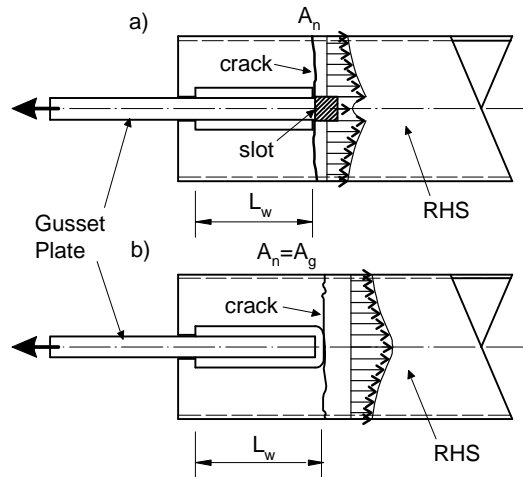


Figure 7.2 – Gusset plate-to-slotted RHS joints: Circumferential failure (CF) with: (a) longitudinal welds only and (b) longitudinal welds plus a weld return

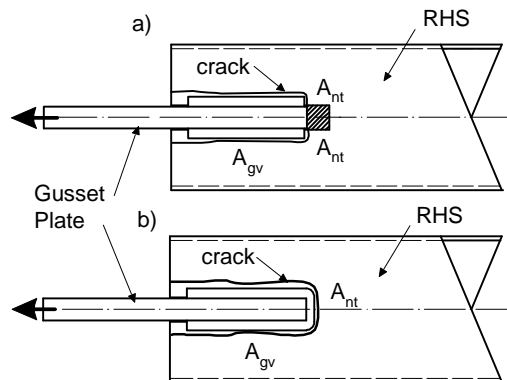


Figure 7.3 – Gusset plate-to-slotted RHS joints: Tear out (TO) failure with: (a) longitudinal welds only ( $A_{nt} = 0$ ) and (b) longitudinal welds plus a weld return



Figure 7.4 – Gusset plates slotted into a diagonal RHS bracing member, in a braced steel frame

### 7.6 Tee joints to the ends of RHS members

When an axial force is applied to the end of an RHS member, via a welded Tee joint as shown in figure 7.5, the possible limit state for the RHS is yielding of the walls (due to applied tension or compression loads). Also, the resistance of the RHS needs to be computed with consideration for shear lag.

In general, the RHS could have dimensions of  $b_1 \times h_1$ , but figure 7.5 shows the bearing width,  $t_w$ , oriented for lateral load dispersion into the RHS wall with dimension  $b_1$ . A conservative assumption for the distribution slope is 2.5:1 from each face of the Tee web (stem) (Kitipornchai and Traves, 1989), which produces a dispersed load width of  $(5t_p + t_w)$ . It is proposed to use this effective width around the perimeter of the RHS member. This is also adopted for CHS members in CIDECT Design Guide No. 1 (Wardenier et al., 2008). Thus the resistance of the RHS can be computed by summing the contributions of the parts of the RHS cross sectional area into which the load is distributed:

$$N_1^* = 2f_{y1} t_1 (t_w + 5t_p) \leq A_1 f_{y1} \quad 7.4$$

A similar load dispersion can be assumed for the capacity of the Tee web. If the web has the same width as the width of the cap plate, i.e.  $(h_1 + 2s)$ , the capacity of the Tee web is:

$$N_1^* = 2f_{yw} t_w (t_1 + 2.5t_p + s) \quad 7.5a$$

$$\leq 2f_{yw} t_w (t_1 + 5t_p) \quad 7.5b$$

In equations 7.4 and 7.5, the size of any weld legs to the Tee web (stem) has been conservatively ignored. If the weld leg size is known, it is acceptable to assume load dispersion from the toes of the welds. If the applied load  $N_1$  (figure 7.5) is compressive, it is assumed that the RHS does not have a slender cross section (i.e. is not class 4).



## 8 Bolted joints

Bolting directly to RHS members is a concern, due to lack of access to the interior of the member (other than near the ends). Welding attachments to the RHS and then bolting remote to the section is a popular option, and normal joint design principles – given in all national and international steel structures codes/specifications – are applicable. Examples of this technique, using angle, fork, channel, tee and plate welded attachments, are given in figure 8.1. Bolted joints are particularly useful for connecting prefabricated sub-assemblies on site and for truss-to-column joints (see figure 8.2).

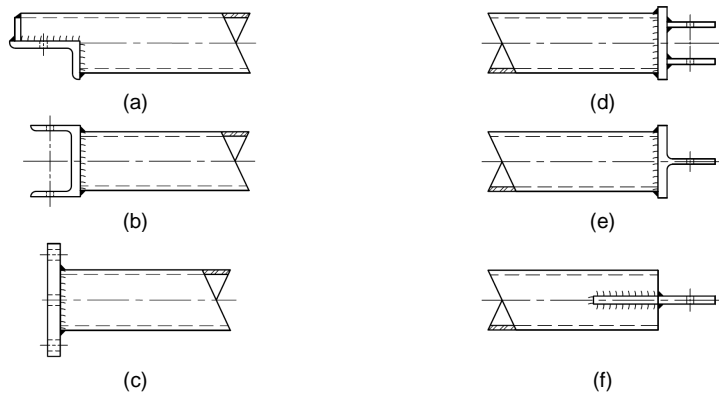


Figure 8.1 – Examples of bolted joints to RHS ends, using welded attachments

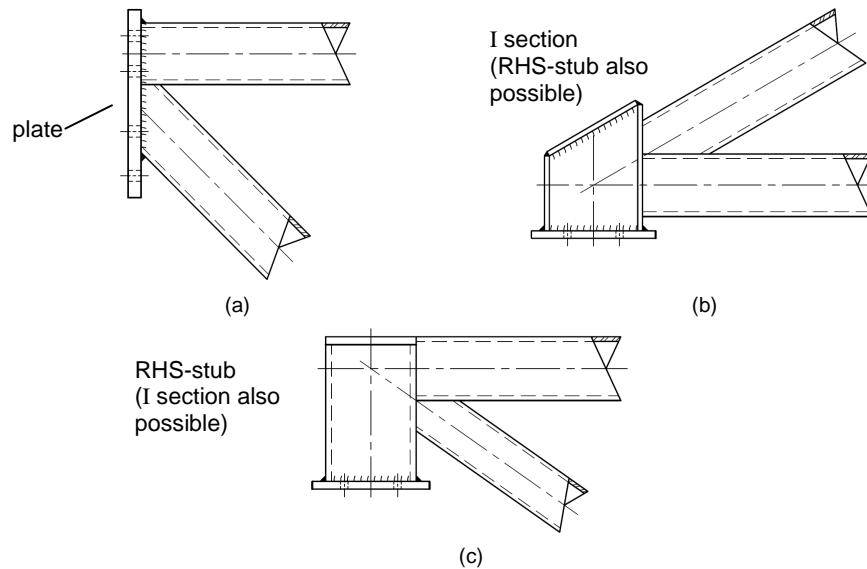
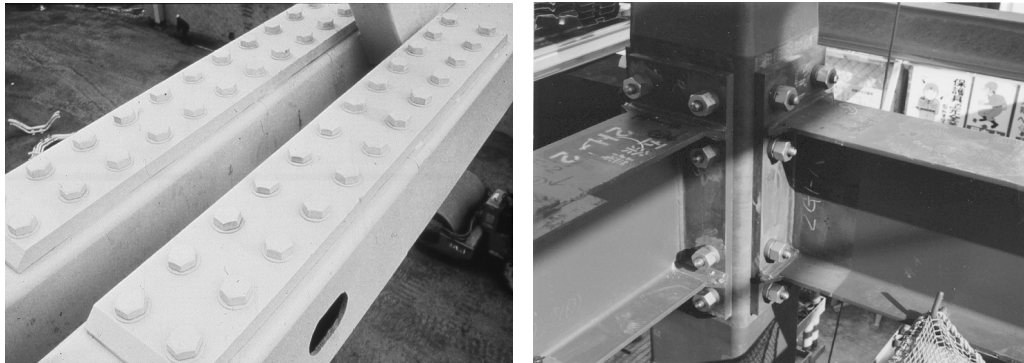


Figure 8.2 – Examples of bolted joints at the ends of RHS trusses

If fastening directly to the RHS wall, several types of mechanical fasteners that can be used are: through-bolts, blind bolts, flow-drilling, welded-on threaded studs and screws. Fasteners can generally be categorized as either loaded in shear or loaded in tension (although a combination of both sometimes occurs); examples of each are shown in figure 8.3 for direct fastening to RHS. Many more details about direct fastening methods to hollow sections are given in CIDECT Design Guide No. 7 (Dutta et al., 1998).



(a) A splice joint in a double chord truss where the bolts (loaded in shear) have been tightened with the aid of access holes  
 (b) A beam-to-column end-plate joint under moment loading, where the bolts (loaded in tension) are blind bolts

Figure 8.3 – Examples of direct fastening to RHS

### 8.1 Flange-plate joints

Flange-plate joints, as shown in figure 8.1(c), are a very popular means of joining the ends of RHS together, whether by bolting on two sides of the RHS or by bolting on all four sides of the RHS. Design procedures for both of these options are given in the following sections, for axial tension loading on the RHS member. In such joints the high-strength bolts should be fully pre-tensioned, particularly if there is any dynamic loading on the joint. Under axial compression loading, the bolts will be non-critical and the flange-plates will be in bearing. A method for handling axial load plus bending moment on the RHS member is given in section 8.1.3.

#### 8.1.1 Bolted on two sides of the RHS – tension loading

Preliminary tests on flange-plate joints bolted along two sides of the RHS were performed by Mang (1980) and Kato and Mukai (1985) followed by a more extensive study by Packer et al. (1989), illustrated in figure 8.4.

The latter tests showed that one could, by selecting specific joint parameters, fully develop the tensile resistance of the member by bolting along only two sides of the RHS. This form of joint lends itself to analysis as a two-dimensional prying problem, and a modified T stub design procedure, based on that of Struik and de Back (1969), has been advocated to evaluate the joint limit states (Packer and Henderson, 1997).



Figure 8.4 – Tension test of a flange-plate joint bolted along two RHS sides, showing plate flexure

In order for the design criteria to be valid, the centreline of the bolts in the flange-plate joint should not be positioned beyond the corner of the RHS. The limit states for the flange-plate joint, bolted on two sides, are:

- yielding of the end plate
- tensile strength of the bolts, including prying action
- strength of the weld connecting the flange-plate to the RHS

Important geometric parameters are illustrated in figure 8.5. Most codes/specifications stipulate bolts with tensile loads be fully pretensioned. This is an essential requirement for any dynamic loading situation. It has been shown that spacers placed between the flange-plates, in line with the RHS walls and parallel to the bolt lines, can preclude prying action and improve fatigue performance (Bouwman, 1979).

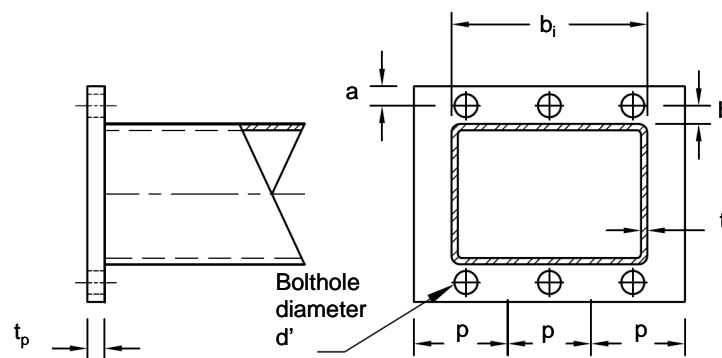


Figure 8.5 – Rectangular flange-plate joint with bolts along two sides of RHS

The modified T stub design procedure (Birkemoe and Packer, 1986) involved a redefinition of some parameters to reflect the observed location of the inner (hogging) plastic hinge line and to also represent the joint behaviour exhibited by more complex analytical models. The distance  $b$  (shown on figure 8.5) was adjusted to  $b'$ , where:

$$b' = b - (d/2) + t_f \quad 8.1$$

The term  $\alpha$  has been used in Struik and de Back's T stub prying model to represent the ratio of the (sagging) bending moment per unit plate width at the bolt line, to the bending moment per unit plate width at the inner (hogging) plastic hinge. Thus, for the limiting case of a rigid plate,  $\alpha = 0$ , and for the limiting case of a flexible plate in double curvature with plastic hinges occurring both at the bolt line and the edge of the T stub web,  $\alpha = 1.0$ . Hence, the term  $\alpha$  in Struik and de Back's model was restricted to the range  $0 \leq \alpha \leq 1.0$ . For bolted RHS flange-plate joints, this range of validity for  $\alpha$  was changed to simply  $\alpha \geq 0$ . This implies that the sagging moment per unit width at the bolt line is allowed to exceed the hogging moment per unit width, which was proposed because the RHS member tends to yield adjacent to the hogging plastic hinge and participate in the general failure mechanism. This behaviour is confirmed by the inward movement of the hogging plastic hinge (see figure 8.4).

Thus, a suitable design method for this joint type follows below. A design example, that also follows these steps, is given in section 10.5.

1. Estimate the number  $n$ , grade and size of bolts required, knowing the applied tensile force  $N_t$  and allowing for some amount of prying. In general, the applied external load per bolt should be only 60% to 80% of the bolt tensile resistance in anticipation of bolt load amplification due to prying. Hence, determine a suitable joint arrangement. The bolt pitch  $p$  should generally be about 4 to 5 bolt diameters (although closer pitches are physically possible if required), and the edge distance  $a$  about  $1.25b$ , which is the maximum allowed in calculations. Prying decreases

as the edge distance  $a$  is increased up to  $1.25b$ , beyond which there is no advantage. Then, from the joint layout, determine the ratio of the net plate area at the bolt line to the gross plate area at the hogging hinge line:

$$\delta = 1 - \frac{d'}{p} \quad 8.2$$

where:

$d'$  = the bolt hole diameter

$p$  = the length of flange-plate tributary to each bolt, or bolt pitch (see figure 8.5).

Determine a trial flange-plate thickness  $t_p$  from:

$$\sqrt{\frac{K P_f}{1 + \delta}} \leq t_p \leq \sqrt{K P_f} \quad 8.3$$

where  $P_f = \frac{N_i}{n}$  = the external factored tensile load on one bolt ( $n$  is the number of bolts), and

$$K = \frac{4 b' 10^3}{\phi_p f_{yp} p} \quad (f_{yp} \text{ in N/mm}^2 \text{ or MPa}) \quad 8.4$$

where  $\phi_p$  = flange-plate resistance factor =  $0.9 = 1/\gamma_M$ .

2. With the number, size and grade of bolts preselected, plus a trial flange-plate thickness, calculate the ratio  $\alpha$  necessary for equilibrium by:

$$\alpha = \left( \frac{K T^*}{t_p^2} - 1 \right) \left( \frac{a + (d/2)}{\delta (a + b + t_i)} \right) \text{ but } \geq 0 \quad 8.5$$

where  $T^*$  is the factored tensile resistance of one bolt. Note that the bolt tensile resistance is used in equation 8.5, because the actual total bolt force  $T_f$ , is unknown.

3. Calculate the joint factored resistance  $N_i^*$  by using  $\alpha$  from equation 8.5:

$$N_i^* = \frac{t_p^2 (1 + \delta \alpha) n}{K} \text{ but } \geq N_i \quad 8.6$$

where  $n$  is the number of bolts.

The actual total bolt tension, including prying, can be calculated by:

$$T_f \approx P_f \left( 1 + \frac{b'}{a'} \left( \frac{\delta \alpha}{1 + \delta \alpha} \right) \right) \text{ but } \leq T^* \quad 8.7$$

where:

$T_f$  = the total bolt tension

$a' = a_{\text{effective}} + d/2$

$a_{\text{effective}} = a$  but  $\leq 1.25b$  (see figure 8.5)

The  $\alpha$  value for use in equation 8.7 is given by:

$$\alpha = \left( \frac{K P_f}{t_p^2} - 1 \right) \frac{1}{\delta} \quad 8.9$$

This design method was validated experimentally and analytically (Birkemoe and Packer, 1986; Packer et al., 1989) over a flange-plate thickness range from 12 to 26 mm. It should be borne in

mind that when a joint with bolts in tension is subject to repeated loads, the flange-plate must be made thick enough and stiff enough so that deformation of the flange is virtually eliminated ( $\alpha \approx 0$ ).

### 8.1.2 Bolted on four sides of the RHS – tension loading

Research projects on flange-plate joints bolted along all four sides, as in figure 8.6, have been undertaken by Mang (1980) and Kato and Mukai (1985), but a reliable joint design procedure was not generated. Kato and Mukai proposed a complex model based on yield line theory with an estimate of the prying force. Depending on the relative strengths of the flange plate to the bolts, the ultimate strength of the joint was determined by one of six failure modes. Failure modes 1 to 3 involved failure of the flange plates, while modes 4 to 6 involved bolt failure. However, Kato and Mukai's method for proportioning flange-plate thickness does not consider the plate yield strength; furthermore, later tests showed that this model could even overestimate the strength by 25% (Caravaggio, 1988).

A thorough study of this type of bolted joint has recently been undertaken by Willibald et al. (2001, 2002, 2003a). An analysis of three-dimensional prying action and plate curvature is complex (see figure 8.7), but this work revealed that RHS flange-plate joints bolted on all four sides could still be proportioned on the basis of the two-dimensional T stub prying model of Struik and de Back (1969), with some minor modifications. Following the procedure in section 8.1.1, the inner yield lines in the flange-plate can now be expected adjacent to the RHS outer face and hence the term  $t_i$  should be deleted from equation 8.1. If the RHS is not square, or if the bolting layout is not the same on all four sides, then the bolt pitch (or the length of flange-plate tributary to each bolt) used should be the minimum of the bolt pitch for the long and the short side (assuming equal values of  $a$  and  $b$  for the long and short sides). Thus, the bolt pitch to be used is the *minimum* of  $p$  and  $p'$  in figure 8.6. This "minimum  $p$ " value is then used in equations 8.2 and 8.4 and the joint analysis then proceeds on the basis of a two-dimensional prying model. In order for this design model to be valid, the centres of the bolt holes should not be positioned beyond the corners of the RHS (as illustrated in figure 8.6). Hence, the bolts should be positioned near the RHS walls, where the tension load acts, not at the plate corners. Also, the range of experimental verification covered joints with up to 10 bolts, RHS up to 254 mm in size, and RHS aspect ratios up to 1.7.

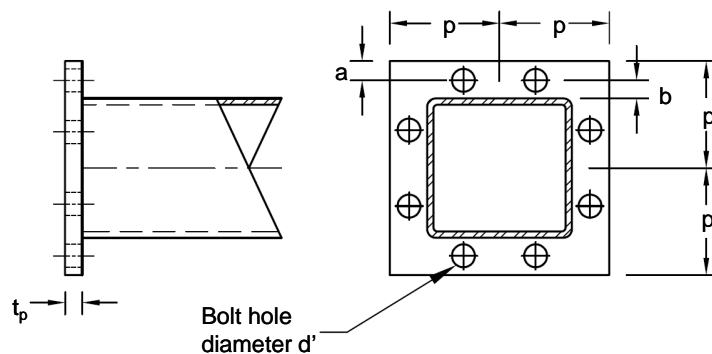


Figure 8.6 – Rectangular flange-plate joint with bolts along four sides of RHS



Figure 8.7 – Tension test of a flange-plate joint bolted along one side of an RHS (four bolts; thin plates)

When two or more bolts are used along one side of an RHS, the distance between adjacent bolts,  $c$ , should be as low as possible. (The dimension  $c$  is also illustrated in section 10.5). Figure 8.8 illustrates that as the ratio  $c/h_i$  decreases (where  $h_i$  is the depth of the RHS wall adjacent to the bolts), the magnitude of the bolt prying force decreases. This figure further shows the trade-off between thick flange-plates (with low bolt prying) and thin flange-plates (with high bolt prying).

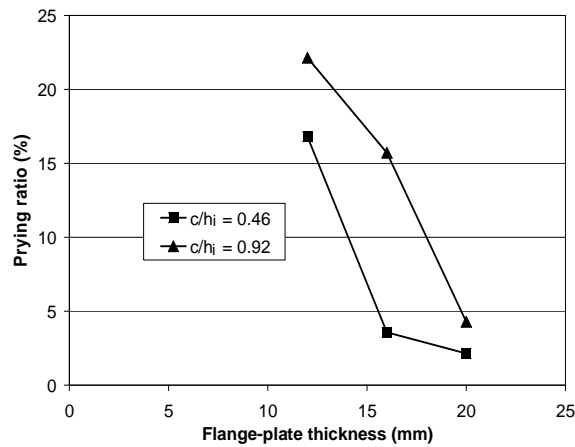


Figure 8.8 – Effect of distance between bolts,  $c$ , on one side of an RHS, on the magnitude of prying

### 8.1.3 Flange-plate joints under axial load and moment loading

Design methods for bolted flange-plate joints to date have generally been developed for axial tension loading on the RHS member. Frequently, however, hollow sections are subjected to both axial tension load ( $N_i$ ) and bending moment ( $M_i$ ). In such cases, a hypothetical “effective” axial load can be computed (Kurobane et al., 2004) for use with the flange-plate joint design procedures given in sections 8.1.1 and 8.1.2:

$$\text{Effective axial} = \left( \frac{N_i}{A_i} \pm \frac{M_i}{W_i} \right) A_i \quad 8.10$$

where:

$A_i$  = cross sectional area of the RHS

$W_i$  = RHS elastic (or plastic) section modulus

This procedure will be conservative as it computes the maximum tensile normal stress in the RHS and then applies this to the whole member cross section.

## 8.2 Gusset plate-to-RHS joints

### 8.2.1 Design considerations

RHS brace members can be field bolted to gusset plates which have been shop welded to RHS chord members, thus producing bolted shear joints as shown in figure 8.9. Such configurations are an option when transportation constraints compel field joints, and bolting has been selected over site welding.

If dynamic loading is a design consideration, this type of joint has an advantage over bolted flange-plate joints in that flange plates must be proportioned to eliminate all prying when fatigue loads are present. In general static load applications, however, the gusset-plate joint is less aesthetically pleasing and often more expensive than its flange-plate counterpart.

An important limitation to the use of RHS gusset-plate joints is the need to have closely matching member widths. Equal width members may be connected directly as in figure 8.9(a), but the gussets often need to be spread slightly by jacking after welding is complete in order to allow field assembly (since welding contraction tends to pull the gussets inwards). Small width differences can be adjusted by the use of filler plates welded on the sides of the brace member. Larger differences allow the further option of extra shim plates, figure 8.9(b), which can be more convenient in the field.

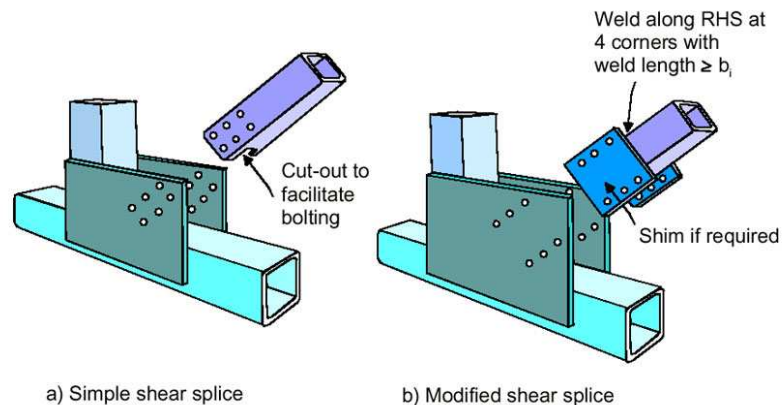


Figure 8.9 – Bolted RHS gusset-plate joints

### 8.2.2 Net area and effective net area

The concept of gross area, net area and effective net area can be used to describe various failure modes for a tension member with holes or openings and these concepts will be utilized herein. Most codes/specifications have very similar checks, with the resistance or safety factors that are applied sometimes varying. The three basic checks are exemplified by (CSA, 2009):

- |  |   |      |
|--|---|------|
| (1) $T^* = \phi A_g f_y$                                 | (yielding of gross area)                        | 8.11 |
| (2) $T^* = \phi_u (A_n f_u + 0.58 A_{gv} (f_y + f_u)/2)$ | (rupture of areas in tension and shear)         | 8.12 |
| (3) $T^* = \phi_u A_{ne} f_u$                            | (rupture of effective net area, with shear lag) | 8.13 |

where  $\phi$  ( $= 1/\gamma_M$  in Eurocode 3 (CEN, 2005a, 2005b)) is a resistance factor for ductile yielding which can be taken as 0.9 (CSA, 2009; AISC, 2005) or 1.0 (Eurocode 3). The  $\phi_u$  resistance factor for brittle rupture is taken as 0.75 by CSA (2009) and AISC (2005), and  $1/\gamma_M = 0.80$  in Eurocode 3 (CEN, 2005a, 2005b).

The net area,  $A_n$ , is the total net area in tension along a potential failure path through the member. The gross area in shear,  $A_{gv}$ , represents the total area failing in shear, for the same failure path through the member. Equation 8.12 recognizes that the failure path can incorporate segments loaded in tension, in shear, or even combinations of the two, and thus includes the “block shear” failure mode where a chunk of material tears out of the member. For the segment loaded in shear in equation 8.12, the gross area (ignoring bolt holes) is taken as the critical area and at a failure stress that is an average of  $0.58f_y$  and  $0.58f_u$  (Driver et al., 2006).

An illustrative example of the application of equation 8.12, which includes area segments loaded in tension, shear and a combination thereof, is the gusset plate Y joint in figure 8.10, where the “block shear” area of the gusset plate is calculated from the proposed failure line A-B-C-D-E-F-G-H-J-K-L-M.

- The tension segment, normal to the load (AB) has:

$$A_n = (g_1 - d'/2) t$$

- Shear segments parallel to the load (G to M) have, in total:

$$A_{gv} = Lt$$

- Each inclined segment (CD or EF), subject to both tension and shear, can be treated as quasi-tension segments with an adjusted net area such that, for each segment:

$$A_n = (g_2 - d') t + (s^2/4g_2) t$$

For bolted joints, the effective net area reduced for shear lag,  $A_{ne}$ , is the net tensile area  $A_n$  multiplied by a shear lag reduction factor ( $\leq 1.0$ ). Shear lag applies when a member is connected by some – but not all – of its cross sectional area and the critical failure path includes parts of the unconnected cross section. Thus, equation 8.13 may not always be applicable. It is not applicable, for example, in considering any failure path of the gusset plate in figure 8.10, because the whole “tension member” (the gusset plate) is loaded.

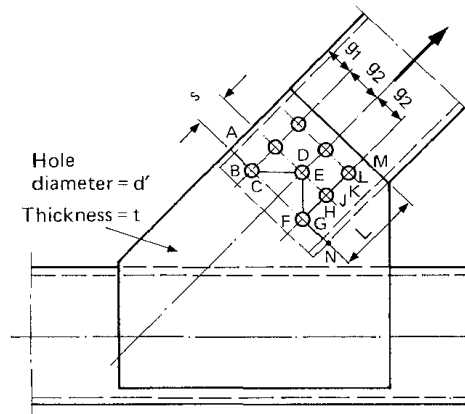


Figure 8.10 – Calculation of net area  $A_n$  (in tension) and gross area  $A_{gv}$  (in shear) for a gusset plate

The shear lag factor to be applied to  $A_n$  ( $A_{ne} = \text{shear lag factor} \times A_n$ ), is given in most codes/specifications for bolted joints; for example, for CSA (2009) this shear lag factor is:

- 0.90 when shapes like I sections (or tees cut from them) are connected only by their flanges with at least three transverse rows of fasteners (flange width  $\geq 2/3$  the depth),
- 0.85 for structural shapes such as RHS connected with three or more transverse rows of fasteners,
- 0.75 for structural shapes such as RHS connected with two transverse rows of fasteners.

For example, if the brace member in figure 8.10 was an RHS and it was bolted to gusset plates on two sides, as suggested in the figure, with each side having eight bolts in three rows (as shown), then the reduced effective net area,  $A_{ne}$ , to be applied to the RHS tension member in equation 8.13 would be  $0.85A_n$ . In this instance, the net area  $A_n$  would be the gross RHS cross sectional area minus the  $2 \times 3$  bolt holes in the first bolt row. An example of the failure mode of an RHS tension member, bolted to gusset plates along just two RHS sides, is given in figure 8.11.



Figure 8.11 – Tear out failure mode for a bolted RHS (with a hand access hole cut-out) in tension

The effective net area reduced for shear lag,  $A_{ne}$ , also applies to *welded* joints when a member is not welded all around its cross section, for example when an element (i.e. a part of the cross section) is connected along its edge(s) by welds parallel to the direction of load. Such a case is illustrated in figure 8.9(b) where bolting plates are welded to the sides of the RHS brace member. For welds parallel to the direction of load (as the four flare groove welds would be in figure 8.9(b), along the four corners of the RHS), the shear lag factor is a function of the weld lengths and the distance between them. The distance between these welds would be  $b_i$  or  $h_i$ , for orthogonal sides of the RHS brace. Also, the RHS brace can be reduced to four area elements, with the approximate gross area of the brace being equal to  $2t(b_i - t_i) + 2t(h_i - t_i)$ . Thus, shear lag reduction factors can be applied to each of the four element areas (two of width  $w = b_i - t_i$ , and two of width  $w = h_i - t_i$ ), to produce a total effective net area of the RHS reduced by shear lag,  $A_{ne}$ , for use in equation 8.13. Suggested shear lag reduction factors for these four element areas, in terms of the weld length  $L_w$ , are (CSA, 2009):

- 1.00 when the weld lengths ( $L_w$ ) along the RHS corners are  $\geq 2b_i$  (or  $2h_i$  as applicable)
- $(0.5 + 0.25L_w/b_i)$  when the weld lengths along the RHS corners are  $b_i \leq L_w < 2b_i$ , or
- $(0.5 + 0.25L_w/h_i)$  when the weld lengths along the RHS corners are  $h_i \leq L_w < 2h_i$
- $0.75L_w/b_i$  when the weld lengths along the RHS corners are  $L_w < b_i$  (or  $h_i$  as applicable)

Section 7.5 of this Design Guide discusses another application of shear lag to welded plate-to-RHS joints, where again the shear lag effect is a function of the weld length divided by the distance between the welds.

Another failure that must be checked, in gusset-plate joints such as shown in figures 8.9 and 8.10, is yielding across an effective dispersion width of the plate. This can be calculated using the Whitmore (1952) effective width concept, illustrated in figure 8.12. For this failure mode (for two gusset plates):

$$N_i^* = 2 \phi f_{yp} t_p (g + 1.15 \Sigma p)$$

8.14

where  $\phi = 0.9 (= 1/\gamma_M)$  is conservative. The term  $\Sigma p$  represents the sum of the bolt pitches in a bolted joint or the length of the weld in a welded joint.

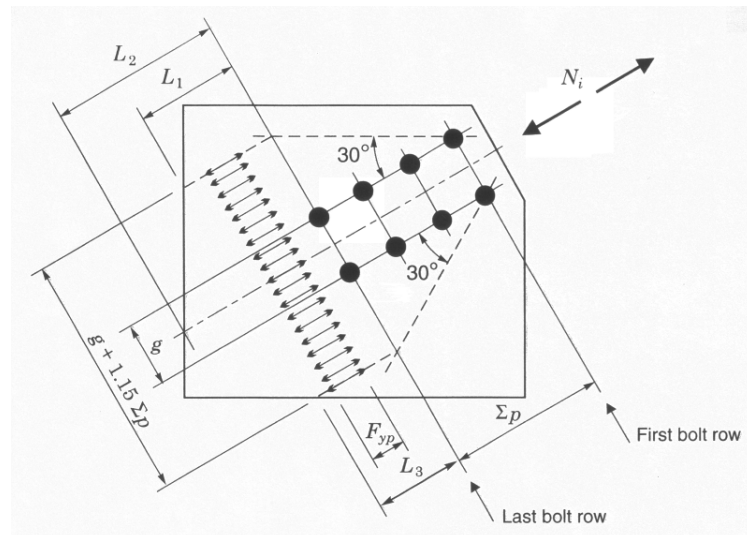


Figure 8.12 – Whitmore criterion for gusset-plate yielding or buckling

The use of  $N_i^*$  indicates that this check applies to both tension and compression load cases. If the member is in compression, buckling of the gusset plate must also be prevented. A suitable method for checking the buckling resistance is given by Thornton (1984). The gusset plate compressive resistance is the column resistance given by an applicable code/specification for a column having a width of  $(g + 1.15 \Sigma p)$ , a depth equal to the gusset-plate thickness, a length equal to the minimum of  $L_1$ ,  $L_2$  and  $L_3$  and an effective length factor  $K$  of 0.65.  $L_1$ ,  $L_2$  and  $L_3$  (see figure 8.12) are determined by points on the connected edges of the gusset plate, depending on the shape of the gusset plate.

### 8.3 Hidden bolted joints

In some projects, such as where Architecturally Exposed Structural Steel (AESS) has been specified for aesthetic purposes, it may not be possible to have bolts exposed to view, yet the alternative of full site welding may be extremely costly. In such situations, RHS members may be site-bolted together using the technique shown in figure 8.13. Initially, single splice plates are shop-welded into adjoining RHS ends, these are then site-bolted together (preferably keeping the shear plane of the connection coaxial with the two members), and then the joint is finished by adding non-structural cover plates – in the shape of the RHS. Small gaps can be filled with epoxy before painting, thus giving the appearance of a welded joint.

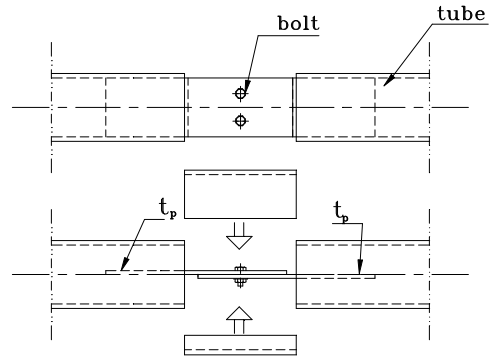
Experimental and numerical research on this RHS joint type, under tension loading, has been undertaken by Willibald et al. (2003b). This has confirmed that existing design methods can be used to analyze the pertinent limit states of the RHS, which are:

- (1) yielding of the gross area of the cross section (equation 8.11)
- (2) block shear tear-out of two opposite RHS walls (equation 8.12)
- (3) fracture of the gross area of the RHS, induced by shear lag (equation 8.13).

Access inside the RHS to make adequate welds can be a problem, hence short weld lengths will be typical and welding of the plate to the longer RHS wall will be beneficial. With short weld lengths, block shear tear-out can be expected to become the governing limit state.



(a) Insertion of plate and welding to the RHS



(b) Completion with a non-structural cover, after bolting

Figure 8.13 – Construction of a hidden bolted joint

## 9 Other uniplanar welded joints

### 9.1 Reinforced joints

Instances may occur when a truss joint has an inadequate resistance, and a designer needs to resort to some form of joint reinforcement. Such a situation might arise if RHS material was ordered on the basis of member selection only, without joint capacity checks being performed. Alternatively, only one or a few joints of a truss may be inadequate due to the selection of a particular chord member, and hence, just these critical joints could be reinforced. The labour costs associated with joint reinforcement are significant, and the resulting structure may lose its aesthetic appeal, but in many cases it may be an acceptable solution.

#### 9.1.1 With stiffening plates

The most common method of strengthening RHS joints is to weld a stiffening plate (or plates) to the RHS chord member. It is particularly applicable to gap K joints with rectangular chord members, although an unstiffened overlap joint is generally preferable from the viewpoints of economy and fatigue. However, a gap joint with a stiffening plate eliminates the necessity for double cuts on the brace members, and in certain cases may prove more acceptable to the fabricator. The addition of a flat plate welded to the connecting face of the chord member greatly reduces local deformations of the joint and consequently the overall truss deformations are reduced. It also permits a more uniform stress distribution in the brace members.

The type of reinforcement required depends upon the governing failure mode which causes the inadequate joint capacity. Two types of plate reinforcement – in one case to the chord connecting face and in the other to the chord side walls – are shown in figure 9.1. Both of these would be applicable to joints with RHS chord members and either CHS or RHS brace members. An alternative to stiffening a joint with plates is to insert a length of chord material of the required thickness at the connection, the length of which would be the same as  $L_p$  given below. This is equivalent to the use of a “joint can” in offshore steel structures, see section 4.6 of CIDECT Design Guide No. 1 (Wardenier et al., 2008).

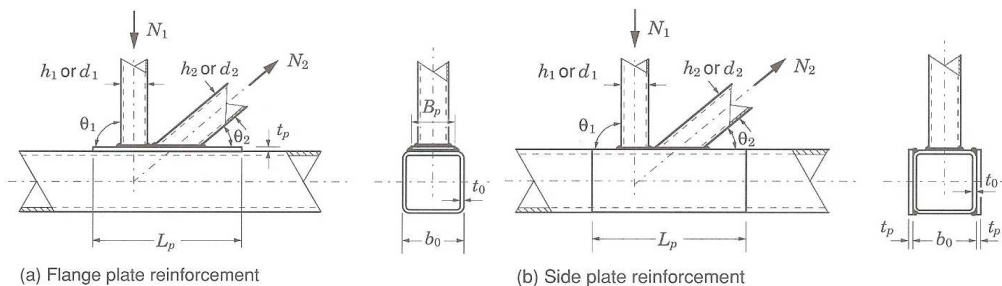


Figure 9.1 – Pratt truss joint with plate stiffening  
 (a) Flange plate reinforcement  
 (b) Side plate reinforcement

#### 9.1.1.1 T, Y and X joints

Under tension or compression brace loading, the capacity of a T, Y or X joint is typically controlled by either chord face plastification or chord side wall failure, as summarized in table 4.1. When chord face plastification governs, the joint capacity can be increased by using flange plate reinforcement similar to the joint shown in figure 9.1(a). This will usually occur when  $\beta \leq 0.85$ . When chord side wall failure controls, the joint capacity can be increased by reinforcing with a pair of side plates similar to the joint shown in figure 9.1(b). This failure mode will usually govern when  $\beta \approx 1.0$ .

For T, Y and X joints stiffened with side plate reinforcement, a recommended procedure for calculating the necessary stiffening plate thickness is to use the chord side wall resistance expression in table 4.1, by replacing  $t_0$  with  $(t_0 + t_p)$  for the side walls. The stiffening plates should have a length  $L_p$  (see figure 9.1(b)), such that for T and Y joints:

$$L_p \geq \frac{1.5h_1}{\sin \theta_1} \quad 9.1$$

For T, Y and X joints stiffened with a flange plate, there is a difference in behaviour of the stiffening plate, depending on the sense of the load in the brace member. With a tension load in the brace, the plate tends to lift off the chord member and behaves as a plate clamped (welded) along its four edges. The strength of the joint thereby depends only on the plate geometry and properties, and not on the chord connecting face. Thus, for tension brace loading, if one applies yield line theory to the plate-reinforced T, Y or X joint with rectangular members, the joint factored resistance can be reasonably estimated by the equation for chord face plastification in table 4.1, if

- $f_{y0}$  is replaced by:  $f_{yp}$
- $t_0$  is replaced by:  $t_p$
- $\beta$  is replaced by:  $\beta_p = b_1/B_p$
- $\eta$  is replaced by:  $\eta_p = h_1/B_p$

where  $B_p$  is the plate width.

In order to develop the yield line pattern in the stiffening plate, the length of the plate  $L_p$ , should be at least:

$$L_p \geq \frac{h_1}{\sin \theta_1} + \sqrt{B_p (B_p - b_1)} \quad 9.2$$

Also, the plate width  $B_p$  should be such that a good transfer of loading to the side walls is achieved; for example  $B_p \approx b_0$  (see figure 9.1(a)).

For T, Y and X joints stiffened with a flange plate, and under compression brace loading, the plate and connecting chord face can be expected to act integrally with each other. This type of joint has been studied by Korol et al. (1982), also using yield line theory. Hence for  $\beta_p \leq 0.85$  (a reasonable upper limit for application of yield line analysis also employed for unreinforced joints), the following plate design recommendations (Korol et al., 1982) are made to obtain a full strength joint:

- $B_p \geq$  flat width of chord face
- $L_p \geq 2b_0$
- $t_p \geq 4t_1 - t_0$

The application of the above guidelines, for compression loaded X, T and Y joints, should ensure that the joint capacity exceeds the brace member capacity, provided that chord side wall failure by web crippling is avoided (Korol et al., 1982).

### 9.1.1.2 K and N joints

The capacity of gap K joints is controlled by criteria either related to the chord face or to the chord side wall, as summarized in tables 4.1 and 4.2. When chord face plastification, chord punching shear or local yielding of a brace controls, the joint capacity can be increased by using flange plate reinforcement as shown in figure 9.1(a). This will usually occur when  $\beta < 1.0$ . When chord shear controls, the joint capacity can be increased by reinforcing with a pair of side plates as shown in figure 9.1(b). This failure mode will usually govern when  $\beta = 1.0$  or  $h_0 < b_0$ .

The first design guidance available for K joints stiffened with a flange plate, as shown in figure 9.1(a), was given by Shinouda (1967). However, this method was based on an elastic deformation requirement of the connection plate under specified (service) loads. A more logical limit states approach which is recommended for calculating the necessary stiffening plate thickness for gap K joints is to use the joint resistance expressions in table 4.1 (general), and table 4.2 (for SHS or CHS

brace members to SHS chord members) by considering  $t_p$  as the chord face thickness and neglecting  $t_0$ . Also, the plate yield stress should be used. It is suggested that proportioning of the stiffening plate be based on the principle of developing the capacity of the brace members ( $A_i f_{yi}$ ). Dutta and Würker (1988) consider that in most cases this will be achieved providing  $t_p \geq 2t_1$  and  $2t_2$ . The required thickness can also easily be determined with the design graphs in chapter 4. Careful attention should be paid to the stiffening plate-to-chord welds which should have a weld throat size at least equal to the wall thickness of the adjacent brace member (Dutta and Würker, 1988). The stiffening plate should have a minimum length  $L_p$  (see figure 9.1(a)), such that:

$$L_p \geq 1.5 \left( \frac{h_1}{\sin \theta_1} + g + \frac{h_2}{\sin \theta_2} \right) \quad 9.3$$

A minimum gap between the brace members, just sufficient to permit welding of the brace members independently to the plate is suggested. All-round welding is generally required to connect the stiffening plate to the chord member, and in order to prevent corrosion on the two inner surfaces. It may also be advisable to drill a small hole in the stiffening plate under a brace to allow entrapped air to escape prior to closing the weld. This will prevent the expanding heated air from causing voids in the closing weld (Stelco, 1981).

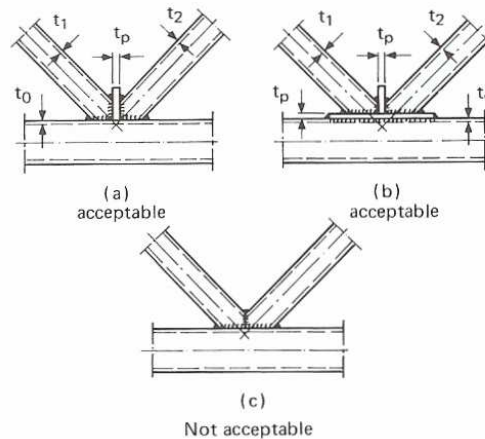


Figure 9.2 – Some acceptable and unacceptable, non-standard truss K joints

In order to avoid partial overlapping of one brace member onto another in a K joint, fabricators may elect to weld each brace member to a vertical stiffener as shown in figure 9.2(a).

Another variation on this concept is to use the reinforcement shown in figure 9.2(b). For both of these joints,  $t_p \geq 2t_1$  and  $2t_2$  is recommended (Dutta and Würker, 1988). Designers should note that the K joint shown in figure 9.2(c) is not acceptable, as it does not develop the strength of an overlapped K joint. Also, it is difficult to create and ensure an effective saddle weld between the two brace members.

If the capacity of a gap K joint is inadequate and the chord shear criterion is the governing failure mode, then as mentioned before, one should stiffen with side plate reinforcement, as shown in figure 9.1(b). A recommended procedure in this case for calculating the necessary stiffening plate thickness is to use the chord shear resistance expression in table 4.1, by calculating  $A_v$  as  $2h_0(t_0 + t_p)$ . The stiffening plates should again have a minimum length,  $L_p$  (see figure 9.1(b)), given by equation 9.3 and have the same depth as the chord member.

### 9.1.2 With concrete filling

A less visible alternative to adding stiffening plates to the exterior of an RHS is to fill the hollow section chord with concrete or grout. Filling the chord members of an RHS truss, either along the full length of the chord or just in the vicinity of critical joints, has two main disadvantages: the concrete will increase the dead weight of the structure, and it involves a secondary trade with its associated costs. On the other hand, the strength of certain joints may increase, and if the members are completely filled, there are further benefits of enhanced member capacity (due to composite action), increased truss stiffness and improved fire endurance. Further, as shown in figure 9.3, the joint deformations are considerably reduced.

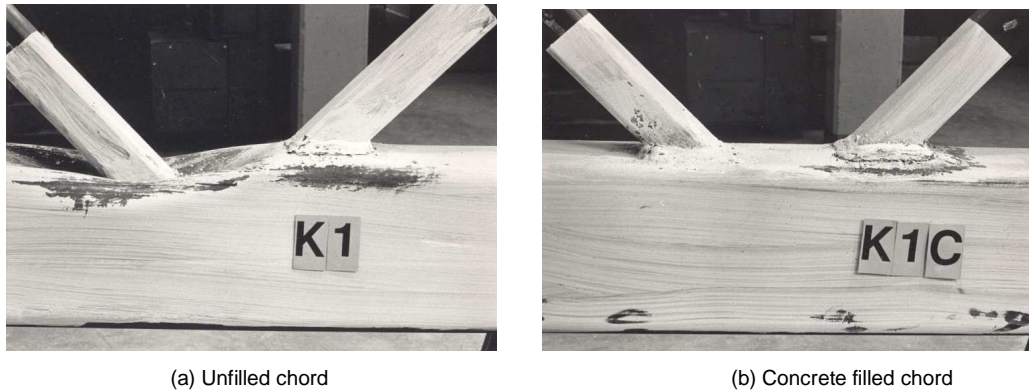


Figure 9.3 – K joint with (a) unfilled chord and (b) concrete filled chord

Concrete filling of chord members can be done in the fabrication shop by tilting the truss and using a concrete or grout with a high fluidity.

The joints which benefit most from concrete filling are X joints with the brace members loaded in compression; i.e. joints at which a compression force is being transferred through the RHS. Examples of such joints are truss reaction points, truss joints at which there is a significant external concentrated load, and beam-to-RHS column moment joints, as illustrated in figure 9.4.

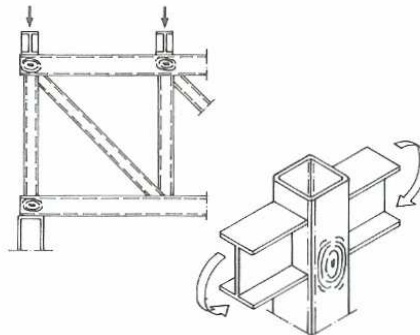


Figure 9.4 – Applications for which concrete filling of RHS may improve the joint resistance

Packer (1995) has performed experimental research on a variety of concrete filled RHS joints, resulting in the design recommendations below. The RHS provides confinement for the concrete, which allows it to reach bearing capacities greater than its crushing strength as determined by cylinder compression tests (Packer and Fear, 1991). It has also been shown that a moderate amount of shrinkage of the concrete (or grout) away from the RHS inside walls does not have a negative impact on the strength of a concrete filled joint.

### 9.1.2.1 X joints with braces in compression

The factored resistance of a concrete filled RHS, compression loaded X joint can be taken as:

$$N_1^* = \phi_c f_c' \frac{A_1}{\sin \theta_1} \sqrt{A_2 / A_1} \quad 9.4$$

where:

$\phi_c$  = resistance factor for concrete in bearing (0.65 may be used)

$f_c'$  = crushing strength of concrete by cylinder tests

$A_1$  = bearing area over which the transverse load is applied

$A_2$  = dispersed bearing area

and:

- $A_2$  should be determined by dispersion of the bearing load at a slope of 2:1 longitudinally along the chord member, as shown in figure 9.5 for transverse compression ( $\theta_1 = 90^\circ$ ). For an inclined brace,  $h_1$  in the expression for  $A_2$  should be replaced by  $h_1/\sin \theta_1$
- the value of  $A_2$  may be limited by the length of concrete
- $\sqrt{A_2 / A_1}$  cannot be taken greater than 3.3

The following are also recommended for general design application of equation 9.4:

$$- h_0/b_0 \leq 1.4$$

$$- L_c \geq \frac{h_1}{\sin \theta_1} + 2h_0$$

where  $L_c$  is the length of concrete in RHS chord member.

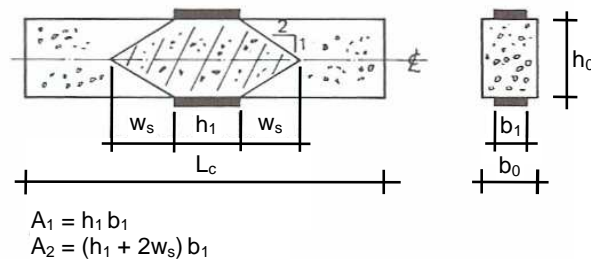


Figure 9.5 – Applied load area ( $A_1$ ) and dispersed load area ( $A_2$ ) for a concrete filled RHS loaded in transverse compression

### 9.1.2.2 T and Y joints with brace in compression

Since for T and Y joints subjected to brace compression, the load is being resisted by shear forces in the chord rather than being transferred through the chord, the dispersed bearing area  $A_2$  should be calculated assuming a stress distribution longitudinally at a slope of 2:1 through the *entire* depth of the chord, rather than to an ( $A_2/A_1$ ) limit. Thus, with respect to figure 9.5, the dispersed bearing area ( $A_2$ ) would be adjusted (for an inclined branch) to:

$$A_2 = \left( \frac{h_1}{\sin \theta_1} + 4h_0 \right) b_1 \quad 9.5$$

Similarly, the limit of validity for  $L_c$  would need to be adjusted to  $L_c \geq \frac{h_1}{\sin \theta_1} + 4h_0$ . The resistance of these joints can then be calculated using equation 9.4.

### 9.1.2.3 T, Y and X joints with brace(s) in tension

In tests, none of the concrete filled joints with brace(s) in tension exhibited a decrease in joint yield or ultimate strength, relative to their unfilled counterparts, by more than a few percent. The concrete filled joints still had large joint deformations, so their design should also be based on the joint yield load. Thus, it is recommended that the design capacity of these joints be calculated using existing design rules for unfilled RHS joints (tables 4.1 and 4.2).

### 9.1.2.4 Gap K joints

For the range of joint parameters studied experimentally (Packer, 1995), gap K joints with concrete filled chords were found to have superior joint yield strengths and ultimate strengths relative to their unfilled counterparts. Also, concrete filling of such joints has been found to produce a significant change in joint failure mode, as illustrated in figure 9.3.

It is recommended that the joint resistance be calculated separately for the compression brace and the tension brace. For the compression brace, which presses on a relatively rigid foundation of concrete, the joint strength would appear to be limited by bearing failure of the concrete. Hence, calculations should be performed for a Y joint with the brace in compression (see above). For the tension brace, the concrete filling only permits two possible failure modes: (i) premature (local) yielding of the tension brace, and (ii) punching shear of the chord face around the brace. These two failure modes are a subset of the possible limit states experienced with unfilled gap K joints, and resistance formulae are given in table 4.1.

## 9.2 Cranked-chord joints

“Cranked-chord” joints arise in certain Pratt or Warren trusses such as the one shown in figure 9.6 and are characterized by a crank or bend in the chord member at the joint noding point. The crank is achieved by butt (groove) welding two common sections together at the appropriate angle, and the intersection of the three member centre-lines is usually made coincident. The uniqueness of this cranked-chord joint lies both in its lack of a straight chord member and the role of the chord member as an “equal width brace member”.

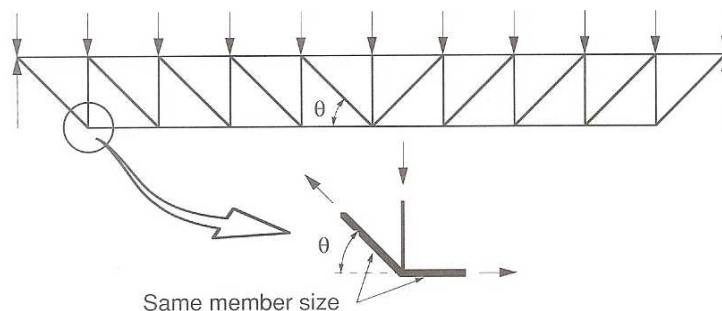


Figure 9.6 – Cranked-chord joint in a Pratt truss

An experimental research programme with SHS and RHS members (Packer, 1991) has revealed that unstiffened, welded, cranked-chord RHS joints behave generally in a manner dissimilar to RHS T or Y joints, despite their similar appearance (they all have a single brace member welded to a uniform-size chord member). Instead, cranked-chord RHS joints have been shown to behave as overlapped K or N joints, and their capacity can be predicted using the criterion for local yielding of the overlapping brace given in table 4.3. Note: the brace shear criterion and the chord yielding criterion based on the interaction of moment and axial load are not applicable here.

Thus, cranked-chord joints can be interpreted as overlapped K joints as shown in figure 9.7, wherein one chord member can be given an imaginary extension and the cranked-chord member is considered to be the overlapped brace member. A design example for a cranked-chord joint is given in section 10.4.

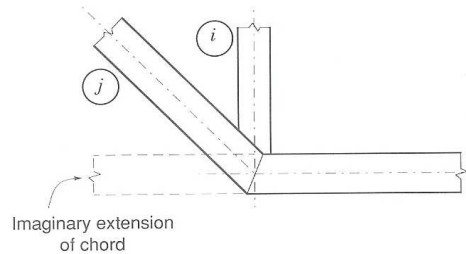


Figure 9.7 – Cranked-chord joint represented as an overlapped N joint

### 9.3 Trusses with RHS brace (web) members framing into the corners of the RHS chord (bird-beak joints)

With multiplanar or uniplanar RHS trusses, it is also possible to have the truss brace members framing into the corners of an RHS chord member, as shown in figure 9.8. This necessitates very careful profiling of the brace member end, particularly where corner radii are large, into so called “bird-beak”, “bird mouth” or “bill-shaped” joints. Such a member arrangement has been used occasionally in North America, for example in the Minneapolis Convention Center Roof and in the Minneapolis/St. Paul Twin Cities Airport Skyway.

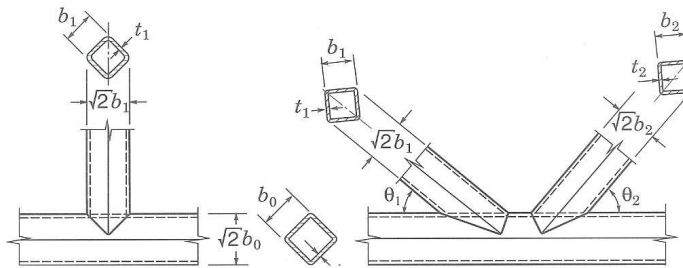


Figure 9.8 – RHS “bird beak” T and K joints

It has also been used in Japan, where in this case a robot was developed to profile the ends of the brace members. By framing into the corners of the RHS chord member a high joint strength and stiffness is achieved, regardless of the brace to chord member width ratio. Ono et al. (1991, 1993, 1994) and Ishida et al. (1993) have undertaken experimental studies of such square RHS T and K joints. In their tests, both the chord and braces were rotated through 45° about the member axis, as shown in figure 9.8. All of the 25 T joints tested had the brace loaded in compression, and the 16 K joints had all brace members inclined at  $\theta_1 = \theta_2 = 45^\circ$  to the chord. It was found that for low to medium  $\beta$  ratios, the “bird beak” joints are much stronger than their conventional RHS counterparts.

Ono et al. (1991) and Ishida et al. (1993) concluded that the joint ultimate strengths for axially loaded T joints could be given by:

$$N_{u1} = f_{y0} t_0^2 \left( \frac{1}{0.211 - 0.147 b_1/b_0} + \frac{b_0/t_0}{1.794 - 0.942 b_1/b_0} \right) f(n') \quad 9.6$$

For K joints, however, the equations in their publications differ, whereas no explanation is given. Furthermore, considering the various modes of failure and the many parameters influencing the joint strength, the K joint tests only give an indication for the range investigated. Thus the equations have to be used with care and are only given for indication. As an example, Ono et al. (1991) give for axially loaded K joints:

$$N_{u1} = \frac{f_{y0} t_0^2}{\sqrt{1 + 2 \sin^2 \theta_1}} 4\alpha b_0/t_0 f(n') \quad 9.7$$

where the effective area coefficient  $\alpha$  is given for 45°K joints in figure 9.9.

$f(n')$  is the chord stress function previously used for CHS joints in the 1<sup>st</sup> edition of CIDECT Design Guide No. 1 (Wardenier et al., 1991) to allow for the influence of normal stresses in compression chords, and is given by:

$$f(n') = 1.0 + 0.3n' - 0.3n'^2 \quad \text{for } n' < 0 \text{ (chord compression prestress)} \quad 9.8a$$

$$f(n') = 1.0 \quad \text{for } n' \geq 0 \text{ (chord tension prestress)} \quad 9.8b$$

$$\text{where } n' = f_{op}/f_{y0} \quad 9.8c$$

For consistency, it is recommended to use the  $Q_f$  function of table 4.1 instead of  $f(n')$ .

As these equations are based on a regression analysis of the test data, one should be careful to ensure that they are only applied within the approximate bounds of parameter ranges examined in the tests, i.e.:

$$16 \leq b_0/t_0 \leq 42 \text{ and } 0.3 \leq b_1/b_0 \leq 1.0 \quad \text{for T joints}$$

$$16 \leq b_0/t_0 \leq 44, 0.2 \leq b_1/b_0 \leq 0.7 \text{ and } \theta_i \approx 45^\circ \text{ for K joints}$$

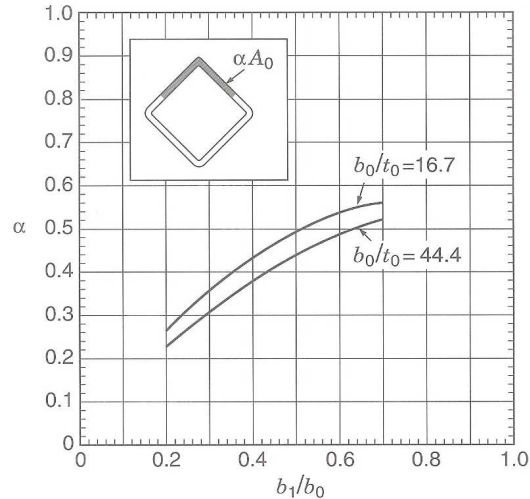


Figure 9.9 – Effective area coefficient  $\alpha$ , for “bird beak” 45°K joints

Further work is reported on T joints loaded by in-plane bending (Ono et al., 1993) and for out-of-plane bending (Ono et al., 1994). These equations also require further investigation and analysis before they can be presented as design recommendations.

Davies and Kelly (1995), Davies et al. (1996, 2001) and Owen et al. (1996) investigated several aspects of these bird beak joints numerically, however without proposing design equations.

#### 9.4 Trusses with flattened and cropped-end CHS brace members to RHS chords

For statically loaded hollow section trusses of small to moderate span, cropping – a procedure in which a CHS brace member is simultaneously flattened and sheared – can simplify fabrication and reduce cost. The procedure is faster than sawing or profiling, the conventional methods of preparing CHS brace members for welding to RHS and CHS chords, respectively, and it simplifies the welding process. Typical cropped-brace Warren truss joints to an RHS chord member are shown in figure 9.10. Note that the flattened ends of the brace member can be aligned in the direction of the truss or transverse to it. For all trusses with flattened or cropped-brace members, an effective length factor ( $K$ ) of 1.0 should be used for the design of the brace members.

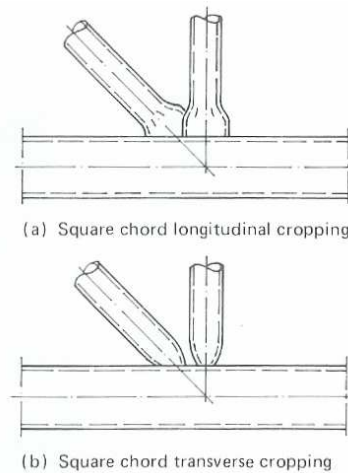


Figure 9.10 – Cropped-brace joints to an RHS chord

Flattening the CHS brace in the plane of the truss (figure 9.10(a)) does not provide as good a structural performance, nor the economies of fabrication, compared to transverse flattening (Grundy and Foo, 1991). Although this has been argued for CHS chord members, the transverse flattening of CHS brace members and welding to RHS chord members is the basis of the “Starch” roof system (Papanikolas et al., 1990). At this stage, no design guidance is available for such joints to RHS chords.

Various types of flattening can be performed on CHS brace members, as illustrated in figure 9.11. In the case of full or partial flattening, the maximum taper from the tube to the flat should remain within 25% (or 1:4). For  $d/t$  ratios exceeding 25, the flattening will reduce the brace member compressive strength (CIDECT, 1984). For welded joints, the length of the flat part should be minimized for compression brace members to avoid local buckling in the flattened region.

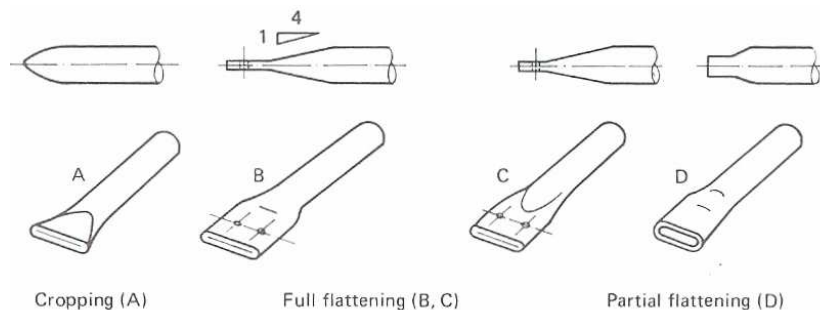


Figure 9.11 – Various types of flattening for CHS brace members

Considerable research has been performed on in-plane cropped-end CHS braces to RHS trusses by Ghosh and Morris (1981), Morris (1985) and Lau et al. (1985). The latter tests had the geometry shown in figure 9.12, in which the toes of the flattened brace members just met at the chord face, with no overlap or gap between them, and with braces at 45°.

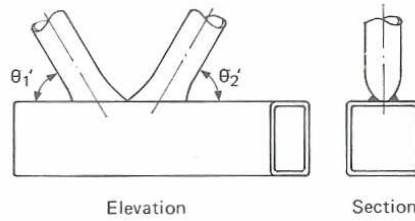


Figure 9.12 – Cropped-brace, zero gap Warren joints

For the joint configuration in figure 9.12, with symmetrical brace members, Morris and Packer (1988) showed that the joint resistance is given by:

$$N_1^* = 0.4N_{y1} \left( 1 + 0.02 \frac{b_0}{t_0} \right) \left( 1 + 1.71 \frac{d_1}{b_0} \right) \quad 9.9$$

where:

$$N_{y1} = \frac{f_{y0} t_0^2}{\sin \theta_1} \left( \frac{\pi}{2} + \frac{b_1' + 2h_1'}{b_0 - b_1'} + \frac{1.32}{t_0} \sqrt{\frac{f_{y1}}{f_{y0}} \tan \theta_1' b_0 t_1} \right) Q_f \quad 9.10$$

$$- b_0' = b_0 - t_0$$

-  $b_1'$  = width of flattened brace member. (With full cropping and flattening, this can be assumed to be  $2t_1$ . If fillet welding is used, this effective contact width can be increased to include the fillet weld leg dimensions).

$$- h_1' = \frac{\pi(d_1 - t_1) + t_1}{2 \sin \theta_1}$$

-  $\theta_1'$  = slope of brace member face at the cropped end, relative to the chord (see figure 9.12).

Conservatively, a value of  $\theta_1' = \theta_1$  can be used.

Equations 9.9 and 9.10 apply to symmetrical joints where:  $\theta_1 = \theta_2$ ,  $d_1 = d_2$ ,  $t_1 = t_2$ ,  $d_1/b_0 \geq 0.3$  and  $b_0/t_0 \leq 32$ .

## 9.5 Double chord trusses

Limitations on the largest available RHS member size have restricted the application range of RHS structures. For very long span roof trusses, such as sports centres and auditoria, the use of double RHS chord members will enable longer clear spans than those available from single chord trusses. Immediate advantages of double chord RHS trusses include not only their greater span capacity, but also more efficient and stiffer joints compared to some single chord trusses. Enhanced lateral stiffness can reduce lateral bracing requirements as well as facilitate handling and erection of the structural components.

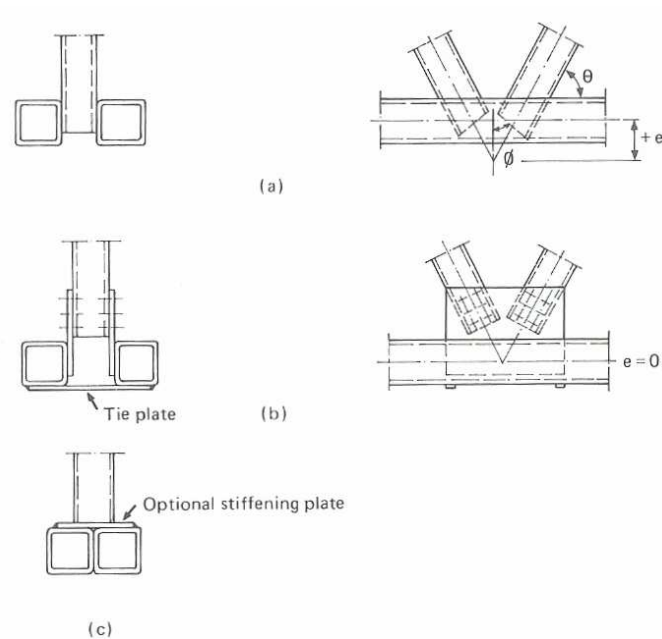


Figure 9.13 – Types of RHS double chord joints  
 (a) Separated chord welded joint  
 (b) Separated chord bolted joint  
 (c) Back-to-back chord joint

Research has been undertaken in Canada (Korol and Chidiac, 1980; Korol, 1983; Korol et al., 1983; Korol and Mitri, 1985; Luft et al., 1991) on isolated joints and trusses of the types shown in figure 9.13. The two separated chord truss types require that all the brace members have the same width; in such cases the brace member sizes can be varied by changing the brace member wall thickness ( $t_i$ ) or depth ( $h_i$ ). For the separated chord bolted joints (figure 9.13(b)), it is recommended that tie plates be used between the RHS chord members on the outside of the truss as they significantly increase the truss stiffness by maintaining the alignment of the sections.

For RHS double chord trusses, it is recommended that a pin-jointed analysis be used with effective length factors ( $K$ ) as given in section 3.3, when designing the compression members. Joint resistance expressions have been proposed for the separated chord welded joints, based on the limit state of chord shear. Thus:

$$N_i^* = \frac{0.58 f_{y0} A_v}{\sin \theta_i} \quad (\text{see table 4.1}) \quad 9.11$$

where:

$$A_v = 2.6h_0t_0 \quad \text{for } h_0/b_0 \geq 1 \quad 9.11a$$

$$A_v = 2h_0t_0 \quad \text{for } h_0/b_0 < 1 \quad 9.11b$$

Equations 9.11a and 9.11b take into account the reduced effectiveness of the chord outer side walls in resisting shear forces, at different chord aspect ratios.

The interaction between axial force and shear force in the gap region of the double chord joint should also be checked. The joint eccentricity has been found to have little effect on the joint strength, when not too large, and a pin-jointed analysis is recommended for the truss analysis, ignoring moments acting on the joint. The axial force/shear force interaction can be checked in a manner similar to that used in table 4.1, such that:

$$N_{\text{gap},0} \leq N_{\text{gap},0}^* = (2A_0 - A_v) f_{y0} + A_v f_{y0} \sqrt{1 - \left( \frac{V_{\text{gap},0}}{V_{\text{pl},0}} \right)^2} \quad 9.12$$

where:

$N_{\text{gap},0}$  = axial force in the gap

$V_{\text{gap},0}$  = shear force in the gap (i.e.  $N_i \sin \theta_i$ ; assuming no "purlin load")

$A_0$  = area of one chord member

$A_v$  is given by equations 9.11a and 9.11b

$V_{\text{pl},0}$  is given by:

$$V_{\text{pl},0} = 0.58 f_{y0} A_v \quad 9.13$$

An economic comparison of single chord and double chord RHS trusses (Luft et al., 1991) showed that for short spans, single chord trusses were the lightest and most economical, being around 20% less expensive than back-to-back double chord trusses. (Back-to-back double chord trusses are generally the heaviest and most expensive option for welded trusses.) Thus, for long spans, separated double chord welded joints are preferable and should again prove more economical than back-to-back joints.



Double chord truss

## 10 Design examples

### 10.1 Uniplanar truss

#### • Truss layout and member loads

An example has been selected to illustrate the use of the joint design methods given in chapters 4 and 5, as well as the truss design principles described in chapter 3. A Warren truss consisting of SHS members is presented since this configuration is often the preferred solution. A Warren configuration with low brace member angles, such as used here and shown in figure 10.1, keeps the number of joints to a minimum. All members chosen are cold-formed hollow sections with dimensions conforming to EN 10219-2 (CEN, 2006b). The steel grade throughout is S355 with a minimum specified yield strength of  $355 \text{ N/mm}^2$ .

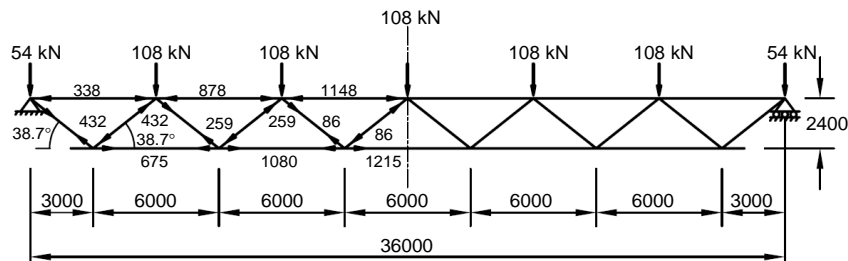


Figure 10.1 – Example Warren truss showing applied loads and resulting member forces (in kN)

Figure 10.1 shows the truss and factored loads along with member axial forces, determined by a pin-jointed analysis. The top (compression) chord is considered to be laterally supported at each purlin position. The span-to-depth ratio is 15, which is around the optimal upper limit considering service load deflections and overall costs (section 3.1).

#### • Design of members

For member selection, one could use either member resistance tables for the compression members, with the appropriate effective length, or the applicable strut buckling curve or equation. In practice, one would also pay attention to the availability of member sizes selected. For this truss design example, compression member resistance has been determined in accordance with Eurocode 3 (CEN, 2005a) using buckling curve “c”. The resistance has been calculated assuming  $\gamma_M = 1.0$ . (i.e. no partial safety factor or resistance factor), since this factor may be different for various countries (1.0 and higher). Since the joints at the truss ends are generally critical, the chord walls selected should not be too thin, as a single size member will be used for the top chord and another single size member selected for the bottom chord.

#### **Top chord**

Use a continuous section with an effective length, for both in-plane and out-of-plane buckling, of  $0.9L = 0.9 \times 6000 = 5400 \text{ mm}$ , as noted in section 3.3.1, equations 3.1 and 3.2.

Maximum force = -1148 kN (compression)

Possible section sizes are shown in table 10.1, along with their compressive resistances. As noted in section 3.6, use  $b_0/t_0$  ratios which are between 15 and 25. Hence, select the  $180 \times 180 \times 10.0 \text{ RHS}$  at this stage. Although the  $200 \times 200 \times 8.0$  is lighter, the joint capacities were shown to be insufficient.

Table 10.1 – Possible section sizes for top (compression) chord

$f_{y0}$ (N/mm <sup>2</sup> )	$N_0$ (kN)	KL (m)	Possible sections (mm x mm x mm)	$A_0$ (mm <sup>2</sup> )	$b_0/t_0$	$\bar{\lambda}$	$\chi$	$\chi f_{y0}A_0$ (kN)
355	-1148	5.4	200 x 200 x 8.0	5920	25.0	0.91	0.60	1261
			180 x 180 x 10.0	6460	18.0	1.03	0.52	1192

### Bottom chord

Table 10.2 – Possible section sizes for bottom (tension) chord

$f_{y0}$ (N/mm <sup>2</sup> )	$N_0$ (kN)	Possible sections (mm x mm x mm)	$A_0$ (mm <sup>2</sup> )	$b_0/t_0$	$f_{y0}A_0$ (kN)
355	1215	150 x 150 x 6.3	3480	23.8	1235
		160 x 160 x 6.0	3600	28.6	1278
		180 x 180 x 5.0	3440	36.0	1221

For joint capacity, it is preferred to keep the tension chord as compact and stocky as possible. Hence, select the 150 x 150 x 6.3 RHS at this stage.

### Diagonals

By aiming for gap joints (instead of overlap joints), reference to the chart in table 4.8 shows that the highest joint efficiency will be achieved when the ratio ( $f_{y0}t_0 / f_{y1}t_1$ ) is maximized. Therefore, try to select brace members such that ( $f_{y0}t_0 / f_{y1}t_1$ ) > 2.0, which in this case implies  $t_1 < 3.15$  mm, or near this thickness if possible.

For the compression brace members, use an effective length of 0.75 L (equation 3.3, section 3.3.1)

$$KL = 0.75 \sqrt{2.4^2 + 3.0^2} = 2.881\text{m}$$

### Compression diagonals

Table 10.3 – Possible section sizes for compression diagonals

$f_{y1}$ (N/mm <sup>2</sup> )	$N_1$ (kN)	KL (m)	Possible sections (mm x mm x mm)	$A_1$ (mm <sup>2</sup> )	$b_1/t_1$	$\bar{\lambda}$	$\chi$	$\chi f_{y1}A_1$ (kN)
355	-432	2.881	140 x 140 x 4.0	2130	35.0	0.68	0.72	544
			120 x 120 x 5.0	2240	24.0	0.81	0.65	517
355	-259	2.881	100 x 100 x 4.0	1490	25.0	0.96	0.56	296
355	-86	2.881	70 x 70 x 3.0	781	23.3	1.39	0.35	97
			80 x 80 x 3.0	901	26.7	1.21	0.43	137

### Tension diagonals

Table 10.4 – Possible section sizes for tension diagonals

$f_{y2}$ (N/mm <sup>2</sup> )	$N_2$ (kN)	Possible sections (mm x mm x mm)	$A_2$ (mm <sup>2</sup> )	$b_2/t_2$	$f_{y2}A_2$ (kN)
355	432	90 x 90 x 4.0	1330	22.5	472
355	259	70 x 70 x 3.0	781	23.3	277
355	86	30 x 30 x 2.5	259	12.0	92

### Member selection

The number of sectional dimensions depends on the total tonnage to be ordered. In this example, only two different sections will be selected for the brace members. A comparison of the members suitable for compression diagonals and tension diagonals shows that the following are most convenient:

- Braces: - 120 x 120 x 5.0 RHS  
 - 80 x 80 x 3.0 RHS
- Notes: - 140 x 140 x 4.0 RHS does not meet the limit for a class 2 section  
 - 80 x 80 selected, rather than 70 x 70 to conform to  $0.6 \leq (b_1+b_2)/2b_i \leq 1.3$
- Top chord: - 180 x 180 x 10.0 RHS
- Bottom chord: - 150 x 150 x 6.3 RHS

Checking the width-to-thickness ratios with the validity range of table 4.2 shows that the sections satisfy the limits. The locations of the sections selected, along with joint numbers, are shown in figure 10.2.

A further check to be made is whether or not gap joints can be applied, by examining the joints with the largest  $\beta$  (smallest gap) and smallest  $\beta$  (largest gap) ratios.

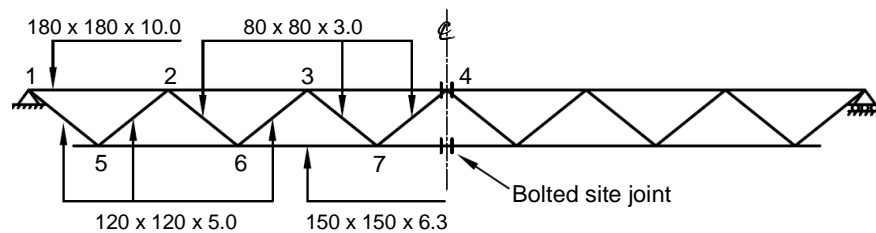


Figure 10.2 – Member dimensions and joint numbers

### Check for gap joints

Joint 5 (largest  $\beta$  ratio):

$\beta = 120/150 = 0.8$ , thus according to table 4.1, the gap  $g$  has to satisfy:

$$0.5(1-0.8) \leq g/150 \leq 1.5(1-0.8) \quad \text{or} \quad 15 \leq g \leq 45$$

The eccentricity ( $e$ ) corresponding to the minimum gap of 15 mm, giving the minimum value for  $e$ , can be calculated with:

$$e = \left( \frac{h_1}{2 \sin \theta_1} + \frac{h_2}{2 \sin \theta_2} + g \right) \frac{\sin \theta_1 \sin \theta_2}{\sin(\theta_1 + \theta_2)} - \frac{h_0}{2} = \left( \frac{120}{\sin \theta_1} + 15 \right) \frac{\sin \theta_1 \sin \theta_2}{\sin(\theta_1 + \theta_2)} - \frac{150}{2} = +8 \text{ mm}$$

Joint 7 (smallest  $\beta$  ratio):

$\beta = 80/150 = 0.53$ , thus according to table 4.1, the gap has to satisfy:

$$0.5(1-0.53) \leq g/150 \leq 1.5(1-0.53) \quad \text{or} \quad 35 \leq g \leq 105$$

The eccentricity corresponding to the maximum gap of 105 mm, giving the maximum value for  $e$ , is:

$$e = \left( \frac{80}{\sin \theta_1} + 105 \right) \frac{\sin \theta_1 \sin \theta_2}{\sin(\theta_1 + \theta_2)} - \frac{150}{2} = +18 \text{ mm} = 0.12h_0, \text{ thus not decisive.}$$

These checks show that gap joints are possible with a small eccentricity of 8 mm, so the members selected allow gap joints. Although no eccentricity is required for joints 6 and 7, for fabrication it might be easier to adopt the same eccentricity for all joints at the bottom chord. Similar checks for the top chord show that gap joints can be applied without eccentricity.

#### • Joint strength checks and commentary

At joints 1 and 4, the top chord member is welded to a flange-plate for connecting to a column and an adjacent chord member, respectively. At joint 1, the minimum required half gap for  $\beta = 120/180 = 0.67$  is chosen between the toe of the tension brace member and the plate, being 16 mm. This joint is checked as a K joint, rather than Y, because the flange plate provides similar restraint to the chord face as an adjacent compression brace member of the same size as the tension brace.

Joint 4 is also checked as a K joint since the plates (see figure 10.2) again stiffen the joint, despite the loading being similar to an X joint. Considering the joint classification in figure 4.2, it is clear that joints 2 and 3 require an additional check based on the K and X joint capacities; all others only need a K gap joint check. Hence, in table 10.5 all joints are initially examined as K (or N) joints for which the chart in table 4.8 can be used. Afterwards, joints 2 and 3 are further evaluated for a combination of K gap and X joint resistances.

The eccentricity of 8 mm for the joints with the tension chord has a small influence on the chord stress parameter  $n$  as will be shown:

$$\text{For tension: } Q_f = (1 - |n|)^{0.10}$$

$$\text{with: } n = \frac{N_0}{N_{pl,0}} + \frac{M_0}{M_{pl,0}}$$

$$\text{and } \frac{M_0}{M_{pl,0}} = \frac{0.5(N_0 - N_{0p})e}{W_{pl,0} f_{y0}}$$

where  $N_0 - N_{0p}$  = the difference between the chord loads on either side of the joint, which is equal to the summation of horizontal components of the brace loads.

The factor 0.5 in the equation for the chord bending moment  $M_0$  only applies to joints 6 and 7 where two chord members at each side of the joint are sharing the moment. For joint 5, the full eccentricity moment  $N_0e$  is taken by the chord member between joints 5 and 6 (the end part is assumed to be only supported in the out-of-plane direction).

Table 10.5 shows that especially for joints 6 and 7, the effect of the eccentricity moment on the chord stress parameter  $n$  is negligible.

Table 10.5 gives the joint resistance calculations based on the K gap joint resistances. However joints 2 and 3 have to be further examined for the combined effects of a K gap joint and an X joint.

Table 10.5 – Check for joint resistances, assuming K joint action only

Joint	Chord (mm)	Braces (mm)	Joint parameters			Chord loading		
			$\beta$	$2\gamma$	e (mm)	$\frac{N_0}{A_0 f_{y0}}$	$\frac{M_0}{M_{pl,0}}$ (*)	n
1	180 x180x10	Plate	0.67	18	0	-0.15	-	-0.15
		120x120x5						
2	180x180x10	120x120x5	0.56	18	0	-0.38	-	-0.38
		80x80x3						
3	180x180x10	120x120x5	0.56	18	0	-0.50	-	-0.50
		80x80x3						
4	180x180x10	80x80x3	0.44	18	0	-0.50	-	-0.50
		80x80x3						
5	150x150x6.3	120x120x5	0.80	23.8	8	0.55	-0.08	0.46
		120x120x5						
6	150x150x6.3	120x120x5	0.67	23.8	8	0.87	-0.02	0.85
		80x80x3						
7	150x150x6.3	80x80x3	0.53	23.8	8	0.98	-0.01	0.98
		80x80x3						

Joint	Actual efficiency	Joint efficiency parameters						Check
	$\frac{N_i}{A_i f_{yi}}$	$C_k$ (**)	$\frac{b_1 + b_2}{2b_i}$	$Q_f$ (***)	$\frac{f_{y0} t_0}{f_{yi} t_i}$	$\frac{1}{\sin \theta_i}$	$\frac{N_i^*}{A_i f_{yi}}$	$N_i^* \geq N_i$
1	-		-	0.97				
	0.54	0.40	1.0		2.0	1.60	> 1.0	o.k.
2	0.54	0.40	0.83	0.90	2.0	1.60	0.96	o.k.
	0.81	0.40	1.25		3.33	1.60	> 1.0	o.k.
3	0.33	0.40	0.83	0.86	2.0	1.60	0.91	o.k.
	0.27	0.40	1.25		3.33	1.60	> 1.0	o.k.
4	0.27	0.40	1.0	0.83	3.33	1.60	> 1.0	o.k.
	0.27	0.40	1.0		3.33	1.60	> 1.0	o.k.
5	0.54	0.32	1.0	0.94	1.26	1.60	0.61	o.k.
	0.54	0.32	1.0		1.26	1.60	0.61	o.k.
6	0.33	0.32	0.83	0.83	1.26	1.60	0.44	o.k.
	0.81	0.32	1.25		2.1	1.60	> 1.0	o.k.
7	0.27	0.32	1.0	0.69	2.1	1.60	0.74	o.k.
	0.27	0.32	1.0		2.1	1.60	0.74	o.k.

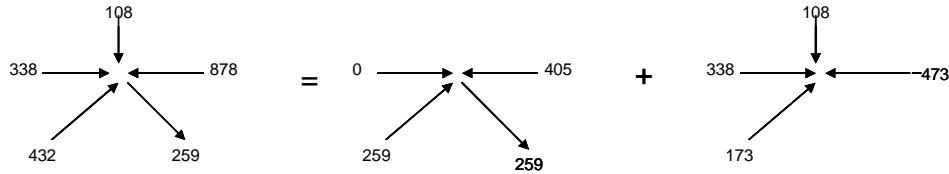
(\*) For joints 6 and 7:  $M_0 = 0.5(N_0 - N_{op}) e$ ; for joint 5:  $M_0 = (N_0 - N_{op}) e$  with  $N_{op} = 0.0$  kN  
 Bending moments giving tensile stress in the chord connecting face are taken as positive.

(\*\*) See table 4.8

(\*\*\*) See figure 4.7

## Joint 2

For joint 2 with  $\beta \approx 0.6$ , the force -338 kN in the chord member might have been located on either the "pure K joint" or the X joint as shown below. This force is added to the X joint because for this  $\beta$  value, the  $Q_f$  effect for X joints is more punitive than that for K gap joints, (see figures 4.5 and 4.7).



Joint 2 – K joint action:

$$n = \frac{N_0}{A_0 f_{y0}} = \frac{-405}{6460 \times 0.355} = -0.18 \text{ compression; thus } Q_f = 0.96 \text{ (see figure 4.7)}$$

For  $2\gamma = 18$ :  $C_K = 0.40$  (see table 4.8)

$$\text{For brace 1: } \frac{N_1^*}{A_1 f_{y1}} = 0.40 \times \frac{10}{5} \times \frac{0.96}{0.625} \times 0.83 > 1.0$$

$$\text{Due to acting load: } \frac{N_1}{A_1 f_{y1}} = \frac{259}{2240 \times 0.355} = 0.33$$

$$\text{Hence, the utilization ratio for K joint action is } \frac{N_1}{N_1^*} = \frac{0.33}{1.0} = 0.33$$

$$\text{For brace 2: } \frac{N_2^*}{A_2 f_{y2}} = 0.40 \times \frac{10}{3} \times \frac{0.96}{0.625} \times 1.25 > 1.0$$

$$\text{Due to acting load: } \frac{N_2}{A_2 f_{y2}} = \frac{259}{901 \times 0.355} = 0.81$$

$$\text{Hence, the utilization ratio for K joint action is } \frac{N_2}{N_2^*} = \frac{0.81}{1.0} = 0.81$$

Joint 2 – X joint action (brace 1 only):

$$n = \frac{N_0}{A_0 f_{y0}} = \frac{-473}{6460 \times 0.355} = -0.21 \text{ compression; } \frac{b_1}{b_0} = \frac{120}{180} = 0.67, \text{ thus } Q_f = 0.94 \text{ (see figure 4.5)}$$

For  $\frac{b_1}{b_0} = \frac{120}{180} = 0.67$  and  $2\gamma = 18$ :  $C_X = 0.27$  (see table 4.7)

$$\frac{N_1^*}{A_1 f_{y1}} = 0.27 \times \frac{10}{5} \times \frac{0.94}{0.625} = 0.81$$

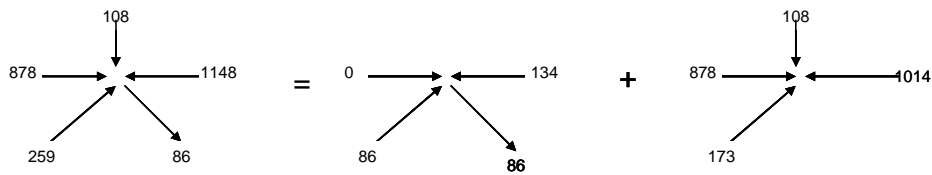
$$\text{Due to acting load: } \frac{N_1}{A_1 f_{y1}} = \frac{173}{2240 \times 0.355} = 0.22$$

$$\text{Hence, the utilization ratio for X joint action is } \frac{N_1}{N_1^*} = \frac{0.22}{0.81} = 0.27$$

The combined acting efficiency due to K joint and X joint action for brace 1 is  $0.33 + 0.27 = 0.60 < 1.0$  and the criteria are satisfied.

*Note: Based on the check as a K joint only (table 10.5), the utilization ratio (for brace 1) is  $\frac{N_1}{N_1^*} = \frac{0.54}{0.96} = 0.56$ . Hence, in this case, the difference is 4% in usage.*

### Joint 3



Joint 3 – K joint action:

$$n = \frac{N_0}{A_0 f_{y0}} = \frac{-134}{6460 \times 0.355} = -0.06 \text{ compression; thus } Q_f = 0.99 \text{ (see figure 4.7)}$$

For  $2\gamma = 18$ :  $C_K = 0.40$  (see table 4.8)

$$\text{For brace 1: } \frac{N_1^*}{A_1 f_{y1}} = 0.40 \times \frac{10}{5} \times \frac{0.99}{0.625} \times 0.83 > 1.0$$

$$\text{Due to acting load: } \frac{N_1}{A_1 f_{y1}} = \frac{86}{2240 \times 0.355} = 0.11$$

$$\text{Hence, the utilization ratio for K joint action is } \frac{N_1}{N_1^*} = \frac{0.11}{1.0} = 0.11$$

$$\text{For brace 2: } \frac{N_2^*}{A_2 f_{y2}} = 0.40 \times \frac{10}{3} \times \frac{0.99}{0.625} \times 1.25 > 1.0$$

$$\text{Due to acting load: } \frac{N_2}{A_2 f_{y2}} = \frac{86}{901 \times 0.355} = 0.27$$

$$\text{Hence, the utilization ratio for K joint action is } \frac{N_2}{N_2^*} = \frac{0.27}{1.0} = 0.27$$

Joint 3 – X joint action (brace 1 only):

$$n = \frac{N_0}{A_0 f_{y0}} = \frac{-1014}{6460 \times 0.355} = -0.44 \text{ compression; } \frac{b_1}{b_0} = \frac{120}{180} = 0.67, \text{ thus } Q_f = 0.86 \text{ (see figure 4.5)}$$

$$\text{For } \frac{b_1}{b_0} = \frac{120}{180} = 0.67 \text{ and } 2\gamma = 18: C_X = 0.27 \text{ (see table 4.7)}$$

$$\frac{N_1^*}{A_1 f_{y1}} = 0.27 \times \frac{10}{5} \times \frac{0.86}{0.625} = 0.74$$

$$\text{Due to acting load: } \frac{N_1}{A_1 f_{y1}} = \frac{173}{2240 \times 0.355} = 0.22$$

$$\text{Hence, the utilization ratio for X joint action is } \frac{N_1}{N_1^*} = \frac{0.22}{0.74} = 0.30$$

The combined acting efficiency due to K joint and X joint action for brace 1 is  $0.11 + 0.30 = 0.41 < 1.0$  and the criteria are satisfied.

*Note: Based on the check as K joint only (table 10.5), the utilization ratio (for brace 1) is  $\frac{N_1}{N_1^*} = \frac{0.33}{0.91} = 0.36$ . Hence, the difference is 5% in usage.*

From table 10.5 and the above calculations, it is concluded that all joints are adequate. This was possible due to an astute selection of member sizes, in which the ratio ( $f_{y0}t_0/f_{yi}t_i$ ) was kept as high as possible. Furthermore, realizing that a large brace member would be adjacent to a much smaller brace member at joints 2, 3 and 6, the 80 x 80 RHS was selected instead of the 70 x 70 RHS to satisfy the  $0.6 \leq (b_1+b_2)/2b_i \leq 1.3$  limit. Along the compression chord, all joints have zero nodding eccentricity, which is usually the first choice of designers, provided that a sufficient gap results. On the tension chord, a nodding eccentricity has been introduced at all the joints, but, as shown before, this only marginally influences the design of the tension chord or the joints.

Although the actual efficiency for the braces at joint 7 is low, the design efficiency is significantly reduced by the chord load effect, because  $n > 0.95$ . As shown in figure 4.7, for these high chord loads, the chord stress effect is considerable. Hence, it is recommended to design initially for actual efficiencies not exceeding 0.9.

#### • Purlin joints

Depending on the type of purlins, various purlin joints are possible. If light gauge purlins for small spans are used, such as cold-formed channel shapes for example, a popular form of purlin cleat is a section of angle welded to the top face of the chord member, extending across the full width of the RHS. The purlin would then be bolted to the outstanding leg of the angle.

If longer span purlins are used, these are likely to be I sections, in which case, angle cleats could be welded to each side of the RHS chord member and the purlin bolted through its flange to the outstanding leg of the angle as shown in figure 10.3.

If lattice girder (open-web steel joist) purlins are used, these can be connected at their ends to the top chord with a cleat or an end plate and depending on this detail, the truss has to be provided with a plate to which these lattice purlin ends can be attached.

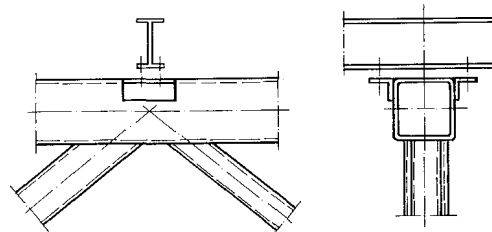


Figure 10.3 – Possible purlin cleat joint at truss joint no. 2

## 10.2 Vierendeel truss

### • Truss layout

The Vierendeel truss shown in figure 10.4 is to be designed for a factored panel load  $P$  of 17 kN. All the joint locations are laterally braced, perpendicular to the truss, by secondary members. The top and bottom chord members will be the same, and one section size will be used for all vertical (brace) members. A statically admissible set of moments and shears follows in figure 10.5. Members will be designed using plastic analysis. All members chosen are hot-finished sections with dimensions conforming to EN 10210-2 (CEN, 2006a). The steel grade throughout is S355 with a minimum specified yield strength of  $355 \text{ N/mm}^2$ . Reductions in plastic moment capacity due to axial force or shear force can be shown to be negligible (Horne and Morris, 1985).

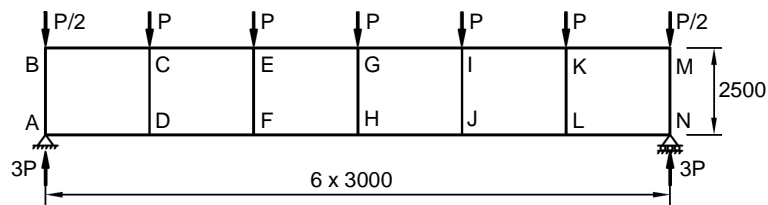
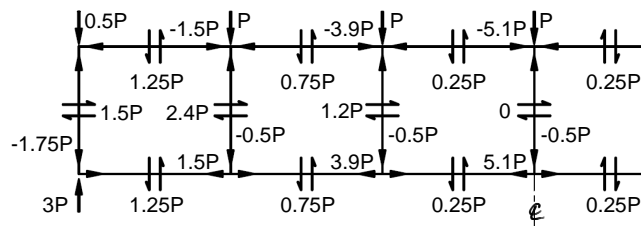
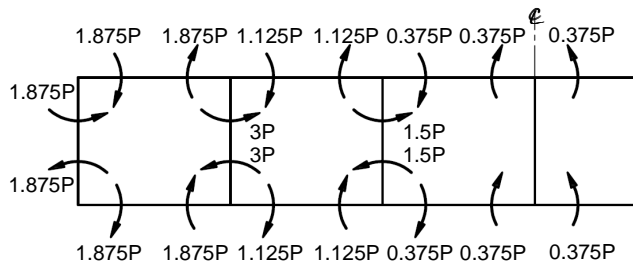


Figure 10.4 – Example Vierendeel truss



(a) Member axial forces and shear forces



(b) Bending moments

Figure 10.5 – Forces and moments within Vierendeel truss (shown applied at the nodes)

### • Design of members

**Chords: select 150 x 150 x 10 RHS**

Note that  $b_0/t_0 < 16$ , as recommended in chapter 5, below equation 5.8.

Confirm that this section is class 1 (suitable for plastic design) at the worst axial load condition.

- Maximum moment =  $1.875 P = 31.9 \text{ kNm}$
- Plastic moment of resistance =  $W_{pl,0} f_{y0} = 286 \times 0.355 = 101.5 \text{ kNm} > 31.9 \text{ kNm} \rightarrow \text{o.k.}$

Note that the member resistance above has been calculated assuming  $\gamma_M = 1.0$  (i.e. no partial safety factor or resistance factor), to be consistent with the other examples. Designers should introduce the appropriate partial safety factor or resistance factor for member design.

Therefore, 150 x 150 x 10 RHS is suitable for the chords.

**Vertical members: select 150 x 150 x 6.3 RHS**

Note that  $\beta = 1.0$ , as recommended in chapter 5, below equation 5.8.

Again, confirm that this section is class 1 (suitable for plastic design) at the worst axial load condition.

- Maximum moment =  $3 P = 51.0 \text{ kNm}$
- Plastic moment of resistance =  $W_{pl,1} f_{y1} = 192 \times 0.355 = 68.2 \text{ kNm} \geq 51.0 \text{ kNm} \rightarrow \text{o.k.}$

This again ignores any partial safety factor or resistance factor to be consistent with member design elsewhere.

Therefore, 150 x 150 x 6.3 RHS is suitable for the vertical members.

**• Plastic collapse mechanism**

Figure 10.6 illustrates the collapse mechanism. Let  $\lambda'$  be the additional multiplication factor by which the already factored loads of 17 kN have to be increased to cause plastic collapse. By the principle of virtual work:

$$17\lambda' \times (3\theta + 6\theta + 6\theta + 6\theta + 3\theta) = M_{pl,0} \times 4\theta + M_{pl,1} \times 8\theta = 101.5 \times 4\theta + 68.2 \times 8\theta$$

Solving this equation gives:  $\lambda' = 2.33$

Therefore, adequate reserve capacity exists for ultimate strength as  $\lambda' \geq 1.0$ .

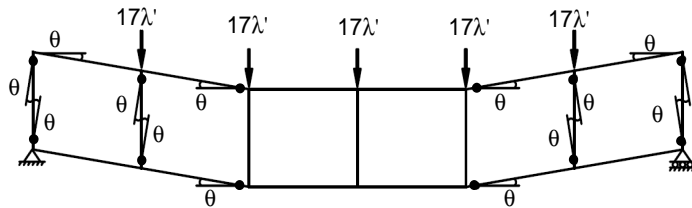


Figure 10.6 – Plastic collapse mechanism for Vierendeel truss

**• Joint capacity check**

As  $\beta = 1.0$ , the brace in-plane bending moment and axial resistances of the joint could be limited by cracking in or local yielding of the brace member, or by chord side wall failure (see tables 4.1 and 5.1).

**Moment resistance – local yielding of the brace**

$$M_{ip,1}^* = f_{y1} \left( W_{pl,1} - \left(1 - \frac{b_e}{b_1}\right) b_1 (h_1 - t_1) t_1 \right)$$

where:

$$b_e = \left( \frac{10}{b_0/t_0} \right) \left( \frac{t_0}{t_1} \right) b_1 = \frac{10}{15} \times \frac{10}{6.3} \times 150 = 158.7 \text{ mm} > b_1, \text{ thus use } b_1$$

$$M_{ip,1}^* = 0.355 \times 192 = 68.2 \text{ kNm} \geq 51.0 \text{ kNm} \rightarrow \text{o.k.}$$

**Moment resistance – chord side wall failure**

$$M_{ip,1}^* = 0.5 f_k t_0 (h_1 + 5t_0)^2 Q_f$$

with  $f_k = f_{y0}$  for T joints under brace in-plane bending (table 5.1)

$Q_f$  will be most punitive in the top (compression) chord. The in-plane bending resistance of joints B, C, E and G will be different because the axial force and bending moment combinations at each joint vary. For top (and bottom) chord,  $N_{pl,0} = 1949 \text{ kN}$  and  $M_{pl,0} = 101.5 \text{ kNm}$ .

Table 10.6 – Determination of  $Q_f$  factors for the joint limit state of chord side wall failure

Joint	Axial compression (kN)	Bending moment (*) (kNm)	$n = \frac{N_0}{N_{pl,0}} + \frac{M_0}{M_{pl,0}}$	$Q_f$
B <sub>right</sub>	-25.5	-31.9	-0.33	0.96
C <sub>left</sub>		31.9	0.30	0.97
C <sub>right</sub>	-66.3	-19.1	-0.22	0.98
E <sub>left</sub>		19.1	0.15	0.98
E <sub>right</sub>	-86.7	-6.4	-0.11	0.99
G <sub>left</sub>		6.4	0.02	1.0

(\*) Bending moments giving tensile stress in the chord connecting face are taken as positive

Thus, take  $Q_f = 0.96$  for all joints.

$$M_{ip,1}^* = 0.5 \times 0.355 \times 10 \times (150 + 50)^2 \times 0.96 = 68.2 \text{ kNm} \geq 51.0 \text{ kNm} \rightarrow \text{o.k.}$$

Thus, the limiting moment resistance  $M_{ip,1}^*$  is 68.2 kNm.

**Axial resistance – local yielding of the brace**

$$N_1^* = f_{y1} t_1 (2h_1 + 2b_e - 4t_1)$$

with  $b_e = b_1$  as before

$$N_1^* = 0.355 \times 6.3 \times (300 + 300 - 25.2) = 1286 \text{ kN}$$

**Axial resistance – chord side wall failure**

$$N_1^* = \frac{f_k t_0}{\sin \theta_1} \left( \frac{2h_1}{\sin \theta_1} + 10t_0 \right) Q_f$$

with  $f_k = \chi f_{y0}$  and  $\lambda$  determined from:  $\lambda = 3.46 \left( \frac{h_0}{t_0} - 2 \right) \sqrt{\frac{1}{\sin \theta_1}} = 3.46 \times (15 - 2) = 45$  thus,  $\bar{\lambda} = 0.59$

Hence,  $\chi = 0.89$  according to curve "a" for hot-finished RHS, see EN 1993-1-1 (CEN, 2005a).

$$N_1^* = 0.89 \times 0.355 \times 10 \times (300 + 100) \times 0.96 = 1213 \text{ kN}$$

Thus, the decisive value of  $N_1^*$  is 1213 kN.

### Interaction

Check if the interaction between in-plane bending moment and axial force in the brace (equation 5.9) is satisfied according to:

$$\frac{N_1}{N_1^*} + \frac{M_{ip,1}}{M_{ip,1}^*} \leq 1.0$$

One should examine the joints at the outside posts (maximum axial compression force of  $N_1 = 1.75 P = 29.8$  kN), and the joints at the most critical interior vertical (having a maximum moment of  $M_{ip,1} = 3 P = 51$  kNm).

For outside posts:

$$\frac{N_1}{N_1^*} + \frac{M_{ip,1}}{M_{ip,1}^*} = \frac{29.8}{1213} + \frac{31.9}{68.2} = 0.49 \leq 1.0 \quad \rightarrow \text{o.k.}$$

For interior verticals:

$$\frac{N_1}{N_1^*} + \frac{M_{ip,1}}{M_{ip,1}^*} = \frac{8.5}{1213} + \frac{51.0}{68.2} = 0.75 \leq 1.0 \quad \rightarrow \text{o.k.}$$

Therefore, the joint resistance is adequate and the truss is satisfactory.

The members would also be suitable by elastic design procedures, and even with the introduction of a partial safety factor (resistance factor) applied to member resistance. By either design method, the chord thickness is still sufficient to provide adequate joint strength.

The end joints (at A, B, M and N) can be made by welding the vertical posts to the chord to form T joints, and then adding cap plates to the ends of the chord sections.

### 10.3 Reinforced joints

Suppose the 45° X joint given in figure 10.7 is subjected to the factored loads shown. The resistance of the joint will be examined to see if it is adequate. The members are hot-finished hollow sections with dimensions conforming to EN 10210-2 (CEN, 2006a). The steel grade is S355 with a minimum specified yield strength of 355 N/mm<sup>2</sup>.

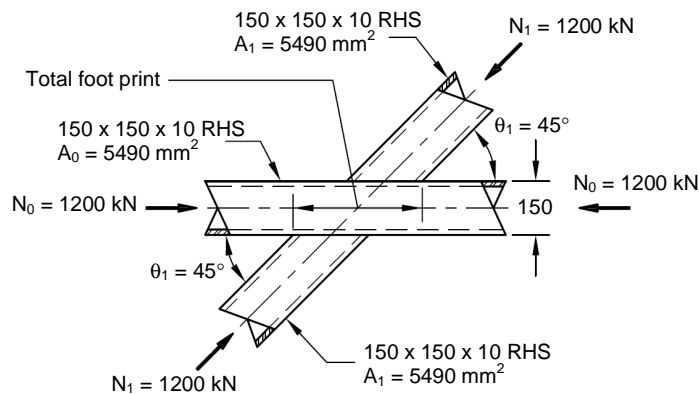


Figure 10.7 – RHS X joint example

### Local yielding of the brace

From table 4.1, for the local yielding of the brace limit state:

$$N_1^* = f_{y1} t_1 \ell_{b,eff.} = f_{y1} t_1 (2h_1 + 2b_e - 4t_1)$$

where:

$$b_e = \left( \frac{10}{b_0/t_0} \right) \left( \frac{f_{y0} t_0}{f_{y1} t_1} \right) b_1 = \frac{10}{15} \times 150 = 100 \text{ mm} \leq b_1$$

$$N_1^* = 0.355 \times 10 \times (300 + 200 - 40) = 1633 \text{ kN}$$

### Chord side wall failure

From table 4.1, for the chord side wall failure limit state:

$$N_1^* = \frac{f_k t_0}{\sin \theta_1} \left( \frac{2h_1}{\sin \theta_1} + 10t_0 \right) Q_f$$

with  $f_k = 0.8 \chi f_{y0} \sin \theta_1$  and  $\lambda$  determined from  $\lambda = 3.46 \left( \frac{h_0}{t_0} - 2 \right) \sqrt{\frac{1}{\sin \theta_1}} = 53.5$  thus,  $\bar{\lambda} = 0.70$

Hence,  $\chi = 0.85$  according to curve "a" for hot-finished RHS, see EN 1993-1-1 (CEN, 2005a).

$$f_k = 0.8 \times 0.85 \times 355 \times 0.707 = 170 \text{ N/mm}^2$$

$$\text{With } \beta = 150/150 = 1.0, b_0/t_0 = 150/10 = 15 \text{ and } n = \frac{N_0}{A_0 f_{y0}} = \frac{-1200}{5490 \times 0.355} = -0.62 \text{ gives:}$$

$$Q_f = 0.91 \text{ (figure 4.5)}$$

$$N_1^* = \frac{0.170 \times 10}{0.707} \left( \frac{2 \times 150}{0.707} + 10 \times 10 \right) 0.91 = 1147 \text{ kN} < 1200 \text{ kN}$$

Hence, the joint resistance is inadequate due to the chord side wall capacity and must be reinforced, either by using plate reinforcement or concrete filling. Since  $\cos \theta_1 < h_1/h_0 (= 1.0)$ , the chord does not need to be checked for shear (table 4.1).

### 10.3.1 Reinforcement by side plates

For the X joint in figure 10.7, a pair of side plates will be added to the chord side walls, with the side plates also having a yield strength of 355 N/mm<sup>2</sup>.

As shown in the section above, a joint capacity of 1147 kN was found for failure mode "Chord side wall failure" for the X joint illustrated in figure 10.7 (with  $\beta = 1.0$  and  $\theta_1 = 45^\circ$ ).

If a plate thickness of 10 mm (same as the chord) is chosen and assuming that the chord side wall and plate act independently, both will have approximately the same compression resistance. Hence, it is evident that the joint resistance will double when reinforced in this manner.

$$\text{Hence } N_1^* = 2294 \text{ kN} > 1200 \text{ kN} \rightarrow \text{o.k.}$$

For the length of the side plates,  $L_p$ , the intent of equation 9.1 for T and Y joints is that the plates extend 50% further than the brace member "footprint". Applying the same guidance to the X joint of figure 10.7, with two offset brace member "footprints":

$$L_p \geq 1.5 \left( \frac{150}{\tan 45^\circ} + \frac{150}{\sin 45^\circ} \right) = 543 \text{ mm}$$

Make the stiffener plates 600 mm long x 150 mm high x 10 mm thick, and weld all around the plate perimeter.

### 10.3.2 Reinforcement by concrete filling of the chord

Fill the chord member of the X joint shown in figure 10.7, with concrete having a crushing strength,  $f'_c = 40 \text{ N/mm}^2$ . The joint resistance is calculated using equation 9.4:

$$N_1^* = \phi_c f'_c \frac{A_1}{\sin \theta_1} \sqrt{A_2 / A_1}$$

$$A_1 = 150 \times 150 / \sin 45^\circ = 31820 \text{ mm}^2$$

$$A_2 \text{ is taken conservatively as: (total footprint length} + 2h_0) b_1 = (362 + 2 \times 150) \times 150 = 99300 \text{ mm}^2$$

$$A_2 / A_1 = 3.121 \text{ and } \sqrt{A_2 / A_1} = 1.767 < 3.3 \rightarrow \text{o.k.}$$

$$N_1^* = 0.65 \times 0.040 \times \frac{31820}{0.707} \times 1.767 = 2067 \text{ kN} > 1200 \text{ kN} \rightarrow \text{o.k.}$$

An appropriate minimum length of concrete would be the "total footprint" length (362 mm) plus  $2h_0$ , say 0.75 m.

### 10.4 Cranked chord joint (and overlapped joint)

The  $45^\circ$  cranked-chord joint given in figure 10.8 is subjected to the factored loads shown. The resistance of the joint will be determined to see whether or not it is adequate. The cold-formed RHS members have dimensions conforming to EN 10219-2 (CEN, 2006b) and the steel grade is S355 with a minimum specified yield strength of  $355 \text{ N/mm}^2$ .

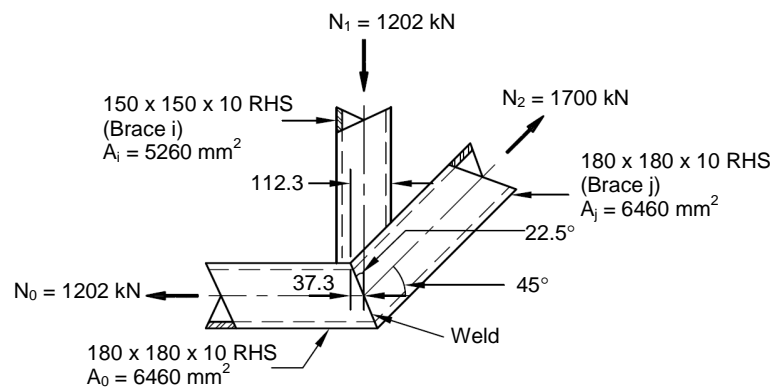


Figure 10.8 – RHS cranked chord joint example, with all RHS perimeters welded

Imagine the horizontal chord member extending as shown in figure 9.7 and both of the other members joining on top of the extended chord member.

$$\text{Overlap (see figure 1.1)} = q/p \times 100\% = (112.3/150) \times 100 = 75\%.$$

Eccentricity  $e = 0 \text{ mm}$

Check range of validity for an overlapped K joint in table 4.3:

- $b/b_0 = 0.83$  and  $b/b_0 = 1.0$ , respectively,  $\geq 0.25 \rightarrow$  o.k.
- $b/b_j = 0.83 \geq 0.75 \rightarrow$  o.k.;  $t/t_j = 1.0 \leq 1.0 \rightarrow$  o.k.
- $25\% \leq Ov = 75\% \leq 100\% \rightarrow$  o.k.;  $0.5 \leq h_0/b_0 = h/b_i = h_j/b_j = 1.0 \leq 2.0 \rightarrow$  o.k.
- $b_1/t_1 = 15$  ( $\leq$  class 1 or 2 limit or 40)  $\rightarrow$  o.k.;  $b_2/t_2 = 18$  ( $\leq 40$ )  $\rightarrow$  o.k.;  $b_0/t_0 = 18 \leq 40 \rightarrow$  o.k.

From table 4.3, for  $50\% \leq Ov < 100\%$ :

$$N_i^* = f_{yi} t_i (2h_i + b_{ei} + b_{e,ov} - 4t_i)$$

where:

$$b_{ei} = \left( \frac{10}{b_0/t_0} \right) \left( \frac{f_{y0} t_0}{f_{yi} t_i} \right) b_i = \frac{10}{18} \times 1.0 \times 150 = 83.3 \text{ mm} = b_{e,ov} \text{ also}$$

$$N_i^* = 0.355 \times 10 \times (300 + 2 \times 83.3 - 40) = 1514 \text{ kN} \geq 1202 \text{ kN} \rightarrow \text{o.k.}$$

Alternatively, one could use table 4.9 to calculate  $N_i^*$ :

$$\text{For } b_0/t_0 = 18 \text{ and } f_{y0}t_0/f_{yi}t_i = 1.0 \rightarrow 0.25 b_{ei}/b_i = 0.13$$

$$\text{For } b_j/t_j = 18 \text{ and } f_{yj}t_j/f_{yi}t_i = 1.0 \rightarrow 0.25 b_{e,ov}/b_i = 0.13$$

$$\text{Total efficiency} = 0.5 + 2 \times 0.13 = 0.76$$

$$\text{or } N_i^* = 0.76 \times A_i \times f_{yi} = 0.76 \times 5260 \times 0.355 = 1419 \text{ kN} \geq 1202 \text{ kN}$$

(This approach is slightly more conservative than direct use of the equations).

Check the efficiencies of the overlapping and overlapped braces (see "General note" in table 4.3): the efficiency (i.e. design resistance divided by the yield load) of the overlapped brace j should not exceed that of the overlapping brace i, hence:

$$N_j^* = N_i^* \frac{A_j f_{yj}}{A_i f_{yi}} = 1514 \times \frac{0.355 \times 6460}{0.355 \times 5260} = 1859 \text{ kN} \geq 1700 \text{ kN} \rightarrow \text{still o.k.}$$

Note: For  $e = 0$ ,  $M_0 = 0$  and hence the check for local chord yielding interaction (i.e. interaction between bending moment and axial load in the chord) is not necessary. Further, the brace shear check is not necessary here, because the brace force is directly transferred to the chord (the same member). If it would have been a real overlap joint, the brace shear check is not necessary either, because the perimeters of all RHS members in the joint are fully welded and hence  $Ov_{limit} = 80\% > Ov = 75\%$  (see table 4.3).

## 10.5 Bolted flange-plate joint

In this example, two RHS 320 x 200 x 12.5, produced to EN 10219-2 (CEN, 2006b) grade S355 (minimum yield stress = 355 N/mm<sup>2</sup> or MPa), will be connected by means of a flange-plate joint with bolts on all four sides. The joint is subjected to an axial tension load of 2200 kN. The flange-plate material has a yield strength of 350 N/mm<sup>2</sup>. The design procedure follows that given in section 8.1.2 (which also refers to section 8.1.1). The pertinent geometric variables for such a joint are shown in figure 10.9.

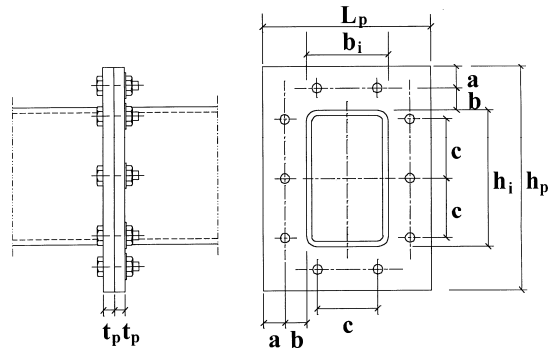


Figure 10.9 – Tension splice with bolts on four sides of RHS

A 12-bolt arrangement as illustrated in figure 10.10 is tried, implying that the applied load per bolt – neglecting prying – would be  $P_f = 2200/12 = 183.3$  kN. ASTM A325M M24 bolts are selected, having a diameter of 24 mm and a tensile resistance of 225 kN/bolt. (ASTM grade A325 bolts are very similar to Grade 8.8 bolts, but one should also be aware that resistance (or partial safety) factors vary for bolts between codes/specifications as well). With a bolt tensile resistance of  $T = 225$  kN, there is an allowance of 23% for prying action. This joint size (RHS size, aspect ratio, and number of bolts) is similar to joints verified experimentally.

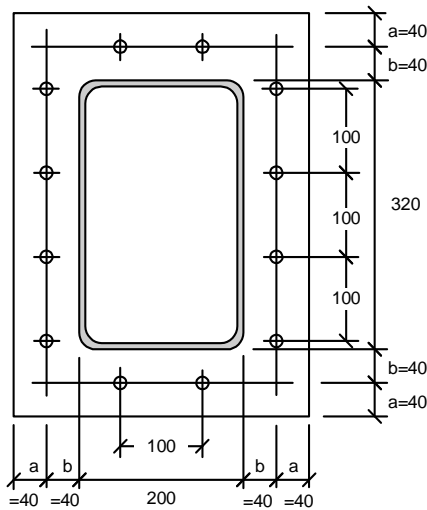


Figure 10.10 – Flange-plate layout selected for bolted joint

Next, a suitable bolt layout is postulated. As noted in section 8.1.1, a bolt pitch of  $4d$  to  $5d$  (96 to 120 mm) is typical, but the distance between adjacent bolts,  $c$ , should be as low as possible. A value of  $c = 100$  mm is therefore chosen and the layout shown in figure 10.10 also results in the bolt centres lying within the depth and width dimensions of the RHS. Dimensions of  $a = b = 40$  mm are selected, which allows sufficient space for bolt tightening, and this results in a flange-plate size of  $480 \times 360$  mm. For bolts on all sides of the RHS, the bolt pitch,  $p$ , to be used in calculations is the minimum of  $(480/4 \text{ and } 360/2) = 120$  mm (see section 8.1.2).

The edge distance,  $a \leq 1.25b$ , hence:

$$a' = a + d/2 = 40 + 24/2 = 52 \text{ mm (equation 8.8) and}$$

$$b' = b - d/2 = 40 - 24/2 = 28 \text{ mm (equation 8.1 with the } t_i \text{ term deleted).}$$

One now follows the steps 1 to 3 as outlined in section 8.1.1 for a two-dimensional prying model, also deleting the term  $t_i$  from equation 8.5.

A drilled bolt hole diameter of  $d' = 26 \text{ mm}$  will be selected.

$$\delta = 1 - \frac{d'}{p} = 1 - \frac{26}{120} = 0.783 \quad 8.2$$

$$K = \frac{4b'10^3}{\phi_p f_{yp} p} = \frac{4 \times 28 \times 10^3}{0.9 \times 350 \times 120} = 2.963 \quad 8.4$$

$$t_{\min} = \sqrt{\frac{KP_f}{1+\delta}} = \sqrt{\frac{2.963 \times 183.3}{1+0.783}} = 17.5 \text{ mm} \quad 8.3$$

$$t_{\max} = \sqrt{KP_f} = \sqrt{2.963 \times 183.3} = 23.3 \text{ mm} \quad 8.3$$

Therefore, select a flange-plate with  $t_p = 20 \text{ mm}$ .

$$\alpha = \left( \frac{KT^*}{t_p^2} - 1 \right) \left( \frac{a + (d/2)}{\delta(a+b)} \right) = \left( \frac{2.963 \times 225}{20^2} - 1 \right) \left( \frac{40 + (24/2)}{0.783 \times (40 + 40)} \right) = 0.553 \quad \text{based on equation 8.5}$$

The splice tensile resistance  $N_t^*$  is thus:

$$N_t^* = \frac{t_p^2 (1 + \delta\alpha)n}{K} = \frac{20^2 (1 + 0.783 \times 0.553)12}{2.963} = 2321 \text{ kN} > 2200 \text{ kN} \quad 8.6$$

For general interest, calculate the actual total bolt tension, including prying force:

$$T_f \approx P_f \left( 1 + \frac{b'}{a'} \left( \frac{\delta\alpha}{1 + \delta\alpha} \right) \right) = 183.3 \left( 1 + \frac{28}{52} \left( \frac{0.783 \times 0.457}{1 + 0.783 \times 0.457} \right) \right) = 209 \text{ kN} < T^* = 225 \text{ kN} \quad 8.7$$

$$\text{using } \alpha = \left( \frac{KP_f}{t_p^2} - 1 \right) \frac{1}{\delta} = \left( \frac{2.963 \times 183.3}{20^2} - 1 \right) \frac{1}{0.783} = 0.457 \quad 8.9$$

Thus, the prying ratio for the bolts is  $T_f/P_f = 209/183.3 = 1.14$ , or 14% prying.

## 11 List of symbols and abbreviations

### 11.1 Abbreviations of organisations

AISC	American Institute of Steel Construction
ASTM	American Society for Testing and Materials
AWS	American Welding Society
CEN	European Committee for Standardization
CSA	Canadian Standards Association
IIW	International Institute of Welding
ISO	International Organization for Standardization

### 11.2 Other abbreviations

CHS	circular hollow section
FE	finite element
RHS	rectangular or square hollow section
SHS	square hollow section

### 11.3 General symbols

$A_g$	gross cross sectional area of RHS
$A_{gv}$	gross area in shear for block failure
$A_i$	cross sectional area of member $i$ ( $i = 0, 1, 2$ )
$A_n$	net cross sectional area of RHS; net section in a bolted joint
$A_{ne}$	effective net area, reduced by shear lag
$A_{nt}$	net area in tension for block failure
$A_v$	chord effective shear area
$A_1, A_2$	areas (general)
$B_p$	width of stiffening plate
$C_e, C_T, C_x, C_K$	efficiency coefficients
$C_1$	coefficient in chord stress functions
$E$	modulus of elasticity
$K$	effective length factor; parameter for a bolted joint
$L$	distance between chord panel points; length in a bolted or welded joint
$L_p$	length of plate
$L_w$	weld length
$L_1, L_2, L_3$	length parameters on the connected edges of gusset plates
$M^*$	moment or flexural resistance of a joint, expressed as a moment in the brace
$M_i$	bending moment applied to member $i$ ( $i = 0, 1, 2$ )
$M_{ip,i}$	in-plane bending moment applied to member $i$
$M_{op,i}$	out-of-plane bending moment applied to member $i$
$M_{pl,i}$	plastic moment capacity of member $i$ ( $i = 0, 1, 2$ )
$N$	axial force
$N_{gap,0}$	axial chord load in the gap of a gap joint
$N_{gap,0}^*$	design resistance for the axial load in a chord member at the gap location
$N_i$	axial force applied to member $i$ ( $i = 0, 1, 2$ )
$N_i^*$	joint resistance, expressed as an axial force in member $i$
$N_{pl,0}$	axial yield capacity of the chord
$N_s^*$	brace shear resistance at connection with chord face
$N_{ui}$	ultimate capacity of a joint based on the load in brace $i$
$N_{yi}$	yield capacity of a joint based on the load in brace $i$
$N_{op}$	chord "preload" force

$N_{1(3\%)}$	joint capacity at a chord deformation of 3% of $b_0$
$O_v$	overlap $O_v = q/p \times 100\%$
$O_{v,limit}$	limit for overlap $O_v$
$P$	external load
$P_f$	external tensile load applied to a bolt
$Q_f$	function to take account of the effect of chord stress in the connecting face
$Q_u$	function in the design strength equations accounting for the effect of geometric parameters
$T^*$	factored tensile resistance of a bolt or member
$T_f$	total bolt tension, including prying
$V$	shear load
$V_{gap,0}$	shear force in the gap of a gap joint
$V_{pl,0}$	shear yield capacity of the chord
$W_{el,i}$	elastic section modulus of member $i$
$W_{pl,i}$	plastic section modulus of member $i$ (class 1 and 2 sections)
$a$	throat thickness of a fillet weld; edge distance of bolt line
$a'$	$a_{effective} + d/2$
$a_{effective}$	$a$ , but $\leq 1.25b$
$b$	distance from bolt line to the hollow section face
$b'$	$b - d/2 + t_i$
$b_e$	effective width of element
$b_{ei}, b_{ej}, b_{e,ov}$	functions used in the criteria for local yielding of the overlapping brace and brace shear
$b_{e,p}$	effective punching shear width of element
$b_i$	overall out-of-plane width of RHS or I section member $i$ ( $i = 0, 1, 2$ ), or width of branch plate $i$ ( $i = 1$ )
$b_i'$	width parameter for a cropped brace
$b_{sp}$	width of stiffening plate
$c$	distance between adjacent bolts
$c_s$	coefficient for brace shear area
$d$	bolt diameter
$d'$	bolt hole diameter
$d_i$	external diameter of CHS member $i$ ( $i = 0, 1, 2$ )
$d_{ei}, d_{ej}, d_{e,ov}$	functions used in the criteria for local yielding of the overlapping brace and brace shear
$e$	nodding eccentricity for a joint – positive being towards the outside of the truss (see figure 1.2)
$f_c'$	crushing strength of concrete
$f_k, f_{kn}$	buckling stress, using the column slenderness ratio $KL/r$
$f(n)$	chord stress function in 1 <sup>st</sup> edition of CIDECT Design Guide No. 3 (Packer et al., 1992)
$f(n')$	chord prestress function
$f_u$	ultimate tensile stress
$f_{ui}$	ultimate tensile stress of member $i$ ( $i = 0, 1, 2$ )
$f_y$	yield stress
$f_{yi}, f_{yw}, f_{yp}$	yield stress of member $i$ ( $i = 0, 1, 2$ ), web or plate
$f_{op}$	prestress in chord (chord stress excluding effect of the brace load components)
$g$	gap between the brace members (ignoring welds) of a K or N joint, at the face of the chord (see figure 1.2); bolt gauge
$g_1$	bolt edge distance
$g_2$	bolt distance
$h_i$	overall in-plane depth of RHS or I section member $i$ ( $i = 0, 1, 2$ ), or depth of branch plate $i$ ( $i = 1$ )
$h_i'$	depth parameter for a cropped brace
$h_p$	depth of plate
$\ell_{b,eff.}$	effective brace perimeter for local yielding of the (overlapping) brace
$\ell_{p,eff.}$	effective brace perimeter for chord punching shear

n	stress ratio in RHS chord, used in $Q_i$ term ( $n = \frac{N_0}{N_{pl,0}} + \frac{M_0}{M_{pl,0}}$ ); number of bolts
n'	stress ratio used in $f(n')$ term, based on the chord loading excluding the brace force components in the chord
p	length of the projected contact area of the overlapping brace member onto the face of the chord, in the absence of the overlapped brace member, in a K or N joint (see figure 1.1); length of flange plate attributed to each bolt, or bolt pitch
p'	length of flange plate attributed to each bolt, or bolt pitch
q	length of overlap, measured at the face of the chord, between one brace member toe and the position of the other projected brace member toe, in a K or N joint (see figure 1.1)
r	fillet radius of an I or H section; radius of gyration
r <sub>o</sub>	external corner radius of an RHS
s	distance; bolt spacing
t	thickness
t <sub>i</sub>	wall thickness of hollow section member i or flange thickness of I section member i (i = 0, 1, 2)
t <sub>p</sub>	thickness of plate
t <sub>sp</sub>	thickness of stiffening plate
t <sub>w</sub>	thickness of web
w	distance between the welds, measured from plate face-to-plate face, around the perimeter of the RHS ( $w \approx b_i + h_i - t_p$ )
$\alpha$	factor; ratio of bending moments in bolted flange-plate joint
$\beta$	width ratio between brace/branch member(s) and the chord = $d_1/b_0$ , $b_1/b_0$ (for T, Y, X) = $(d_1 + d_2)/2b_0$ , $(b_1 + b_2 + h_1 + h_2)/4b_0$ (for K or N joints)
$\beta^*$	stiffening plate width ratio ( $\beta^* = (b_{sp} - t_1)/(b_0 - t_0)$ )
$\beta_p$	width ratio between brace member and stiffening plate ( $\beta_p = b_1/B_p$ )
$\chi$	reduction factor for (column) buckling
$\delta$	ratio of the net flange-plate area at bolt line to gross area at the RHS face
$\epsilon$	parameter used to define section class limitations
$\phi$	joint resistance (or capacity) factor (approximate inverse of $\gamma_M$ ); angle between two planes in a multiplanar joint
$\phi_c$	resistance factor for concrete in bearing
$\phi_p$	resistance factor for flange-plate
$\phi_u$	resistance factor for rupture
$\gamma$	half width-to-thickness ratio of the chord ( $\gamma = b_0/2t_0$ )
$\gamma_M$	partial safety factor for joint resistance (approximate inverse of $\phi$ )
$\eta$	ratio of brace member depth to the chord width ( $\eta = h_1/b_0$ )
$\eta_p$	ratio of brace member depth to stiffening plate width ( $\eta_p = h_1/B_p$ )
$\lambda$	slenderness
$\bar{\lambda}$	non-dimensional slenderness
$\lambda'$	multiplication factor
$\mu$	factor to be applied to uniplanar joint strength to obtain multiplanar joint strength
$\theta_i$	included angle between brace/branch member i (i = 1, 2) and the chord
$\theta_i'$	slope of brace member face at the cropped end

#### 11.4 Subscripts

e	effective
el	elastic
g	gross
i	subscript used to denote the member of a hollow section joint. Subscript i = 0 designates the chord (or "through member"); i = 1 refers in general to the brace for T, Y and X joints, or it refers to the compression brace member for K and N joints; i = 2 refers to the tension

brace member for K and N joints. For K and N overlap joints, the subscript *i* is used to denote the overlapping brace member (see figure 1.1).

<i>j</i>	subscript used to denote the overlapped brace member for K and N overlap joints
<i>n</i>	net
<i>p</i>	plate; preload force
<i>pl</i>	plastic
<i>t</i>	tension
<i>u</i>	ultimate
<i>v</i>	shear
<i>w</i>	web or weld
<i>y</i>	yield

### 11.5 Superscripts

*	resistance or capacity
---	------------------------

Symbols not shown here are specifically defined at the location where they are used.

In all calculations, the nominal (guaranteed minimum) mechanical properties should be used.



Three-dimensional truss made of RHS members

## 12 References

AISC, 2005: Specification for structural steel buildings. ANSI/AISC 360-05, American Institute of Steel Construction, Chicago, Ill., USA.

ASTM, 2007a: Standard specification for pipe, steel, black and hot-dipped, zinc-coated, welded and seamless. ASTM A53/A53M-07, ASTM International, West Conshohocken, Pa., USA.

ASTM, 2007b: Standard specification for cold-formed welded and seamless carbon steel structural tubing in rounds and shapes. ASTM A500/A500M-07, ASTM International, West Conshohocken, Pa., USA.

ASTM, 2007c: Standard specification for hot-formed welded and seamless carbon steel structural tubing. ASTM A501-07, ASTM International, West Conshohocken, Pa., USA.

AWS, 2008: Structural welding code – Steel. 21<sup>st</sup> Edition, AWS D1.1/D1.1M:2008, American Welding Society, Miami, FI, USA.

Bauer, D., and Redwood, R.G., 1988: Triangular truss joints using rectangular tubes. *Journal of Structural Engineering*, American Society of Civil Engineers, Vol. 114, No. 2, pp. 408-424.

Birkemoe, P.C., and Packer, J.A., 1986: Ultimate strength design of bolted tubular tension connections. *Proceedings Conference on Steel Structures – Recent Research Advances and their Applications to Design*, Budva, Yugoslavia, pp. 153-168.

Björk, T., Marquis, G., Kemppainen, R., and Ilvonen, R., 2003 : The capacity of cold-formed rectangular hollow section K gap joints. *Proceedings 10<sup>th</sup> International Symposium on Tubular Structures*, Madrid, Spain, Tubular Structures X, Swets & Zeitlinger, Lisse, The Netherlands, pp. 227-234.

Bouwman, L.P., 1979: Fatigue of bolted connections and bolts loaded in tension. *Stevin Report 6-79-9*, Delft University of Technology, Delft, The Netherlands.

Brockenbough, R.L., 1972: Strength of square tube connections under combined loads. *Journal of the Structural Division*, American Society of Civil Engineers, Vol. 98, No. ST12, pp. 2753-2768.

Cao, J.J., Packer, J.A., and Kosteski, N., 1998a: Design guidelines for longitudinal plate to HSS connections. *Journal of Structural Engineering*, American Society of Civil Engineers, Vol. 124, No. 7, pp. 784-791.

Cao, J.J., Packer, J.A., and Yang, G.J., 1998b: Yield line analysis of RHS connections with axial loads. *Journal of Constructional Steel Research*, Vol. 48, No. 1, pp. 1-25.

Caravaggio, A., 1988: Tests on steel roof joints for Toronto SkyDome. M.A.Sc. Thesis, University of Toronto, Canada.

CEN, 2005a: Eurocode 3: Design of steel structures – Part 1-1: General rules and rules for buildings. EN 1993-1-1:2005(E), European Committee for Standardization, Brussels, Belgium.

CEN, 2005b: Eurocode 3: Design of steel structures – Part 1-8: Design of joints. EN 1993-1-8:2005(E), European Committee for Standardization, Brussels, Belgium.

CEN, 2006a: Hot-finished structural hollow sections of non-alloy and fine grain steels – Part 2: Tolerances, dimensions and sectional properties. EN 10210-2:2006(E), European Committee for Standardization, Brussels, Belgium.

CEN, 2006b: Cold-formed welded structural hollow sections of non-alloy and fine grain steels – Part 2: Tolerances, dimensions and sectional properties. EN 10219-2:2006(E), European Committee for Standardization, Brussels, Belgium.

Chen, Y., Liu, D.K., and Wardenier, J., 2005: Design recommendations for RHS-K joints with 100% overlap. Proceedings 15<sup>th</sup> International Offshore and Polar Engineering Conference, Seoul, Korea, Vol. IV, pp. 300-307.

CIDECT, 1984: Construction with hollow steel sections. British Steel Plc., Corby, Northants, UK, ISBN 0-9510062-0-7.

Coutie, M.G., Davies, G., Bettison, M., and Platt, J., 1983: Development of recommendations for the design of welded joints between steel structural hollow sections or between steel structural hollow sections and H sections. Final Report, Part 3: Three dimensional joints. Report on ECSC Contract 7210.5A1814, University of Nottingham, UK.

Coutie, M.G., Davies, G., Philiastides, A., and Yeomans, N., 1987: Testing of full-scale lattice girders fabricated with RHS members. Conference on Structural Assessment Based on Full and Large-Scale Testing, Building Research Station, Watford, UK.

CSA, 2004: General requirements for rolled or welded structural quality steel/structural quality steel. CAN/CSA G40.20-04/G40.21-04, Canadian Standards Association, Toronto, Canada.

CSA, 2009: Design of steel structures. CSA-S16-09, Canadian Standards Association, Toronto, Canada.

Cute, D., Camo, S., and Rumpf, J.L., 1968: Welded connections for square and rectangular structural steel tubing. Research Report No. 292-10, Drexel Institute of Technology, Philadelphia, Pa, USA.

Czechowski, A., Gasparski, T., Zycinski, J., and Brodka, J., 1984: Investigation into the static behaviour and strength of lattice girders made of RHS. International Institute of Welding, IIW Doc. XV-562-84, Poland.

Davies, G., and Packer, J.A., 1982: Predicting the strength of branch plate-RHS connections for punching shear. Canadian Journal of Civil Engineering, Vol. 9, pp. 458-467.

Davies, G., and Panjeh Shahi, E., 1984: Tee joints in rectangular hollow sections (RHS) under combined axial loading and bending. Proceedings 7<sup>th</sup> International Symposium on Steel Structures, Gdansk, Poland.

Davies, G., and Morita, K., 1991: Three dimensional cross joints under combined axial branch loading. Proceedings 4<sup>th</sup> International Symposium on Tubular Structures, Delft, The Netherlands, Delft University Press, Delft, The Netherlands, pp. 324-333.

Davies, G., and Kelly, R.B., 1995: Bird beak joints in square hollow sections – A finite element investigation. Proceedings 4<sup>th</sup> Pacific Structural Steel Conference, Singapore.

Davies, G., Owen, J.S., and Kelly, R.B., 1996: Bird beak T-joints in square hollow sections – A finite element investigation. Proceedings 6<sup>th</sup> International Offshore and Polar Engineering Conference, Los Angeles, USA, Vol. IV, pp. 22-27.

Davies, G., Owen, J.S., and Kelly, R.B., 2001: The effect of purlin loads on the capacity of overlapped bird-beak K joints. Proceedings 9<sup>th</sup> International Symposium on Tubular Structures, Düsseldorf, Germany, Tubular Structures IX, Swets & Zeitlinger, Lisse, The Netherlands, pp. 229-238.

- Driver, R.G., Grondin, G.Y., and Kulak, G.L., 2006: Unified block shear equation for achieving consistent reliability. *Journal of Constructional Steel Research*, Vol. 62, No. 3, pp. 210-222.
- Duff, G., 1963: Joint behaviour of a welded beam-column connection in rectangular hollow sections. Ph.D. Thesis, The College of Aeronautics, Cranfield, UK.
- Dutta, D., and Würker, K., 1988: *Handbuch Hohlprofile in Stahlkonstruktionen*. Verlag TÜV Rheinland GmbH, Köln, Germany.
- Dutta, D., Wardenier, J., Yeomans, N., Sakae, K., Bucak, Ö., and Packer, J.A., 1998: Design guide for fabrication, assembly and erection of hollow section structures. CIDECT series 'Construction with hollow sections' No. 7, TÜV-Verlag, Köln, Germany.
- Dutta, D., 2002: *Structures with hollow sections*. Ernst & Sohn, Verlag, Berlin, Germany.
- Eekhout, M., 1996: *Tubular structures in architecture*. CIDECT and Delft University of Technology, Delft, The Netherlands.
- Fleischer, O., and Puthli, R., 2008: Extending existing design rules in EN 1993-1-8 (2005) for gapped RHS K-joints for maximum chord slenderness ( $b_0/t_0$ ) of 35 to 50 and gap size  $g$  to as low as  $4t_0$ . *Proceedings 12<sup>th</sup> International Symposium on Tubular Structures*, Shanghai, China, *Tubular Structures XII*, Taylor & Francis Group, London, UK, pp. 293-301.
- Frater, G.S., and Packer, J.A., 1990: Design of fillet weldments for hollow structural section trusses. CIDECT Report No. 5AN/2-9017, University of Toronto, Canada.
- Frater, G.S., 1991: Performance of welded rectangular hollow structural section trusses. Ph.D. Thesis, University of Toronto, Canada.
- Galambos, T.V. (Ed.), 1998: *Guide to stability design criteria for metal structures*, 5<sup>th</sup> Edition, Structural Stability Research Council, John Wiley & Sons, New York, USA.
- Ghosh, A., and Morris, G., 1981: Behaviour of tubular steel trusses with cropped webs. *Canadian Journal of Civil Engineering*, Vol. 8, No. 1, pp. 51-58.
- Grundy, P., and Foo, E.K.J., 1991: Performance of flattened tube connections. *Proceedings 4<sup>th</sup> International Symposium on Tubular Structures*, Delft, The Netherlands, Delft University Press, Delft, The Netherlands, pp. 251-258.
- Horne, M.R., and Morris, L.J., 1985: *Plastic design of low-rise frames*. Collins, London, UK.
- IIW, 1989: Design recommendations for hollow section joints – Predominantly statically loaded. 2<sup>nd</sup> Edition, International Institute of Welding, Commission XV, IIW Doc. XV-701-89.
- IIW, 2009: Static design procedure for welded hollow section joints – Recommendations. 3<sup>rd</sup> Edition, International Institute of Welding, Commission XV, IIW Doc. XV-1329-09.
- Ishida, K., Ono, T., and Iwata, M., 1993: Ultimate strength formula for joints of new truss system using rectangular hollow sections. *Proceedings 5<sup>th</sup> International Symposium on Tubular Structures*, Nottingham, UK, *Tubular Structures V, E & FN Spon*, London, UK, pp. 511-518.
- Kanatani, H., Fujiwara, K., Tabuchi, M., and Kamba, T., 1980: Bending tests on T-joints of RHS chord and RHS or H-shape branch, CIDECT Report 5AF-80/15.
- Kanatani, H., Kamba, T., and Tabuchi, M., 1986: Effect of the local deformation of the joints on RHS Vierendeel trusses. *Proceedings International Meeting on Safety Criteria in Design of Tubular Structures*, Tokyo, Japan, pp. 127-137.

- Karcher, D., and Puthli, R.S., 2001: The static design of stiffened and unstiffened CHS L-joints. Proceedings 9<sup>th</sup> International Symposium on Tubular Structures, Düsseldorf, Germany, Tubular Structures IX, Swets & Zeitlinger, Lisse, The Netherlands, pp. 221-228.
- Kato, B., and Mukai, A., 1985: Bolted tension flanges square hollow section members. Supplement in 1985: Bolted at two sides of flange. CIDECT Program 8B Report, University of Tokyo, Japan.
- Kitipornchai, S., and Traves, W.H., 1989: Welded tee end connections for circular hollow tubes. Journal of Structural Engineering, American Society of Civil Engineers, Vol. 115, No. 12, pp. 3155-3170.
- Koning, C.H.M. de, and Wardenier, J., 1984: The static strength of welded joints between structural hollow sections or between structural hollow sections and H-sections. Part 2: Joints between rectangular hollow sections. Stevin Report 6-84-19, Delft University of Technology, Delft, The Netherlands.
- Korol, R.M., El-Zanaty, M., and Brady, F.J., 1977: Unequal width connections of square hollow sections in Vierendeel trusses. Canadian Journal of Civil Engineering, Vol. 4, pp. 190-201.
- Korol, R.M., and Mansour, M.H., 1979: Theoretical analysis of haunch-reinforced T-joints in square hollow sections. Canadian Journal of Civil Engineering, Vol. 6, No. 4, pp. 601-609.
- Korol, R.M., and Chidiac, M.A., 1980: K-joints of double-chord square hollow-sections. Canadian Journal of Civil Engineering, Vol. 7, No. 3, pp. 523-539.
- Korol, R.M., and Mirza, F.A., 1982: Finite element analysis of RHS T-joints. Journal of the Structural Division, American Society of Civil Engineers, Vol. 108, No. ST9, pp. 2081-2098.
- Korol, R.M., Mitri, H.S., and Mirza, F.A., 1982: Plate reinforced square hollow section T-joints of unequal width. Canadian Journal of Civil Engineering, Vol. 9, No. 2, pp. 143-148.
- Korol, R.M., 1983: The behaviour of HSS double chord Warren trusses and aspects of design. Canadian Symposium on HSS, CIDECT, Lecture tour to Canadian cities.
- Korol, R.M., Mirza, F.A., and Chiu, E.T.-C., 1983: An experimental investigation of double-chord HSS trusses. Canadian Journal of Civil Engineering, Vol. 10, No. 2, pp. 248-260.
- Korol, R.M., and Mitri, H.S., 1985: Strength analysis of RHS double chord joints with separated chords. Canadian Journal of Civil Engineering, Vol. 12, No. 2, pp. 370-381.
- Kosteski, N., 2001: Branch plate to rectangular hollow section member connections. Ph.D. Thesis, University of Toronto, Toronto, Canada.
- Kosteski, N., and Packer, J.A., 2003a: Welded tee-to-HSS connections. Journal of Structural Engineering, American Society of Civil Engineers, Vol. 129, No. 2, pp. 151-159.
- Kosteski, N., and Packer, J.A., 2003b: Longitudinal plate and through plate-to-HSS welded connections. Journal of Structural Engineering, American Society of Civil Engineers, Vol. 129, No. 4, pp. 478-486.
- Kosteski, N., Packer, J.A., and Puthli, R.S., 2005: Notch toughness of internationally produced hollow structural sections. Journal of Structural Engineering, American Society of Civil Engineers, Vol. 131, No. 2, pp. 279-286.
- Kurobane, Y., Packer, J.A., Wardenier, J., and Yeomans, N., 2004: Design guide for structural hollow section column connections. CIDECT series 'Construction with hollow sections' No. 9, TÜV-Verlag, Köln, Germany.

- Lau, B.L., Morris, G.A., and Pinkney, R.B., 1985: Testing of Warren-type cropped-web tubular truss joints. Canadian Society for Civil Engineering Annual Conference, Saskatoon, Canada.
- Lazar, B.E., and Fang, P.J., 1971: T-type moment connections between rectangular tubular sections. Research Report, Sir George Williams University, Montreal, Canada.
- Liu, D.K., and Wardenier, J., 2001a: Multiplanar influence on the strength of RHS multiplanar gap KK-joints. Proceedings 9<sup>th</sup> International Symposium on Tubular Structures, Düsseldorf, Germany, Tubular Structures IX, Swets & Zeitlinger, Lisse, The Netherlands, pp. 203-212.
- Liu, D.K., and Wardenier, J., 2001b: The strength of multiplanar gap KK joints of rectangular hollow sections under axial loading. Proceedings 11<sup>th</sup> International Offshore and Polar Engineering Conference, Stavanger, Norway, Vol. IV, pp. 15-22.
- Liu, D.K., and Wardenier, J., 2002: The strength of multiplanar overlap KK-joints of rectangular hollow sections under axial loading. Proceedings 12<sup>th</sup> International Offshore and Polar Engineering Conference, Kitakyushu, Japan, Vol. IV, pp. 34-40.
- Liu, D.K., and Wardenier, J., 2003: The strength of multiplanar KK-joints of square hollow sections. Proceedings 10<sup>th</sup> International Symposium on Tubular Structures, Madrid, Spain, Tubular Structures X, Swets & Zeitlinger, Lisse, The Netherlands, pp. 197-205.
- Liu, D.K., and Wardenier, J., 2004: Effect of the yield strength on the static strength of uniplanar K-joints in RHS (steel grades S460, S355 and S235). IIW Doc. XV-E-04-293, Delft University of Technology, Delft, The Netherlands.
- Liu, D.K., Chen, Y., and Wardenier, J., 2005: Design recommendations for RHS-K joints with 50% overlap. Proceedings 15<sup>th</sup> International Offshore and Polar Engineering Conference, Seoul, Korea, Vol. IV, pp. 308-315.
- Lu, L.H., Winkel, G.D. de, Yu, Y., and Wardenier, J., 1994: Deformation limit for the ultimate strength of hollow section joints. Proceedings 6<sup>th</sup> International Symposium on Tubular Structures, Melbourne, Australia, Tubular Structures VI, Balkema, Rotterdam, The Netherlands, pp. 341-347.
- Lu, L.H., 1997: The static strength of I-beam to rectangular hollow section column connections. Ph.D. Thesis, Delft University Press, Delft, The Netherlands.
- Luft, R.T., Korol, R.M., and Huitema, H.A.P., 1991: An economic comparison of single chord and double chord RHS Warren trusses. Proceedings 4<sup>th</sup> International Symposium on Tubular Structures, Delft, The Netherlands, Delft University Press, Delft, The Netherlands, pp. 11-20.
- Mang, F., 1980: Investigation of standard bolted flange connections for circular and rectangular hollow sections. CIDECT Report 8A-81/7-E, University of Karlsruhe, Germany.
- Mang, F., Steidl, G., and Bucak, Ö., 1980: Design of welded lattice joints and moment resisting knee joints made of hollow sections. International Institute of Welding, IIW Doc. XV-463-80, University of Karlsruhe, Germany.
- Mang, F., Bucak, Ö., and Wolfmuller, F., 1983: The development of recommendations for the design of welded joints between steel structural hollow sections (T- and X-type joints). University of Karlsruhe, Germany, Final Report on ECSC Agreement 7210 SA/I 09 and CIDECT Program 5AD.
- Martinez-Saucedo, G., and Packer, J.A., 2006: Slotted end connections to hollow sections. CIDECT Final Report 8G-10/4, University of Toronto, Toronto, Canada.
- Mehrotra, B.L., and Redwood, R.G., 1970: Load transfer through connections between box sections. Canadian Engineering Institute, C-70-BR and ST 10, Canada.

- Mehrotra, B.L., and Govil, A.K., 1972: Shear lag analysis of rectangular full-width tube connections. *Journal of the Structural Division, American Society of Civil Engineers*, Vol. 98, No. ST1, pp. 287-305.
- Morris, G.A., 1985: Tubular steel trusses with cropped webs. *Journal of Structural Engineering, American Society of Civil Engineers*, Vol. 111, No. 6, pp. 1338-1357.
- Morris, G.A., and Packer, J.A., 1988: Yield line analysis of cropped-web Warren truss joints. *Journal of Structural Engineering, American Society of Civil Engineers*, Vol. 114, No. 10, pp. 2210-2224.
- Mouty, J. (Ed.), 1981: Effective lengths of lattice girder members. CIDECT Monograph No. 4, CIDECT.
- Ono, T., Iwata, M., and Ishida, K., 1991: An experimental study on joints of new truss system using rectangular hollow sections. *Proceedings 4<sup>th</sup> International Symposium on Tubular Structures*, Delft, The Netherlands, Delft University Press, Delft, The Netherlands, pp. 344-353.
- Ono, T., Iwata, M., and Ishida, K., 1993: Local failure of joints of new truss system using rectangular hollow sections subjected to in-plane bending moment. *Proceedings 5<sup>th</sup> International Symposium on Tubular Structures*, Nottingham, UK, Tubular Structures V, E & FN Spon, London, UK, pp. 503-510.
- Ono, T., Iwata, M., and Ishida, K., 1994: Local failure of joints of new truss system using rectangular hollow sections subjected to out-of-plane bending moment. *Proceedings 6<sup>th</sup> International Symposium on Tubular Structures*, Melbourne, Australia, Tubular Structures VI, Balkema, Rotterdam, The Netherlands, pp. 441-448.
- Owen, J.S., Davies, G., and Kelly, R.B., 1996: A comparison of the behaviour of RHS bird beak T-joints with normal RHS and CHS systems. *Proceedings 7<sup>th</sup> International Symposium on Tubular Structures*, Miskolc, Hungary, Tubular Structures VII, Balkema, Rotterdam, The Netherlands, pp. 173-180.
- Packer, J.A., and Haleem, A.S., 1981: Ultimate strength formulae for statically loaded welded HSS joints in lattice girders with RHS chords. *Proceedings Canadian Society for Civil Engineering Annual Conference*, Fredericton, Canada, Vol. 1, pp. 331-343.
- Packer, J.A., Bruno, L., and Birkemoe, P.C., 1989: Limit analysis of bolted RHS flange plate joints. *Journal of Structural Engineering, American Society of Civil Engineers*, Vol. 115, No. 9, pp. 2226-2242.
- Packer, J.A., 1991: Cranked-chord HSS connections. *Journal of Structural Engineering, American Society of Civil Engineers*, Vol. 117, No. 8, pp. 2224-2240.
- Packer, J.A., and Fear, C.E., 1991: Concrete-filled rectangular hollow section X and T connections. *Proceedings 4<sup>th</sup> International Symposium on Tubular Structures*, Delft, The Netherlands, Delft University Press, Delft, The Netherlands, pp. 382-391.
- Packer, J.A., and Wardenier, J., 1992: Design rules for welds in RHS K, T, Y and X connections. *IIV International Conference on Engineering Design in Welded Construction*, Madrid, Spain, pp. 113-120.
- Packer, J.A., Wardenier, J., Kurobane, Y., Dutta, D., and Yeomans, N., 1992: Design guide for rectangular hollow section (RHS) joints under predominantly static loading. 1<sup>st</sup> Edition, CIDECT series 'Construction with hollow sections' No. 3, TÜV-Verlag, Köln, Germany.
- Packer, J.A., 1995: Concrete-filled HSS connections. *Journal of Structural Engineering, American Society of Civil Engineers*, Vol. 121, No. 3, pp. 458-467.

Packer, J.A., and Henderson, J.E., 1997: Hollow structural section connections and trusses – A design guide. 2<sup>nd</sup> Edition, Canadian Institute of Steel Construction, Toronto, Canada.

Packer, J.A., 2007: Design with hollow structural sections – A report on recent developments in the USA. Proceedings 5<sup>th</sup> International Conference on Advances in Steel Structures, Singapore, Vol. II, pp. 228-237.

Packer, J.A., Sherman, D.R., and Lecce, M., 2009: HSS connections. Steel Design Guide No. 24, American Institute of Steel Construction, Chicago, Ill., USA.

Papanikolas, P.C., Nowak, J.A., and Kulak, G.L., 1990: Flexible flattened HSS connections. Report by Northern Steel Inc., Edmonton, Canada.

Philiastides, A., 1988: Fully overlapped rolled hollow section welded joints in trusses. Ph.D. Thesis, University of Nottingham, UK.

Qian, X.D., Wardenier, J., and Choo, Y.S., 2007: A uniform approach for the design of CHS 100% overlap joints. Proceedings 5<sup>th</sup> International Conference on Advances in Steel Structures, Singapore, Vol. II, pp. 172-182.

Redwood, R.G., 1965: The behaviour of joints between rectangular hollow structural members. Civil Engineering and Public Works Review, Canada, pp. 1463-1469.

Rondal, J., Würker, K.-G., Dutta, D., Wardenier, J., and Yeomans, N., 1996: Structural stability of hollow sections. 2<sup>nd</sup> Printing, CIDECT series 'Construction with hollow sections' No. 2, TÜV-Verlag, Köln, Germany.

Sedlacek, G., Wardenier, J., Dutta, D., and Grotmann, D., 1991: Evaluation of test results on hollow section lattice girder connections. Background Report to Eurocode 3 'Common unified rules for steel structures', Document 5.07, Eurocode 3 Editorial Group.

Sedlacek, G., Völling, B., Pak, D., and Feldmann, M., 2006: Local buckling behaviour of cold-formed RHS made from S1100. Proceedings 11<sup>th</sup> International Symposium on Tubular Structures, Quebec City, Canada, Tubular Structures XI, Taylor & Francis Group, London, UK, pp. 147-152.

Sherman, D.R., 1995: Simple framing connections to HSS columns. Proceedings National Steel Construction Conference, San Antonio, Tex., USA, American Institute of Steel Construction, Chicago, Ill., USA, pp. 30.1-30.16.

Sherman, D.R., 1996: Designing with structural tubing. Engineering Journal, American Institute of Steel Construction, Vol. 33, No. 3, pp. 101-109.

Shinouda, M.R., 1967: Stiffened tubular joints. Ph.D. Thesis, University of Sheffield, UK.

Standards Australia, 1991: Structural steel hollow sections. Australian Standard AS 1163, Standards Australia, Sydney, Australia.

Staples, C.J.L., and Harrison, C.C., undated: Test results of 24 right-angled branches fabricated from rectangular hollow sections. University of Manchester Institute of Science and Technology (UMIST) Report, Manchester, UK.

Stelco, 1981: Hollow structural sections – Design manual for connections. 2<sup>nd</sup> Edition, Stelco Inc., Hamilton, Canada.

Struik, J.H.A., and Back, J. de, 1969: Tests on bolted T-stubs with respect to a bolted beam-to-column connection. Stevin Report 6-69-13, Delft University of Technology, Delft, The Netherlands.

- Szlendak, J., and Brodka, J., 1985: Strengthening of T moment of RHS joints. Proceedings Institution of Civil Engineers, Part 2, Vol. 79, pp. 717-727.
- Szlendak, J., 1986: Interaction curves for M-N loaded T RHS joints. Proceedings International Meeting on Safety Criteria in Design of Tubular Structures, Tokyo, Japan, pp. 169-174.
- Szlendak, J., and Brodka, J., 1986a: Design of strengthen frame RHS joints. Proceedings International Meeting on Safety Criteria in Design of Tubular Structures, Tokyo, Japan, pp. 159-168.
- Szlendak, J., and Brodka, J., 1986b: Reply to discussion by J.A. Packer on paper "Strengthening of T moment of RHS joints". Proceedings Institution of Civil Engineers, Part 2, Vol. 81, pp. 721-725.
- Szlendak, J., 1991: Beam-column welded RHS connections. Journal of Thin-Walled Structures, Vol. 12, pp. 63-80.
- Thornton, W.A., 1984: Bracing connections for heavy construction. Engineering Journal, American Institute of Steel Construction, Vol. 21, Third Quarter, pp. 139-148.
- Wardenier, J., 1972: Investigation on Vierendeel joints; Determination of  $M-\Phi$  and  $P-\delta$  characteristics and the fatigue behaviour. Stevin Report 6-72-11, Delft University of Technology, Delft, The Netherlands, (in Dutch).
- Wardenier, J., and Stark, J.W.B., 1978: The static strength of welded lattice girder joints in structural hollow sections: Parts 1-10. CIDECT Final Report 5Q-78/4, Delft University of Technology, Delft, The Netherlands.
- Wardenier, J., Davies, G., and Stolle, P., 1981: The effective width of branch plate to RHS chord connections in cross joints. Stevin Report 6-81-6, Delft University of Technology, Delft, The Netherlands.
- Wardenier, J., 1982: Hollow section joints. Delft University Press, Delft, The Netherlands.
- Wardenier, J., Kurobane, Y., Packer, J.A., Dutta, D., and Yeomans, N., 1991: Design guide for circular hollow section (CHS) joints under predominantly static loading. 1<sup>st</sup> Edition, CIDECT series 'Construction with hollow sections' No. 1, TÜV-Verlag, Köln, Germany.
- Wardenier, J., 2002: Hollow sections in structural applications. Bouwen met Staal, Zoetermeer, The Netherlands.
- Wardenier, J., 2007: A uniform effective width approach for the design of CHS overlap joints. Proceedings 5<sup>th</sup> International Conference on Advances in Steel Structures, Singapore, Vol. II, pp. 155-165.
- Wardenier, J., Vegte, G.J. van der, and Liu, D.K., 2007a: Chord stress function for rectangular hollow section X and T joints. Proceedings 17<sup>th</sup> International Offshore and Polar Engineering Conference, Lisbon, Portugal, Vol. IV, pp. 3363-3370.
- Wardenier, J., Vegte, G.J. van der, and Liu, D.K., 2007b: Chord stress functions for K gap joints of rectangular hollow sections. International Journal of Offshore and Polar Engineering, ISOPE, Vol. 17, No. 3, pp. 225-232.
- Wardenier, J., Kurobane, Y., Packer, J.A., Vegte, G.J. van der, and Zhao, X.-L., 2008: Design guide for circular hollow section (CHS) joints under predominantly static loading. 2<sup>nd</sup> Edition, CIDECT series 'Construction with hollow sections' No. 1, CIDECT, Geneva, Switzerland.
- Whitmore, R.E., 1952: Experimental investigation of stresses in gusset plates. Bulletin 16, University of Tennessee Engineering Experiment Station, USA.

Willibald, S., Puthli, R.S., and Packer, J.A., 2001: Experimentelle Studie zu geschraubten Kopfplatten-Verbindungen für Quadrathohlprofile. Stahlbau, Vol. 70, No. 3, pp. 183-192, (in German).

Willibald, S., Packer, J.A., and Puthli, R.S., 2002: Experimental study of bolted HSS flange-plate connections in axial tension. Journal of Structural Engineering, American Society of Civil Engineers, Vol. 128, No. 3, pp. 328-336.

Willibald, S., Packer, J.A., and Puthli, R.S., 2003a: Design recommendations for bolted rectangular HSS flange-plate connections in axial tension. Engineering Journal, American Institute of Steel Construction, Vol. 40, First Quarter, pp. 15-24.

Willibald, S., Packer, J.A., and Puthli, R.S., 2003b: Investigation on hidden joint connections under tensile loading. Proceedings 10<sup>th</sup> International Symposium on Tubular Structures, Madrid, Spain, Tubular Structures X, Swets & Zeitlinger, Lisse, The Netherlands, pp. 217-225.

Yeomans, N.F., and Giddings, T.W., 1988: The design of full width joints in RHS Vierendeel girders. Report No. 800/0/72, British Steel Plc., Corby, UK.

Yu, Y., 1997: The static strength of uniplanar and multiplanar connections in rectangular hollow sections. Ph.D. Thesis, Delft University Press, Delft, The Netherlands.

Zhao, X.-L., Wardenier, J., Packer, J.A., and Vegte, G.J. van der, 2008: New IIW (2008) static design recommendations for hollow section joints, Proceedings 12<sup>th</sup> International Symposium on Tubular Structures, Shanghai, China, Tubular Structures XII, Taylor & Francis Group, London, UK, pp. 261-269.

## Appendix A: Comparison between the new IIW (2009) design equations and the previous recommendations of IIW (1989) and/or CIDECT Design Guide No. 3 (1992)

In this Appendix, the new IIW (2009) design equations for RHS to RHS joints, presented in chapters 4 to 7 in this 2<sup>nd</sup> edition of Design Guide No. 3 are compared with the previous IIW (1989) equations incorporated in the 1<sup>st</sup> edition of this Design Guide (Packer et al., 1992). The latter were also implemented in Eurocode 3 (see e.g. Sedlacek et al., 1991) and other national and international codes. For comparison, the main tables of the previous IIW recommendations are recorded in this Appendix (see tables A1, A2, A6 and A7). This Appendix further notes some changes in scope between the 1<sup>st</sup> and 2<sup>nd</sup> edition of this Design Guide.

### A1 General

In the 2<sup>nd</sup> edition of Design Guide No. 3, it is explicitly indicated that joints have to be classified and designed on the basis of the load transfer through the joint, as illustrated in figure 4.2 and figure 4.3 (which is repeated in figure A1). In the 1<sup>st</sup> edition, only the extremes in loading were considered (e.g. similar to the approach for special types of joints given in table 4.4 of this 2<sup>nd</sup> edition of the Design Guide).

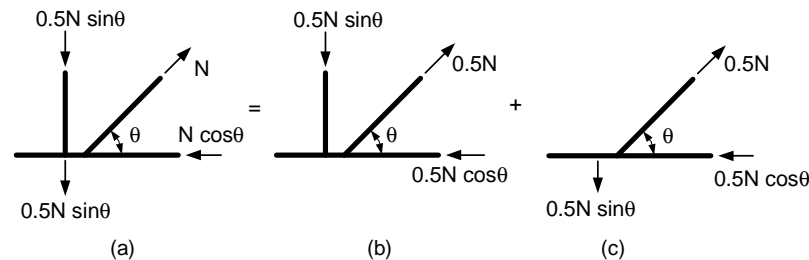


Figure A1 – Checking of a K joint with imbalanced brace loads

For distinction with the formulae in the previous edition, which are incorporated in many national and international codes, a slightly different presentation is used – compare tables 4.1 and 4.2 with tables A1 and A2. For example, the design capacity for chord (face) plastification (equation 4.1) is now presented as follows:

$$N_i^* = Q_u Q_f \frac{f_{y0} t_0^2}{\sin \theta_i} \quad \text{A1}$$

The parameter  $Q_u$  gives the influence function for the parameters  $\beta$  and  $\gamma$ , while the parameter  $Q_f$  accounts for the influence of the chord stress on the joint capacity. In the 1<sup>st</sup> edition of this Design Guide, the design equations in tables A1 and A2 directly incorporated the function of  $Q_u$  through the  $\beta$  and  $\gamma$  terms, but in principle the formulations are the same.

In the 1<sup>st</sup> edition, the chord stress function was given by  $f(n)$ , now it is designated as  $Q_f$ .

Apart from the fact that the chord stress functions have been modified for chord compression loading, a reduction factor is now given for tensile loading, whereas previously this was  $f(n) = 1.0$ .

Table A1 – Design resistance of uniplanar RHS braces or CHS braces to RHS chord joints according to IIW (1989) and the 1<sup>st</sup> edition of Design Guide No. 3 (Packer et al., 1992)

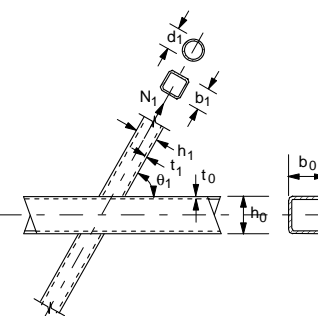
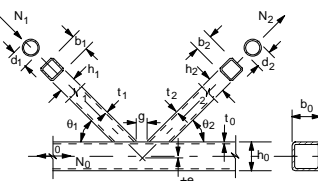
Type of joint	Factored joint resistance ( $i = 1,2$ )	
<b>T, Y and X joints</b>	$\beta \leq 0.85$	basis: chord face plastification
	$N_i^* = \frac{f_{y0} t_0^2}{(1-\beta) \sin \theta_1} \left[ \frac{2\eta}{\sin \theta_1} + 4(1-\beta)^{0.5} \right] f(n)$	
	$\beta = 1.0$ basis: chord side wall failure (*)	For $0.85 < \beta \leq 1.0$ , use linear interpolation between chord face plastification and chord side wall failure criteria
	$N_i^* = \frac{f_k t_0}{\sin \theta_1} \left[ \frac{2h_1}{\sin \theta_1} + 10t_0 \right]$	
	$\beta > 0.85$	basis: local yielding of brace
	$N_i^* = f_{y1} t_1 [2h_1 - 4t_1 + 2b_e]$	
	$0.85 \leq \beta \leq 1-1/\gamma$	basis: chord punching shear
$N_i^* = \frac{f_{y0} t_0}{\sqrt{3} \sin \theta_1} \left[ \frac{2h_1}{\sin \theta_1} + 2b_{e,p} \right]$		
<b>K and N gap joints</b>	basis: chord face plastification	
	$N_i^* = 8.9 \frac{f_{y0} t_0^2}{\sin \theta_i} \left[ \frac{b_1 + b_2 + h_1 + h_2}{4b_0} \right] \gamma^{0.5} f(n) \quad (i=1,2)$	
	basis: chord shear	
	$N_i^* = \frac{f_{y0} A_v}{\sqrt{3} \sin \theta_i}$	
	Also $N_{gap,0} \leq N_{gap,0}^* = (A_0 - A_v) f_{y0} + A_v f_{y0} \sqrt{1 - (V_{gap,0} / V_{pl,0})^2}$	
	basis: local yielding of brace	
	$N_i^* = f_{yi} t_i [2h_i - 4t_i + b_i + b_e]$	
$\beta \leq 1-1/\gamma$	basis: chord punching shear	
$N_i^* = \frac{f_{y0} t_0}{\sqrt{3} \sin \theta_i} \left[ \frac{2h_i}{\sin \theta_i} + b_i + b_{e,p} \right]$		
<b>K and N overlap joints</b>	Similar to joints of SHS (table A2)	
<b>CHS braces</b>	Multiply formulae by $\pi/4$ and replace $b_{1,2}$ and $h_{1,2}$ by $d_{1,2}$	
<b>Functions</b>		
tension: $f_k = f_{y0}$ compression: $f_k = f_{kn}$ (T and Y joints) $f_k = 0.8 \sin \theta_1 f_{kn}$ (X joints)		
$f_{kn}$ = buckling stress according to the relevant steelwork specification, using a column slenderness ratio (KL/r) of $3.46(h_0/t_0 - 2)(1/\sin \theta_1)^{0.5}$		
$f(n) = 1.0$ for $n \geq 0$ (tension) $f(n) = 1.3 + \frac{0.4}{\beta} n$ for $n < 0$ but $\leq 1.0$ (compression)	$V_{pl,0} = \frac{f_{y0} A_v}{\sqrt{3}}$ $\alpha = \sqrt{\frac{1}{1 + (4g^2)/(3t_0^2)}}$ For SHS and RHS braces: $A_v = (2h_0 + \alpha b_0) t_0$ For CHS braces: $A_v = 2h_0 t_0$	
$b_e = \frac{10}{b_0/t_0} \frac{f_{y0} t_0}{f_{yi} t_i} b_i$ but $\leq b_i$	$b_{e,p} = \frac{10}{b_0/t_0} b_i$ but $\leq b_i$	$b_{e,ov} = \frac{10}{b_j/t_j} \frac{f_{yj} t_j}{f_{yi} t_i} b_i$ but $\leq b_i$
(*) For X joints with angles $\theta_1 < 90^\circ$ , the chord side walls must be checked for shear		

Table A1a – Range of validity of table A1

Type of joint	Joint parameters (i = 1 or 2, j = overlapped brace) (*)						
	$b_i/b_0$ $h_i/b_0$	$b_i/t_i, h_i/t_i, d_i/t_i$		$h_i/b_i$	$b_0/t_0$ $h_0/t_0$	Gap/overlap $b_i/b_j, t_i/t_j$	Eccentricity
		Compression	Tension				
<b>T, Y and X joints</b>	$\geq 0.25$	$\leq 1.25 \sqrt{\frac{E}{f_{y1}}}$		$0.5 \leq \frac{h_i}{b_i} \leq 2$	$\leq 35$		
<b>K and N gap joints</b>	$\geq 0.1 + 0.01 \frac{b_0}{t_0}$ $\beta \geq 0.35$				$\leq 35$	$\leq 35$	$\leq 35$
<b>K and N overlap joints</b>	$\geq 0.25$	$\leq 1.1 \sqrt{\frac{E}{f_{y1}}}$			$\leq 40$	$25\% \leq Ov \leq 100\%$ $\frac{t_i}{t_j} \leq 1.0, \frac{b_i}{b_j} \geq 0.75$	
<b>CHS braces (web members)</b>	$0.4 \leq \frac{d_i}{b_0} \leq 0.8$	$\leq 1.5 \sqrt{\frac{E}{f_{y1}}}$	$\leq 50$	Limitations as above for $d_i = b_i$			

(\*)  $f_{yi}$  and  $f_{yj} \leq 355 \text{ N/mm}^2$ ,  $f_{yi}$  (or  $f_{yj}$ )/ $f_{ui} \leq 0.8$

(\*\*) If  $\frac{g}{b_0} >$  the larger of  $1.5(1-\beta)$  and  $(t_1 + t_2)$ , treat as a T or Y joint

Table A2 – Design resistance of uniplanar SHS braces or CHS braces to SHS chord joints according to IIW (1989) and the 1<sup>st</sup> edition of Design Guide No. 3 (Packer et al., 1992)

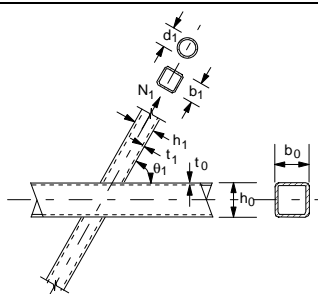
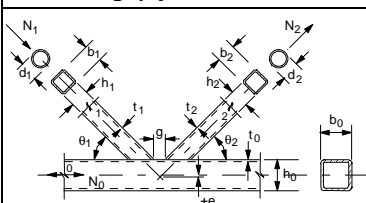
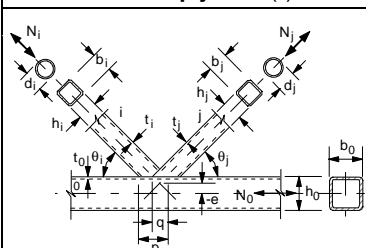
Type of joint	Factored joint resistance (i = 1,2)
<b>T, Y and X joints</b>	$\beta \leq 0.85$ basis: chord face plastification
	$N_i^* = \frac{f_{y0} t_0^2}{(1-\beta) \sin \theta_1} \left[ \frac{2\beta}{\sin \theta_1} + 4(1-\beta)^{0.5} \right] f(n)$
<b>K and N gap joints</b>	$\beta \leq 1.0$ basis: chord face plastification
	$N_i^* = 8.9 \frac{f_{y0} t_0^2}{\sin \theta_i} \left[ \frac{b_1 + b_2}{2b_0} \right] \gamma^{0.5} f(n) \quad (i=1,2)$
<b>K and N overlap joints (*)</b>	25% ≤ Ov < 50% basis: local yielding of overlapping brace
	$N_i^* = f_{yi} t_i \left[ \left( \frac{Ov}{50} \right) (2h_i - 4t_i) + b_e + b_{e,ov} \right]$
	50% ≤ Ov < 80% basis: local yielding of overlapping brace
	$N_i^* = f_{yi} t_i [2h_i - 4t_i + b_e + b_{e,ov}]$
	Ov ≥ 80% basis: local yielding of overlapping brace
	$N_i^* = f_{yi} t_i [2h_i - 4t_i + b_i + b_{e,ov}]$
<b>CHS braces</b>	Multiply by $\pi/4$ and replace $b_{1,2}$ and $h_{1,2}$ by $d_{1,2}$
<b>Functions</b>	
$f(n) = 1.0$ for $n \geq 0$ (tension)	
$f(n) = 1.3 + \frac{0.4}{\beta} n$ for $n < 0$ (compression) but $f(n) \leq 1.0$	
$b_e = \frac{10}{b_0/t_0} \frac{f_{y0} t_0}{f_{yi} t_i} b_i$ but $\leq b_i$	$b_{e,ov} = \frac{10}{b_j/t_j} \frac{f_{yj} t_j}{f_{yi} t_i} b_i$ but $\leq b_i$
(*) Only the overlapping brace need be checked for local yielding. However, the efficiency (the factored joint resistance divided by the yield capacity of the brace) of the overlapped brace should not exceed that of the overlapping brace.	

Table A2a – Range of validity of table A2

Type of joint	Joint parameters (i = 1 or 2; j = overlapped brace) (*)						
	b <sub>i</sub> /b <sub>0</sub>	b <sub>i</sub> /t <sub>i</sub>		b <sub>0</sub> /t <sub>0</sub>	$\frac{(b_1+b_2)/2b_i}{b_i/b_j \ t_i/t_j}$	Gap/overlap	Eccentricity
T, Y and X joints	$0.25 \leq \beta \leq 0.85$ (**)	$\leq 1.25 \sqrt{\frac{E}{f_{y1}}}$		$10^{(**)} \leq \frac{b_0}{t_0} \leq 35$			
K and N gap joints	$\geq 0.1 + 0.01 \frac{b_0}{t_0}$ $\beta \geq 0.35$			$\leq 35$	$15^{(**)} \leq \frac{b_0}{t_0} \leq 35$	$b_i \geq 0.77 \frac{b_1+b_2}{2}^{(**)}$	$0.5(1-\beta) \leq \frac{g}{b_0} \leq 1.5(1-\beta)$ $g \geq t_1 + t_2^{(***)}$
K and N overlap joints	$\geq 0.25$	$\leq 1.1 \sqrt{\frac{E}{f_{y1}}}$	$\leq 35$	$\frac{b_0}{t_0} \leq 40$	$\frac{t_i}{t_j} \leq 1.0$ $\frac{b_i}{b_j} \geq 0.75$	$25\% \leq Ov \leq 100\%$	
CHS braces	$0.4 \leq \frac{d_i}{b_0} \leq 0.8$	$\frac{d_1}{t_1} \leq 1.5 \sqrt{\frac{E}{f_{y1}}}$	$\frac{d_2}{t_2} \leq 50$	Limitations as above for d <sub>i</sub> = b <sub>i</sub>			
<p>(*) <math>f_{yi}</math> and <math>f_{yj} \leq 355 \text{ N/mm}^2</math>, <math>f_{yi}</math> (or <math>f_{yj}</math>)/<math>f_{ui} \leq 0.8</math></p> <p>(**) Outside this range of validity, other criteria may be governing; e.g. chord punching shear, local yielding of the (overlapping) brace, chord side wall failure, chord shear or local buckling. If these particular limits of validity are violated, the joint may still be checked as one having an RHS chord using table A1, provided the limits of validity in table A1a are met.</p> <p>(***) If <math>\frac{g}{b_0} &gt;</math> the larger of <math>1.5(1-\beta)</math> and <math>(t_1 + t_2)</math>, treat as a T or Y joint</p>							

For joints with RHS chords, the validity range in the (2009) IIW recommendations differs from that in the previous (1989) version and the 1<sup>st</sup> edition of Design Guide No. 3 (Packer et al., 1992). Previously the recommendations were given for steel grades with yield stresses  $f_y$  up to 355 N/mm<sup>2</sup> whereas in the IIW (2009) version steels with a nominal yield stress up to 460 N/mm<sup>2</sup> are included. As indicated in section 1.2.1, for yield stresses  $f_y > 355$  N/mm<sup>2</sup>, the design strength should be multiplied by a reduction factor of 0.9. The extension of the yield stress range also affects the range of validity for the diameter-to-thickness and width-to-thickness ratios for compression members and flexural members, and their section classification.

## A2 Welded uniplanar truss joints between RHS chords and RHS or CHS brace (web) members

### A2.1 $Q_u$ factors for axially loaded T, Y, X and K gap joints

The  $Q_u$  functions for joints with RHS chords now included in the resistance equations (chapter 4, tables 4.1 and 4.2) and the expressions indirectly incorporated in the equations in the 1<sup>st</sup> edition of Design Guide No. 3 (given in tables A1 and A2) are, where different, summarised in table A3.

Table A3 – Comparison of  $Q_u$  functions for RHS chord joints

	IIW (2009) formulae (chapter 4)	Previous IIW (1989) and CIDECT (1992) formulae
Function $Q_u$	$Q_u = \frac{N_i \sin \theta_i}{f_{y0} t_0^2 Q_f}$	
X joints	Identical	
T joints		
K gap joints	$Q_u = 14\beta\gamma^{0.3}$	$Q_u = 8.9\beta\gamma^{0.5}$
K overlap joints	Chord member check and brace shear check added	
Brace in-plane bending	Identical	
Brace out-of-plane bending		

#### A2.1.1 T, Y and X joints

For T and X joints, the equations for  $Q_u$  given in the new and previous recommendations are identical, except for the  $\beta$  limit, which is changed from:

$\beta \geq 0.25$  to: the same limit as for K gap joints, i.e.  $\beta \geq 0.1 + 0.01b_0/t_0$  with  $\beta \geq 0.25$ .

With this  $\beta$  limit, the  $N_{1(3\%)}$  data at a deformation limit of 3%  $b_0$  are better covered, and the  $2\gamma$  validity limit could be marginally extended from:

$2\gamma \leq 35$  to: class 1 and 2 sections but with  $b_0/t_0 \leq 40$  and  $h_0/t_0 \leq 40$ .

#### A2.1.2 K gap joints

The new K gap joint formula for chord face plastification is changed such that the equation better fits with the  $N_{1(3\%)}$  test results based on the adopted 3% ultimate deformation limit. It further allows an extension of the range of validity from:

$2\gamma \leq 35$  to: class 1 and 2 sections but with  $b_0/t_0 \leq 40$  and  $h_0/t_0 \leq 40$ .

Table A4 and figure A1 indicate, for K gap joints, the ratio between the  $Q_u$  values in tables 4.1 and 4.2 and the  $Q_u$  function adopted in the 1<sup>st</sup> edition. The new design equation gives for very high  $2\gamma$  values, up to 14% lower strengths than the previous equation, but for ratios  $2\gamma < 20$ , it gives up to 14% higher strengths.

Table A4 – Comparison between the new and previous  $Q_u$  functions for RHS K gap joints

$2\gamma$	$14\gamma^{0.3}$ (IIW, 2009)	$8.9\gamma^{0.5}$ (IIW, 1989)	Ratio $14\gamma^{0.3}/8.9\gamma^{0.5}$
10	22.7	19.9	1.14
15	25.6	24.4	1.05
20	27.9	28.1	0.99
25	29.9	31.5	0.95
30	31.5	34.5	0.92
35	33.0	37.2	0.89
40	34.4	39.8	0.86

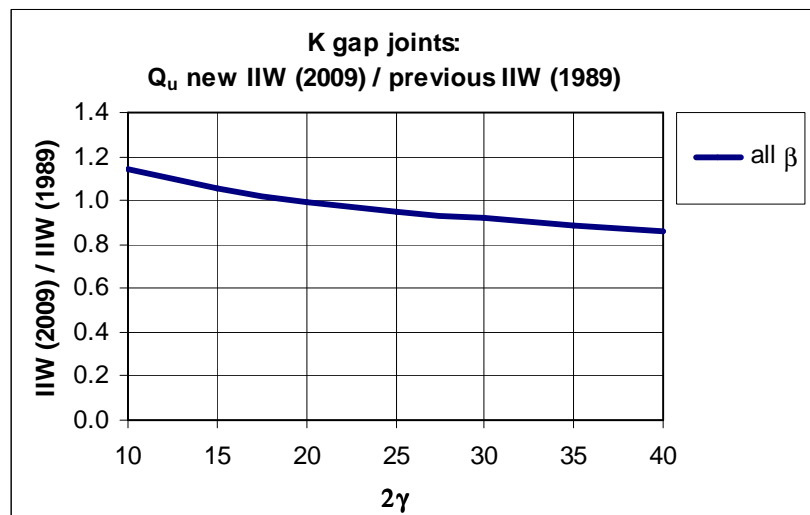


Figure A1 – RHS K gap joints: ratio between the  $Q_u$  function in the new (2009) and the previous (1989) IIW recommendations

## A2.2 $Q_f$ factors for axially loaded T, Y, X and K gap joints

The equations for  $Q_f$  in tables 4.1 and 4.2 and the  $f(n)$  functions in tables A1 or A2 are recorded in table A5.

Figure A2 compares the new expressions for  $Q_f$  given in tables 4.1 and 4.2 (curved lines) with the previous equations for  $f(n)$  (straight lines) as a function of the chord stress ratio  $n$ . This figure shows that the new formulae give, especially for very high chord compression stress and for chord tensile stress, a larger reduction in joint capacity. For chord compression stress, the reduction is especially larger for high  $\beta$  ratios, whereby the effect is more pronounced for T and X joints than for K gap joints.

It should be further mentioned that in the Corrigendum 2009 to Eurocode 3 (CEN, 2005b), the  $Q_f$  function is also added to the chord side wall failure criterion for T, Y and X joints, based on the numerical results of Yu (1997).

Table A5 – Comparison of functions for  $Q_f$  and  $f(n)$

Function $Q_f$ (IIW, 2009) – see table 4.1		
	$Q_f = (1 -  n )^{C_1}$ with $n = \frac{N_0}{N_{pl,0}} + \frac{M_0}{M_{pl,0}}$ in connecting face	
	<b>Chord compression stress (<math>n &lt; 0</math>)</b>	<b>Chord tension stress (<math>n \geq 0</math>)</b>
<b>T, Y and X joints</b>	$C_1 = 0.6 - 0.5\beta$	$C_1 = 0.10$
<b>K gap joints</b>	$C_1 = 0.5 - 0.5\beta$ but $\geq 0.10$	
Function $f(n)$ (IIW, 1989) – see table A1		
	$n = \frac{N_0}{A_0 f_{y0}} + \frac{M_0}{W_{el,0} f_{y0}}$	
	<b>Chord compression stress (<math>n &lt; 0</math>)</b>	<b>Chord tension stress (<math>n \geq 0</math>)</b>
<b>T, Y, X and K gap joints</b>	$f(n) = 1.3 - \frac{0.4}{\beta} n $ but $\leq 1.0$	$f(n) = 1.0$

### A2.3 Combined effect of $Q_u$ and $Q_f$ factors

In general, considering the effect of the  $Q_u$  with the  $Q_f$  functions together, the new IIW formulae for T, Y, X and K gap joints (chapter 4) give smaller or equal strength values compared to the capacities of the IIW (1989) recommendations (tables A1 and A2). Only in selected cases (low  $\gamma$  values combined with low  $\beta$  ratios), the new recommendations may predict larger capacities than the IIW (1989) equations. Especially for joints with tension loaded chords, the new recommendations give lower capacities due to the chord stress function.

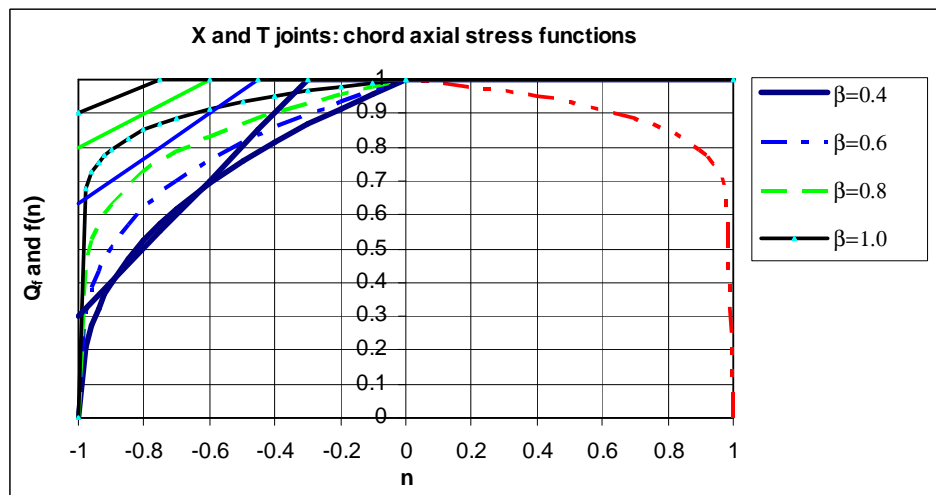


Figure A2(a) – RHS T and X joints: comparison between the  $Q_f$  and  $f(n)$  functions for chord axial loading

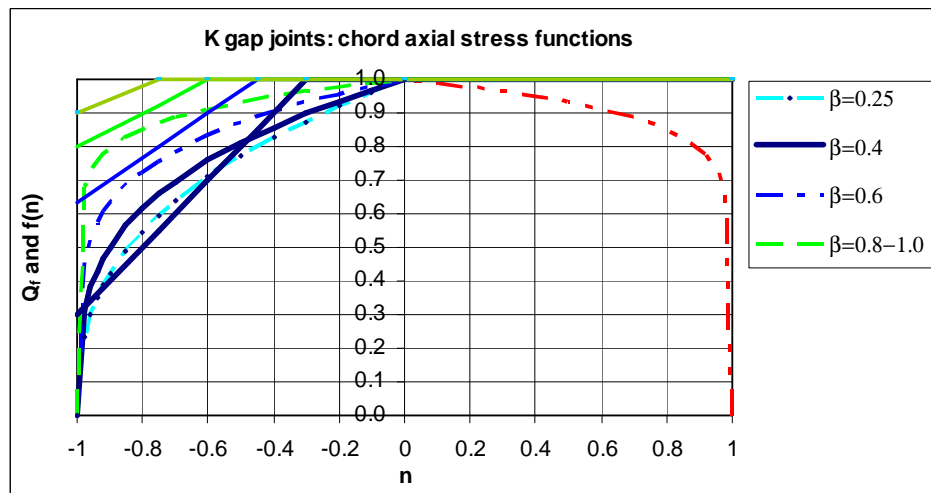


Figure A2(b) – RHS K gap joints: comparison between the  $Q_f$  and  $f(n)$  functions

#### A2.4 K overlap joints

In the 1<sup>st</sup> edition of Design Guide No. 3, only the criterion for local yielding of the overlapping brace was given for overlap joints, whereas the chord member had to be checked for the combination of chord compression loading and bending moment due to eccentricity. However, this last check was sometimes overlooked by designers, and hence, it has now been explicitly included in the design checks.

Further, in case of large overlaps or for  $h_i < b_i$  and/or  $h_j < b_j$ , a brace shear check has been included in order to avoid excessively large concentrated shear at the brace-to-chord face connection. This criterion may become critical for overlaps exceeding 60 or 80%, depending on whether or not the hidden seam of the overlapped brace is welded.

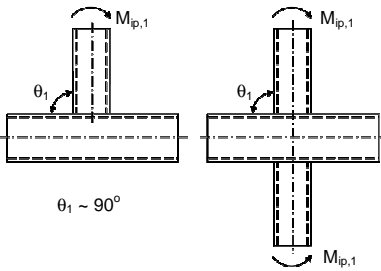
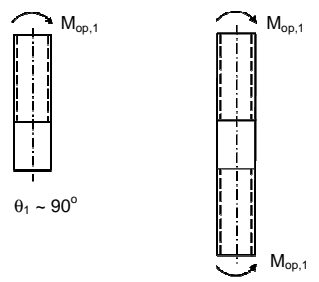
Hence, compared to the IIW (1989) recommendations, a chord member local yielding check and a check for shear between the braces and the chord have been added for K overlap joints. *Although the current Eurocode 3 recommendations are mainly based on the IIW (1989) and the previous version of this CIDECT Design Guide (Packer et al., 1992), in the Corrigendum 2009 to Eurocode 3 (CEN, 2005b) it is mentioned when shear between the braces and the chord has to be checked (see section 4.4).*

#### A3 Welded RHS-to-RHS joints under (brace) moment loading

For welded joints under brace moment loading, with the exception of the format, the equations adopted in the new and previous recommendations are in principle the same (see tables 5.1 and A6 respectively). Only the  $Q_f$  function, which is similar to the expression shown in table A5 and figure A2(a) for T joints, is different from the previous  $f(n)$  function. As discussed in section A2.2, the  $Q_f$  function gives a slightly larger reduction than the previous  $f(n)$  function.

The  $Q_f$  function has also been added to the chord side wall failure check. Further, the buckling coefficient  $\chi$  is now included for chord side wall failure of X joints subjected to brace in-plane bending moment. The last-mentioned effect is mainly due to the extension of the validity range for  $b_0/t_0$  and the extension of the yield stress range up to 460 N/mm<sup>2</sup>. *These effects are also incorporated in the Corrigendum 2009 to Eurocode 3 (CEN, 2005b).*

Table A6 – Design resistance of RHS-to-RHS joints under brace moment loading according to the 1<sup>st</sup> edition of Design Guide No. 3 (Packer et al., 1992)

Type of joint	Factored joint resistance	
<b>T and X joints under in-plane bending moments</b> 	$\beta \leq 0.85$	basis: chord face plastification
	$M_{ip,1}^* = f_{y0} t_0^2 h_1 \left\{ \frac{1}{2h_1/b_0} + \frac{2}{\sqrt{1-\beta}} + \frac{h_1/b_0}{(1-\beta)} \right\} f(n)$	
	$0.85 < \beta \leq 1.0$	basis: local yielding of brace
	$M_{ip,1}^* = f_{y1} \left\{ W_{pl,1} - \left( 1 - \frac{b_e}{b_1} \right) b_1 t_1 (h_1 - t_1) \right\}$	
	$0.85 < \beta \leq 1.0$	basis: chord side wall failure
$M_{ip,1}^* = 0.5 f_k t_0 (h_1 + 5t_0)^2$		
<b>T and X joints under out-of-plane bending moments</b> 	$\beta \leq 0.85$	basis: chord face plastification
	$M_{op,1}^* = f_{y0} t_0^2 \left\{ \frac{h_1 (1+\beta)}{2(1-\beta)} + \sqrt{\frac{2b_0 b_1 (1+\beta)}{(1-\beta)}} \right\} f(n)$	
	$0.85 < \beta \leq 1.0$	basis: local yielding of brace
	$M_{op,1}^* = f_{y1} [W_{pl,1} - 0.5t_1 (b_1 - b_e)^2]$	
	$0.85 < \beta \leq 1.0$	basis: chord side wall failure
$M_{op,1}^* = f_k t_0 (h_1 + 5t_0) (b_0 - t_0)$		
<b>Functions</b>		
$f(n) = 1.0$ for $n \geq 0$ (tension) $f(n) = 1.3 + \frac{0.4}{\beta} n$ for $n < 0$ (compression) but $f(n) \leq 1.0$ $n = \frac{N_0}{A_0 f_{y0}} + \frac{M_0}{W_{el,0} f_{y0}}$	$b_e = \frac{10}{b_0/t_0} \frac{f_{y0} t_0}{f_{y1} t_1} b_1 \leq b_1$ $f_k = f_{y0}$ for T joints $f_k = 0.8f_{y0}$ for X joints	
<b>Range of validity</b>		
$f_{yi} \leq 355 \text{ N/mm}^2$ $b_0/t_0$ and $h_0/t_0 \leq 35$	$b_1/t_1 \leq 1.1 \sqrt{E/f_{y1}}$ $\theta_1 = 90^\circ$	

#### A4 Multiplanar welded joints

Comparison of the multiplanar correction factors in table 6.1 with the recommendations in the 1<sup>st</sup> edition of Design Guide No. 3 (Packer et al., 1992), recorded in table A7, shows that the correction factors have been changed considerably.

Depending on the sense of out-of-plane loading to in-plane loading, the reduction factor for XX joints may be larger for loading in the opposite sense and is more favourable for loading in the same sense.

For KK joints, the new recommendations in table 6.1 do not give a multiplanar correction factor, whereas this was 0.9 in the 1<sup>st</sup> edition, see table A7. Further, the chord shear equation for KK gap

joints given in the 1<sup>st</sup> edition of Design Guide No. 3 had a typing error, which is corrected in table 6.1 of this 2<sup>nd</sup> edition of the Design Guide: for the shear force  $0.5\sqrt{2} V_{\text{gap},0}$  acting in each plane of an SHS chord, a shear area of  $0.5A_0$  is available. In addition, the angle  $\phi$  between the two K planes is now limited to approximately  $90^\circ$ , while in the 1<sup>st</sup> edition of Design Guide No. 3, the multiplanar angle had a range of validity from  $60^\circ$  to  $90^\circ$ .

Table A7 – Correction factors for RHS multiplanar joints according to the 1<sup>st</sup> edition of Design Guide No. 3 (Packer et al., 1992)

Type of joint	Correction factor $\mu$ to uniplanar joint resistance from table A1 or table A2
<b>KK joints</b> $60^\circ \leq \phi \leq 90^\circ$	$\mu = 0.9$
	Also, for KK gap joints, check that: $\left( \frac{N_{\text{gap},0}}{A_0 f_{y0}} \right)^2 + \left( \frac{V}{A_0 f_{y0} / \sqrt{3}} \right)^2 \leq 1.0 \quad (*)$
<b>TT and XX joints</b> $60^\circ \leq \phi \leq 90^\circ$	$\mu = 0.9$

(\*) The denominator of the second term incorrectly states  $A_0 f_{y0} / \sqrt{3}$  instead of  $0.5A_0 f_{y0} / \sqrt{3}$ .

Furthermore, the shear force  $V$  in the second term should be taken as  $0.5\sqrt{2} V_{\text{gap},0}$ .

#### A5 Welded plate-to-RHS chord joints

For welded plate-to-RHS chord joints, this 2<sup>nd</sup> edition of the Design Guide presents considerably more evidence than the previous version. For example, design recommendations for through plate joints, slotted gusset plate joints and end joints with a welded tee are now included besides transverse and longitudinal plate-to-RHS chord joints, which were only covered in the 1<sup>st</sup> edition.

Comparison of the equations for transverse plate joints shows that a chord face plastification check (see table 7.1) is now included, which can become critical if the chord load is high. Further, the chord load function  $Q_f$  differs from  $f(n)$ , as discussed under section A2.2 for T and X joints. Similar to RHS T and X joints, the  $Q_f$  function is now also incorporated in the chord side wall failure check.

For longitudinal plate-to-RHS joints, the only difference is the  $Q_f$  function compared to the  $f(n)$  function adopted in the previous edition of Design Guide No. 3.

#### A6 Bolted joints

This 2<sup>nd</sup> edition of Design Guide No. 3 gives considerably more evidence for bolted joints than the 1<sup>st</sup> edition, especially for end plate joints with bolts on four sides. Compared to the joints covered in the 1<sup>st</sup> edition, there are no principle differences in the design equations, although design recommendations for bolted flange-plate joints with bolts along four sides and for hidden joints have been added.

#### A7 Special types of welded joints

For the special types of welded joints covered in chapter 9, no principle modifications have been made. KT joints included in the 1<sup>st</sup> edition of this Design Guide are not covered within the scope of this 2<sup>nd</sup> edition because of the large number of configurations to be analysed, depending on the relative sizes of the three braces and the relative forces in the braces.



## Comité International pour le Développement et l'Etude de la Construction Tubulaire

### International Committee for the Development and Study of Tubular Structures

CIDECT, founded in 1962 as an international association, joins together the research resources of the principal hollow steel section manufacturers to create a major force in the research and application of hollow steel sections world-wide.

The CIDECT website is [www.cidect.com](http://www.cidect.com)

#### The objectives of CIDECT are:

- to increase the knowledge of hollow steel sections and their potential application by initiating and participating in appropriate research and studies.
- to establish and maintain contacts and exchanges between producers of hollow steel sections and the ever increasing number of architects and engineers using hollow steel sections throughout the world.
- to promote hollow steel section usage wherever this makes good engineering practice and suitable architecture, in general by disseminating information, organising congresses, etc.
- to co-operate with organisations concerned with specifications, practical design recommendations, regulations or standards at national and international levels.

#### Technical activities

The technical activities of CIDECT have centred on the following research aspects of hollow steel section design:

- Buckling behaviour of empty and concrete filled columns
- Effective buckling lengths of members in trusses
- Fire resistance of concrete filled columns
- Static strength of welded and bolted joints
- Fatigue resistance of welded joints
- Aerodynamic properties
- Bending strength of hollow steel section beams
- Corrosion resistance
- Workshop fabrication, including section bending
- Material properties

The results of CIDECT research form the basis of many national and international design requirements for hollow steel sections.

## **CIDECT Publications**

The current situation relating to CIDECT publications reflects the ever increasing emphasis on the dissemination of research results.

The list of CIDECT Design Guides, in the series "Construction with Hollow Steel Sections", already published, is given below. These Design Guides are available in English, French, German and Spanish.

1. Design guide for circular hollow section (CHS) joints under predominantly static loading (1<sup>st</sup> edition 1991 and 2<sup>nd</sup> edition 2008)
2. Structural stability of hollow sections (1992, reprinted 1996)
3. Design guide for rectangular hollow section (RHS) joints under predominantly static loading (1<sup>st</sup> edition 1992 and 2<sup>nd</sup> edition 2009)
4. Design guide for structural hollow section columns exposed to fire (1995, reprinted 1996)
5. Design guide for concrete filled hollow section columns under static and seismic loading (1995)
6. Design guide for structural hollow sections in mechanical applications (1995)
7. Design guide for fabrication, assembly and erection of hollow section structures (1998)
8. Design guide for circular and rectangular hollow section welded joints under fatigue loading (2000)
9. Design guide for structural hollow section column connections (2004)

In addition, as a result of the ever increasing interest in steel hollow sections in internationally acclaimed structures, two books "Tubular Structures in Architecture" by Prof. Mick Eekhout (1996), sponsored by the European Community, and "Hollow Sections in Structural Applications" by Prof. Jaap Wardenier (2002) have been published.

Copies of the Design Guides, the architectural book and research papers may be obtained through the CIDECT website: <http://www.cidect.com>

"Hollow Sections in Structural Applications" by Prof. Jaap Wardenier (2002) is available from the publisher:

Bouwen met Staal  
Boerhaavelaan 40  
2713 HX Zoetermeer, The Netherlands  
P.O. Box 190  
2700 AD Zoetermeer, The Netherlands

Tel. +31(0)79 353 1277  
Fax +31(0)79 353 1278  
E-mail [info@bouwenmetstaal.nl](mailto:info@bouwenmetstaal.nl)

### **CIDECT Organisation (2009)**

- President: J.M. Soto, Grupo Condesa, Spain
- Treasurer/Secretary: R. Murmann, United Kingdom
- A General Assembly of all members meeting once a year and appointing an Executive Committee responsible for administration and execution of established policy.
- A Technical Commission and a Promotion Committee meeting at least once a year and directly responsible for the research work and technical promotion work.

### **Present members of CIDECT are:**

- Atlas Tube, Canada
- Australian Tube Mills, Australia
- Borusan Mannesmann Boru, Turkey
- Corus Tubes, United Kingdom
- Grupo Condesa, Spain
- Industrias Unicon, Venezuela
- Rautaruukki Oyj, Finland
- Sidenor SA, Greece
- Vallourec & Mannesmann Tubes, Germany
- Voest-Alpine Krems, Austria

### **Acknowledgements for photographs:**

The authors express their appreciation to the following firms for making available some photographs used in this Design Guide:

Delft University of Technology, The Netherlands  
Instituto para la Construcción Tubular (ICT), Spain  
University of Toronto, Canada

### **Disclaimer**

Care has been taken to ensure that all data and information herein is factual and that numerical values are accurate. To the best of our knowledge, all information in this book is accurate at the time of publication.

CIDECT, its members and the authors assume no responsibility for errors or misinterpretations of information contained in this Design Guide or in its use.





This Design Guide is a revision and update of the 3<sup>rd</sup> Design Guide in a series that CIDECT has published under the general series heading "Construction with Hollow Steel Sections". The previously published Design Guides in the series, which are all available in English, French, German and Spanish, are:

1. Design guide for circular hollow section (CHS) joints under predominantly static loading (1<sup>st</sup> edition 1991 and 2<sup>nd</sup> edition 2008)
2. Structural stability of hollow sections (1992, reprinted 1996)
3. Design guide for rectangular hollow section (RHS) joints under predominantly static loading (1<sup>st</sup> edition 1992 and 2<sup>nd</sup> edition 2009)
4. Design guide for structural hollow section columns exposed to fire (1995, reprinted 1996)
5. Design guide for concrete filled hollow section columns under static and seismic loading (1995)
6. Design guide for structural hollow sections in mechanical applications (1995)
7. Design guide for fabrication, assembly and erection of hollow section structures (1998)
8. Design guide for circular and rectangular hollow section welded joints under fatigue loading (2000)
9. Design guide for structural hollow section column connections (2004)

This Design Guide is a revision and update of the 3<sup>rd</sup> Design Guide in a series that CIDECT has published under the general series heading "Construction with Hollow Steel Sections". The previously published Design Guides in the series, which are all available in English, French, German and Spanish, are:

1. Design guide for circular hollow section (CHS) joints under predominantly static loading (1<sup>st</sup> edition 1991 and 2<sup>nd</sup> edition 2008)
2. Structural stability of hollow sections (1992, reprinted 1996)
3. Design guide for rectangular hollow section (RHS) joints under predominantly static loading (1<sup>st</sup> edition 1992 and 2<sup>nd</sup> edition 2009)
4. Design guide for structural hollow section columns exposed to fire (1995, reprinted 1996)
5. Design guide for concrete filled hollow section columns under static and seismic loading (1995)
6. Design guide for structural hollow sections in mechanical applications (1995)
7. Design guide for fabrication, assembly and erection of hollow section structures (1998)
8. Design guide for circular and rectangular hollow section welded joints under fatigue loading (2000)
9. Design guide for structural hollow section column connections (2004)